University of Naples "Federico II"
Department of Cellular and Molecular Biology and Pathology "L. Califano"
Pathology and Physiopathology Doctorate Program – XXII Cycle
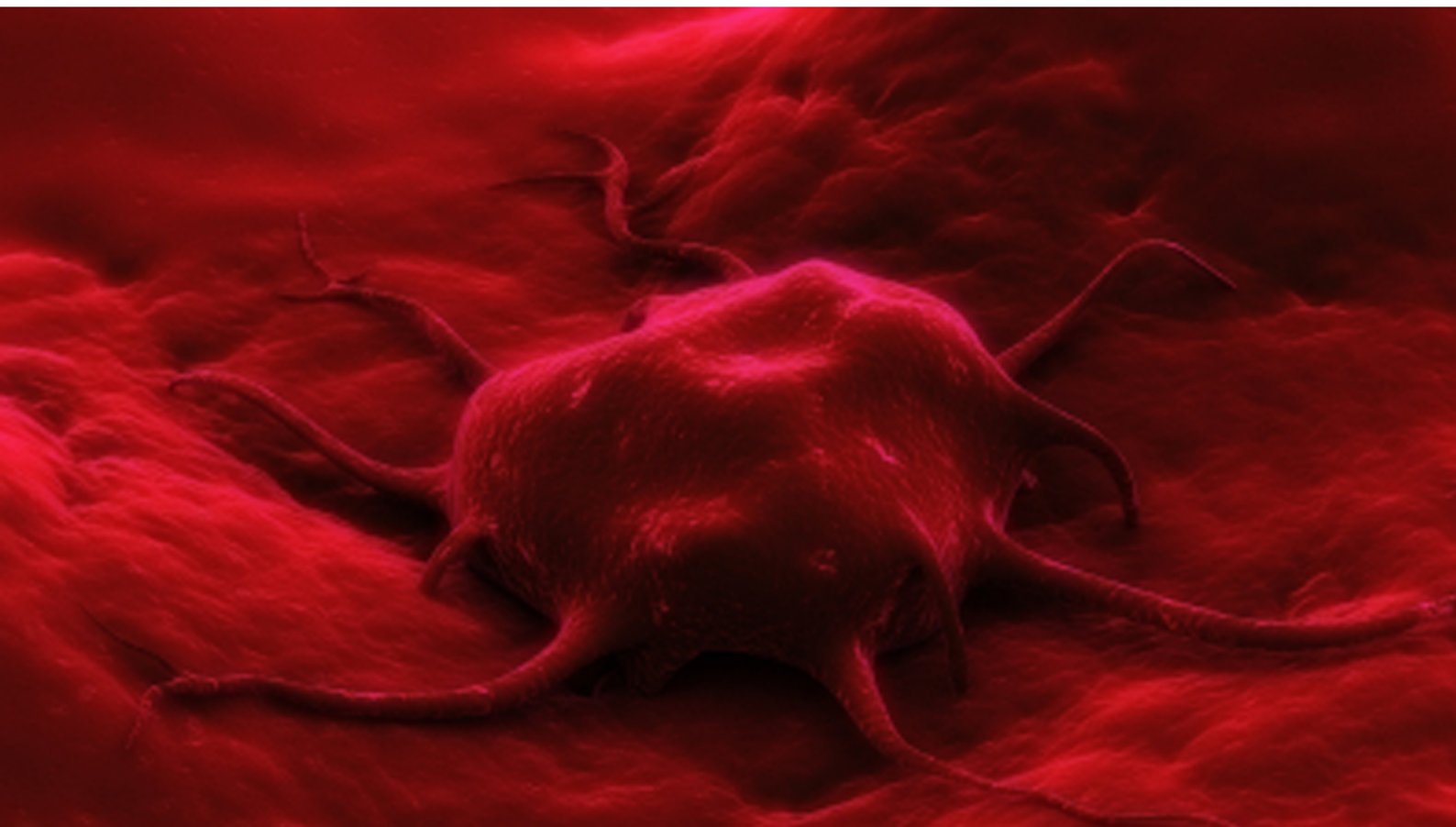
Multifunctional role of PED/PEA15 on cell death and cell motility in human Non Small Cell Lung Cancer (NSCLC)

Candidate
Dott. Ciro Zanca

Supervisor
Prof. Gerolama Condorelli

Coordinator
Prof. Vittorio Enrico Avvedimento

Academic Year 2008/09

Dott. Ciro Zanca

Department of Cellular and Molecular Biology and Pathology "L. Califano"

University of Naples "Federico II", Naples, Italy

Email: ciro.zanca@gmail.com

LUNG CANCER

Lung cancer is the leading cause of cancer deaths in the United States and worldwide. The two major forms of lung cancer are non–small cell lung cancer (NSCLC - about 85% of all lung cancers) and small-cell lung cancer (SCLS - about 15%). This classification is based upon the microscopic appearance of the tumor cells themselves. These two types of cancers grow and spread in different ways and may have different treatment options, so a distinction between these two types is important. Despite advances in early detection and standard treatment, non-small cell lung cancer is often diagnosed at an advanced stage and has a poor prognosis. The treatment and prevention of lung cancer are the major unmet needs that can probably be improved by a better understanding of the molecular origins and evolution of the disease. Non–small-cell lung cancer can be divided into three major histologic subtypes: squamous-cell carcinoma, adenocarcinoma, and large-cell lung cancer. Smoking is a major risk factor of all types of lung cancer but is most strongly linked with small-cell lung cancer and squamous-cell carcinoma; adenocarcinoma is the most common type in patients who have never smoked. (1)

SCLC is the most aggressive and rapidly growing of all lung cancers. SCLC metastasize rapidly to many sites within the body and are most often discovered after they have spread extensively. Referring to a specific cell appearance often seen when examining samples of SCLC under the microscope, these cancers are sometimes called oat cell carcinomas.

Metastatic cancers from other primary tumors in the body are often found in the lung. Tumors from anywhere in the body may spread to the lungs either through the bloodstream, through the lymphatic system, or directly from nearby organs. Metastatic tumors are most often multiple, scattered throughout the lung, and concentrated in the peripheral rather than central areas of the lung. (2)
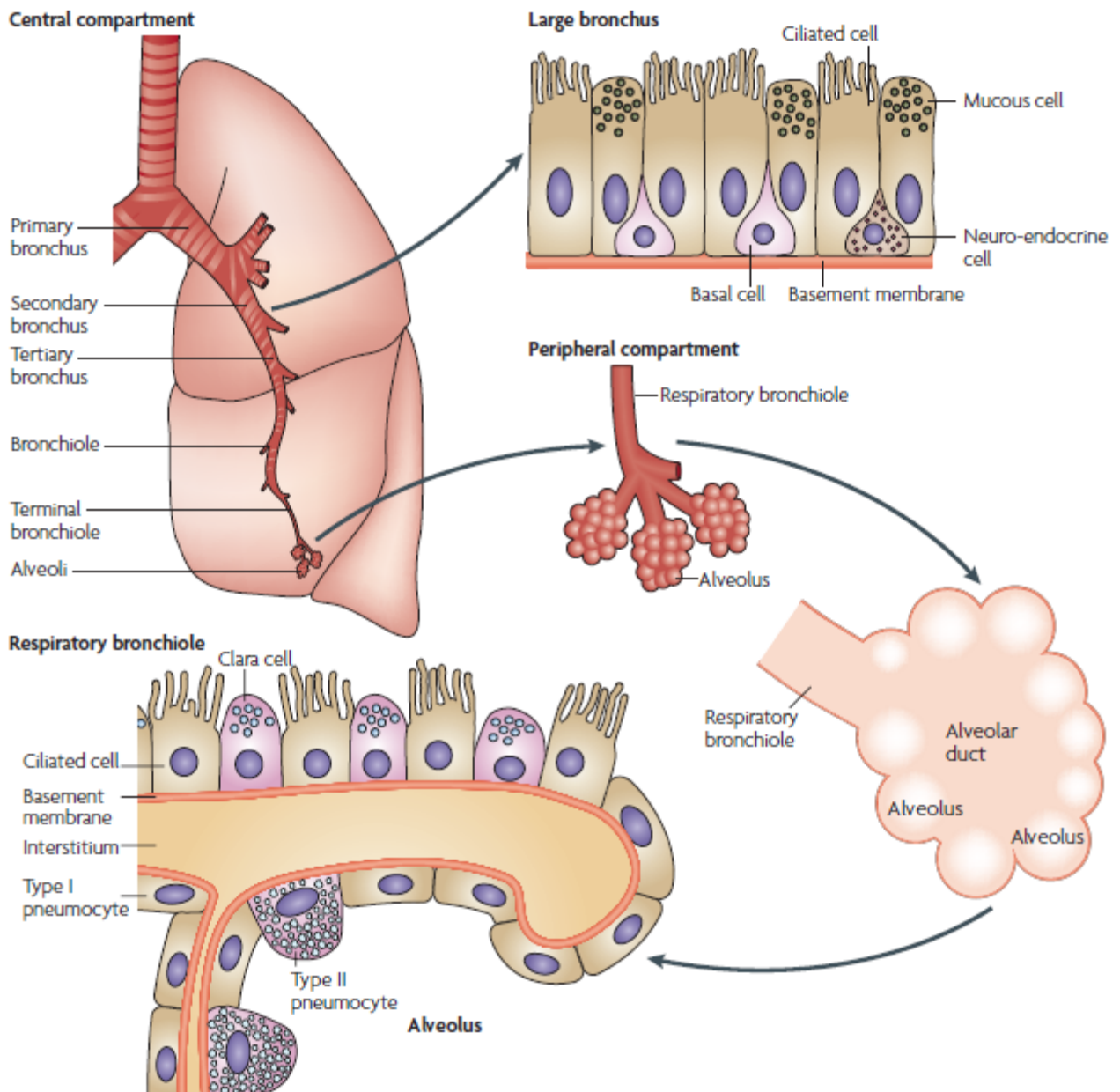
Figure 1. Pathogenesis of lung cancer: targeting a specific anatomical compartment. Lung cancer is one of few malignancies in which the major histological types arise in different anatomical compartments of the organ. The major function of the lungs is respiratory exchange, and inhaled air is conducted to the alveoli (the small sacs in which gaseous exchange occurs) through a network of branching tubes (bronchi and bronchioles). The larger tubes, having muscular walls reinforced with cartilage are the bronchi, while smaller tubes (< 1 mm in diameter) that hav incomplete muscular walls and lack cartilage are called bronchioles, and they connect to the alveoli. The putative stem cell of the bronchus is the basal cell, which is believed to give rise to the differentiated ciliated, mucous and neuroendocrine cells. The terminal bronchioles and alveoli are believed to share a common stem cell, and a putative stem cell has recently been identified in the mouse. However, the peripheral airway stem cell is difficult to identify morphologically, and the cells capable of dividing in these locations are the Clara cells (in the bronchioles) and the surfactant secreting type II pneumocytes (in the alveoli). The secretory products of peripheral airway cells include Clara cell protein 10 (CC10) and surfactant (from type II pneumocytes). Thus, region-specific stem cell niches function to maintain epithelial diversity. Lung cancer may be considered to arise from either the central airway compartment (predominantly SCLC and squamous cell carcinoma) or from the peripheral airway compartment (predominantly adenocarcinoma). (3)

Staging of lung cancer

The stage of a cancer refers to the extent to which a cancer has spread in the body. Staging involves both evaluation of a cancer's size as well as the presence or absence of metastases in the lymph nodes or in other organs. Staging is important for determining how a particular cancer should be treated, since lung-cancer therapies are geared toward specific stages. Staging of a cancer is also critical in estimating the prognosis of a given patient, with higher-stage cancers generally having a worse prognosis than lower-stage cancers. NSCLC are assigned a stage from I to IV in order of severity:

- In stage I, the cancer is confined to the lung.

- In stages II and III, the cancer is confined to the chest (with larger and more invasive tumors classified as stage III).

- Stage IV cancer has spread from the chest to other parts of the body.

  SCLC are staged using a two-tiered system:

- Limited-stage SCLC refers to cancer that is confined to its area of origin in the chest.

- In extensive-stage SCLC, the cancer has spread beyond the chest to other parts of the body.

  The TNM staging system for lung cancer provides a consistent reproducible description of the extent of anatomic involvement. This is achieved by defining the characteristics of primary tumor (T), regional lymph node involvement (N), and metastasis (M). (2)

TNM STAGING OF LUNG CANCER

Stage IV
M1 (any T, any N)

Lymph node (N) columns (vertical headers): Supraclavicular | Scalene(ipsi-/contralateral) | Mediastinal (contralateral) | Mediastinal (ipsilateral) | Subcarinal | Hilar (contralateral) | Hilar (ipsilateral) | Peribronchial (ipsilateral) | LYMPH NODE (N)

+	/ +	/ +				/ +		**N3** — Stage III B
−	−	−	+ &/ +		−			**N2** — Stage III A
−	−	−	−	−	−	*+ &/ +		**N1** — Stage II A / Stage II B
−	−	−	−	−	−	−	−	**N0** — Stage I A / Stage I B / Stage II B

(MO on right side arrow)

Stage 0
(Tis, N0, M0)

PRIMARY TUMOR (T)

	T1	T2	T3	T4	PRIMARY TUMOR (T)
	a&b&c	any of a,b,c,d	(a&c)/b/d	(a&c)/d	Criteria
a. Size	≤ 3 cm	> 3 cm	any	any	
b. Endo-bronchial location	No invasion proximal to the lobar bronchus	Main bronchus (≥ 2 cm distal to the carina)	Main bronchus (< 2 cm distal to the carina)	−	
c. Local Invasion	surrounded by lung or visceral pleura	Visceral pleura	Chest wall **/ diaphragm/ mediastinal pleura/ parietal pericardium	Mediastinum/ trachea/heart/ great vessels/ esophagus/ vertebral body/ carina	
d. Other	−	Atelectasis/ obstructive pneumonitis that extends to the hilar region but doesn't involve the entire lung	Atelectasis/ obstructive pneumonitis of the entire lung	Malignant pleural/peri-cardial effusion or satellite tumor nodule(s) within the ipsilateral primary-tumor lobe of the lung	

METASTASES (M)
M0 : Abscent
M1 : Present
Separate metastatic tumor nodule(s) in the ipsilateral nonprimary-tumor lobe(s) of the lung also are classified M1

Tis : Carcinoma *in situ*

Staging is not relevant for Occult Carcinoma (Tx, N0, M0)

* Including direct extension to intrapulmonary nodes
** Including superior sulcus tumor

(& : and) (/ : or) (&/ : and /or)

Figure 2. The chart lists the comparative characteristics of primary tumor in the vertical columns (including size, endobronchial location, local invasion, and other characteristics). The horizontal columns refer to the lymph node involvement. The different stages are color coded and can be found at the intersection of appropriately matched horizontal and vertical columns. Stages with unique characteristics such as stages 0 and IV are defined in separate boxes. The most recently adopted revisions of TNM staging are reflected in this chart, which include the following: division of stage I into stages IA and IB; splitting of stage II into stage IIA and stage IIB; shifting of T3N0M0 from stage IIIA to stage IIB; and classification of multiple tumor nodules (T4 if the satellite nodule(s) are in the same lobe or M1 if the intrapulmonary ipsilateral nodule(s) are in the nonprimary tumor lobe(s)). (4)

Lung cancer treatment and prognosis

Treatment for lung cancer can involve surgical removal of the cancer, chemotherapy, or radiation therapy, as well as combinations of these treatments. The decision about which treatments will be appropriate for a given individual must take into account the localization and extent of the tumor as well as the overall health status of the patient.

Surgery. Surgical removal of the tumor is generally performed for limited-stage (stage I or sometimes stage II) NSCLC and is the treatment of choice for cancer that has not spread beyond the lung. About 10%-35% of lung cancers can be removed surgically, but removal does not always result in a cure, since the tumors may already have spread and can recur at a later time.

Radiation. Radiation therapy may be employed as a treatment for both NSCLC and SCLC. Radiation therapy uses high-energy X-rays or other types of radiation to kill dividing cancer cells. Radiation therapy may be given as curative therapy, palliative therapy (using lower doses of radiation than with curative regimens), or as adjuvant therapy in combination with surgery or chemotherapy. Combining radiation therapy with chemotherapy can further increase the chances of survival when chemotherapy is administered. External radiation therapy can generally be carried out on an outpatient basis, while internal radiation therapy requires a brief hospitalization. A person who has severe lung disease in addition to a lung cancer may not be able to receive radiotherapy to the lung.

Chemotherapy. Both NSCLC and SCLC may be treated with chemotherapy. Chemotherapy refers to the administration of drugs that stop the growth of cancer cells by killing them or preventing them from dividing. Chemotherapy may be given alone, as an adjuvant to surgical therapy, or in combination with radiotherapy. While a number of chemotherapeutic drugs have been developed, the class of drugs known as the platinum-based drugs have been the most effective in treatment of lung cancers. Chemotherapy is the treatment of choice for

most SCLC, since these tumors are generally widespread in the body when they are diagnosed. Only half of people who have SCLC survive for four months without chemotherapy. With chemotherapy, their survival time is increased up to four- to fivefold. Chemotherapy alone is not particularly effective in treating NSCLC, but when NSCLC have metastasized, it can prolong survival in many cases. Unfortunately, the drugs used in chemotherapy also kill normally dividing cells in the body, resulting in unpleasant side effects.

Targeted therapy. The discovery that signaling by the epidermal growth factor receptor (EGFR) plays a key role in tumorigenesis prompted efforts to target this receptor in anticancer therapy. Two different types of EGFR-targeted therapeutic agents were subsequently developed: mAbs, such as cetuximab and panitumumab, which target the extracellular domain of the receptor, thereby inhibiting ligand-dependent EGFR signal transduction; and small-molecule tyrosine kinase inhibitors, such as gefitinib and erlotinib (Tarceva), which target the intracellular tyrosine kinase domain of the EGFR. (5) This protein is found at abnormally high levels on the surface of some types of cancer cells, including many cases of non-small cell lung cancer. Other attempts at targeted therapy include antiangiogenesis drugs, which block the development of new blood vessels within a cancer. Without adequate blood vessels to supply oxygenated blood, the cancer cells will die. The antiangiogenic drug bevacizumab (Avastin) has recently been found to prolong survival in advanced lung cancer when it is added to the standard chemotherapy regimen (2). Another example of targeted therapy is represented by the use of the Tumour necrosis factor (TNF)-related apoptosis-inducing ligand (TRAIL), which is a potent stimulator of apoptosis. One of the most interesting aspects of this molecule is that tumour cells are significantly more sensitive to TRAIL-induced apoptosis than normal cells. Although the molecular basis for the tumour-selective activity of TRAIL remains to be fully defined, the TRAIL pathway is an attractive therapeutic target for the treatment of cancer. In addition to triggering a pro-apoptotic signal through activation of caspases, TRAIL can activate diverse intracellular

signalling pathways involving NFκB, phosphoinositoide 3-kinase (PI3K) and mitogen activated protein kinase (MAPK)n family proteins that can stimulate cell survival and proliferation. TRAIL is an important immune effector molecule in the surveillance and elimination of developing tumours. Moreover, genetic lesions in various components of the TRAIL pathway have been found in human tumour samples, suggesting that inactivation of the TRAIL pathway and/or escape from TRAIL-mediated immunosurveillance might have an important role in tumour onset and progression. In preclinical trials, recombinant forms of TRAIL and agonistic anti-TRAIL receptor antibodies can have single-agent activity against TRAIL-sensitive tumour cells *in vitro* and *in vivo*. These agents can synergize with chemotherapeutic drugs and novel molecular therapeutic agents to more effectively kill TRAIL-sensitive tumour cells and TRAIL-resistant tumours. Early-phase clinical trials using recombinant TRAIL and agonistic anti-TRAIL receptor antibodies indicate that these agents can be delivered safely and are generally well-tolerated. Although some objective anti-tumour responses have been reported with these agents as monotherapies, they probably hold greater promise for further clinical development when used in combination with other cancer treatments. (6)

Prognosis of lung cancer. SCLC has the most aggressive growth of all lung cancers, with a median survival time of only two to four months after diagnosis when untreated. However, SCLC is also the type of lung cancer most responsive to radiation therapy and chemotherapy. In non-small cell lung cancer (NSCLC), results of standard treatment are generally poor in all but the most localized cancers that can be surgically removed. However, in stage I cancers that can be completely removed, five-year survival approaches 75%. Radiation therapy can produce a cure in a small minority of patients with NSCLC and leads to relief of symptoms in most patients. In advanced-stage disease, chemotherapy offers modest improvements in survival time, although overall survival rates are poor. The overall prognosis for lung cancer is poor when compared with some other cancers. Survival rates for

lung cancer are generally lower than those for most cancers, with an overall five-year survival rate for lung cancer of about 16% compared to 65% for colon cancer, 89% for breast cancer, and over 99% for prostate cancer (2).

Risk factors

Environmental tobacco smoke. The causal relationship between smoking and lung cancer is well established with a 10- to 20-fold increased risk of lung cancer in smokers compared with never smokers. Given the link between active smoking and lung cancer, the association of environmental tobacco smoke (ETS) and lung cancer risk has been widely studied. ETS is a mixture of sidestream smoke released by the burning tip of the cigarette or other smoking device (such as a cigar or pipe) and mainstream smoke exhaled by the smoker. Sidestream smoke is the main component of ETS, and although diluted in air, consists largely of the same toxic substances and carcinogens that are inhaled by the active smoker, although the proportions of the different carcinogens may vary. Even though the dose of carcinogens from ETS is far less than from smoking, urinary metabolites of tobacco-specific carcinogens such as NNK are detectable in nonsmokers exposed to ETS, providing biological evidence for a role of ETS in lung cancer development.

Radon. Radon is a radioactive gas produced from the decay of naturally occurring uranium in rocks and soil. Although chemically inert, radon decays into active products ('radon progeny') that attach themselves to particulate matter in the air and are inhaled, where they adhere to the respiratory epithelium.

Hormonal factors. The higher proportion of lung cancer in female never smokers compared with male never smokers suggests a possible role for gender-dependent hormones in the development of lung cancer. Several studies have provided evidence supporting a biological role for oestrogen in lung carcinogenesis by direct promotion of cell proliferation. Oestrogen receptors (ERα and ERβ) are expressed in healthy lung tissue and lung tumours in both men

and women, and the data are inconsistent as to whether ER expression is biased to any gender. ERβ appears to be expressed more frequently than ERα in lung tissue, and its expression in NSCLC tumours is associated with improved survival, whereas the expression of ERα is a poor prognostic factor. *In vitro* studies have also shown that oestrogens stimulate the proliferation of NSCLC cells through oestrogen receptor-mediated signalling, whereas anti-oestrogens inhibit growth. In addition, oestrogens can potentially alter the metabolic activation of carcinogens such as PAHs, thus promoting carcinogenesis.

Genetic factors. Inter-individual variations in the ability to metabolize carcinogens might contribute to differences in susceptibility to lung cancer. Genetic epidemiological studies have suggested that individuals with cytochrome P450 1A1(*CYP1A1*) polymorphisms (I462V) and/or a homozygous deletion of glutathione S‑transferase (*GSTM1*) are at increased risk of lung cancer, although other studies have found no association. Pooled analyses of case–control studies of *CYP1A1* and *GSTM1* polymorphisms have found that the *CYP1A1‑*I462V polymorphism is associated with a twofold to threefold increased risk of lung cancer in Caucasian (but not in Asian) never smokers with no significant effect of the *GSTM1*-null genotype. However, a combined effect of *CYP1A1‑*I462V and *GSTM1*-null variants has been observed, with a greater than fourfold increased risk of lung cancer with the combination compared with those with two non-variant genotypes, suggesting possible interactions between the phase I and phase II enzymes. Differences in DNA repair capacity might also contribute to susceptibility to lung cancer, with the underlying hypothesis that individuals with lower capacity to repair DNA have a higher risk of lung cancer from DNA-damaging carcinogens. Polymorphisms in DNA repair genes involved in base excision repair (*XRCC1* and *OGG1*), nucleotide excision repair (*ERCC1*, *ERCC2* and *XPA*), DNA double-strand break repair (*XRCC3*) and mismatch repair pathways (*MLH1* and *MSH2*) have been studied in association with lung cancer risk. (3)

Molecular basis of lung cancer

Clonal Evolution. Changes in certain genes (e.g., proinflammatory interleukin-8 [*IL8*] and some DNA-repair genes) occur in nonmalignant lung tissue of smokers and patients with lung cancer, a finding consistent with diffuse tissue injury. These changes probably precede epithelial clonal evolution, an important element of the molecular origins of lung and other cancers. Patches of clonally related cells, or clonal patches containing 40,000 to 360,000 cells, have been mapped in the lung. The size and number of subclones in a clonal patch may contribute to the cancer risk.

Early events in the development of non–small cell lung cancer include loss of heterozygosity at chromosomal region 3p21.3 (site of *RASSF1A*, a member of the Ras association domain family, and *FUS1*), 3p14.2 (*FHIT,* a fragile histidine triadgene), 9p21 (*p16*), and 17p13 (*p53*). All these genes are tumor-suppressor genes. Loss-of-heterozygosity patterns in squamous-cell carcinoma and adenocarcinoma differ (e.g., chromosome 3p deletions are much more extensive in squamous cell carcinoma). Clonal patches with methylation of promoter regions of genes (epigenetic changes), *p53* mutation, *EGFR* mutation, *c-Myc* amplification, loss of heterozygosity, and microsatellite instability can occur in normal tissue surrounding non–small-cell lung tumors and may be associated with a greater risk of recurrence and second primary tumors. These findings suggest that in the future molecular analyses of surgical margins may help identify patients most likely to benefit from adjuvant therapy. (1)
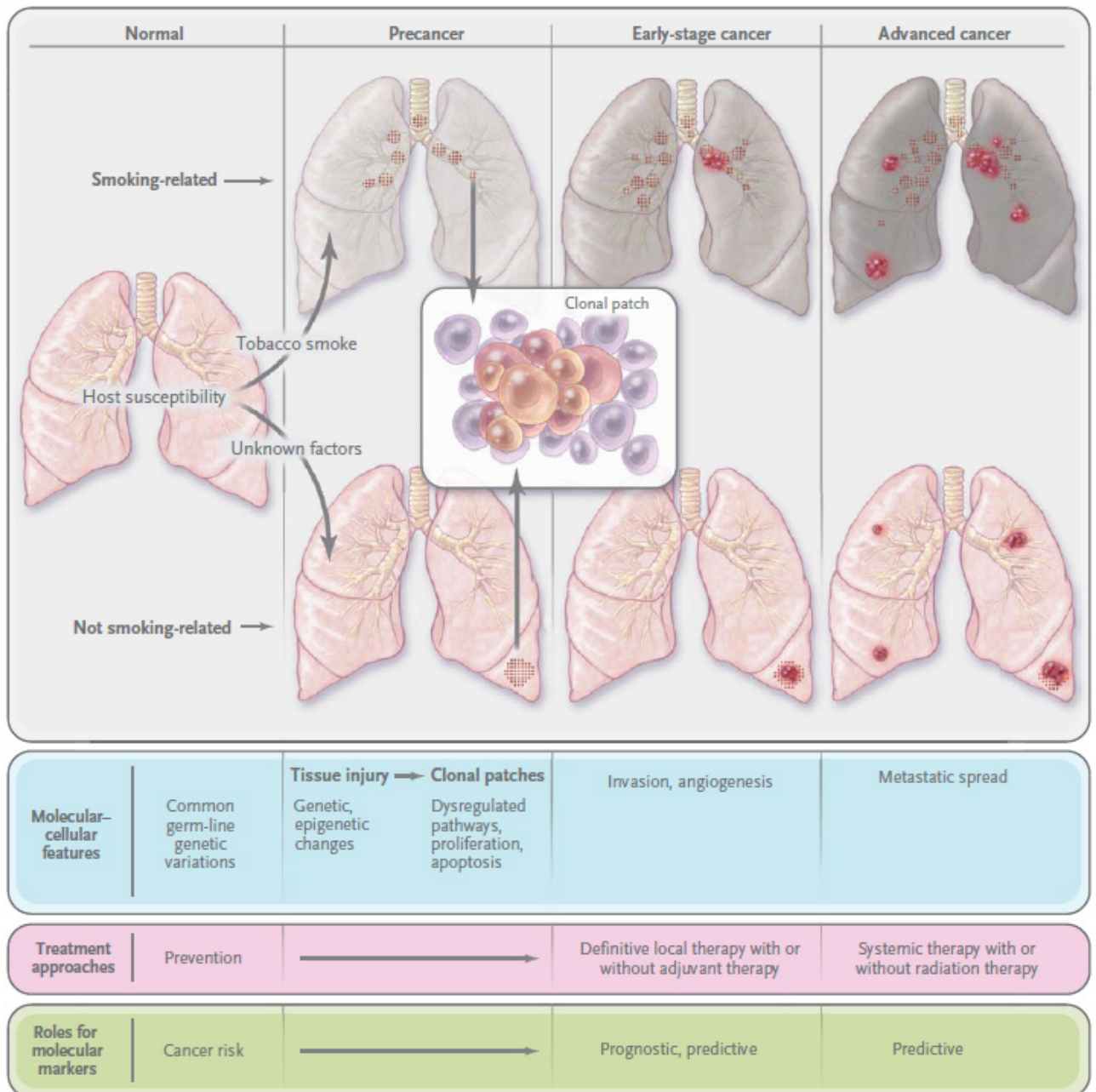
Figure 3. Molecular evolution of Lung Cancer. Environmental factors, such as tobacco smoke, and genetic susceptibility interact to influence carcinogenesis. Factors that are unrelated to smoking — including genetic, hormonal, and viral (e.g., human papillomavirus) factors — have been suggested. Tissue injury (e.g., from tobacco smoke, reflected in the discolored smoking-related lungs) initially occurs in the form of genetic and epigenetic changes (e.g., mutations, loss of heterozygosity, and promoter methylation) and global transcriptome changes (e.g., inflammation and apoptosis pathways). These changes can persist long term and eventually lead to aberrant pathway activation and cellular function (e.g., deregulated proliferation and apoptosis) to produce premalignant changes, including dysplasia and clonal patches. Additional changes can result in
angiogenesis, invasion and early-stage cancer, and advanced cancer and metastasis. Many molecular changes in earliest-stage cancer also occur in advanced disease. Premalignant patches contain clones and subclones (inset), which can involve loss of heterozygosity, microsatellite instability, and mutations (e.g., in *p53* and epidermal growth factor receptor [*EGFR*]). Lung cancers unrelated and related to smoking have strikingly different molecular profiles, including those of mutations in *p53*, *KRAS*, *EGFR,* and *HER2*. Smoking-related patches and primary cancers (usually squamous-cell carcinoma and small-cell lung cancer) most often develop in the central airway. Most tumors that are not related to smoking are adenocarcinomas and develop in the peripheral airways. Molecular markers can signify risk (in people without cancer), prognosis (outcome independent of treatment), and sensitivity to treatment through predictive markers. Such stage-specific markers can span the course of disease from its early stages through its late stages. They also can help define mechanisms of resistance to therapy. (1)

EGFR Family. The EGFR protein belongs to a family of four surface receptor tyrosine kinases and is overexpressed in many cancers, including about 50% of lung cancers. On binding to one of several ligands, EGFR forms homodimers or heterodimers with other family members, initiating a cascade of signaling events that trigger anti-apoptotic signaling, proliferation, angiogenesis, invasion and metastasis. These multiple effects are initiated by the activation of three major pathways: the Akt pathway that leads to survival through the inhibition of apoptosis; activation of the Ras–mitogen-activated protein kinase (MAPK) pathway that leads to increased proliferation; and STAT signalling with effects on many other functions. These observations led to the development and widespread clinical testing of small-molecule tyrosine kinase inhibitors (TKIs) including erlotinib (Tarceva) and gefitinib (Iressa). Although these inhibitors had modest or no effects in most NSCLC cases, dramatic responses were observed in some patients. Subsequently, mutations in the tyrosine kinase domain of *EGFR* associated with drug sensitivity and treatment response were identified. (3) Preclinical and clinical data suggest that *EGFR* mutations are early events in the development of non–small-cell lung cancer. *EGFR* mutations, including those involving exons 18, 19, and 20 and L858R, can transform fibroblasts and lung epithelial cells. Deinduction of mutant *EGFR* expression led to regression of tumors, suggesting the need for persistent mutant *EGFR* activity for continued tumor survival. *HER2* mutations and amplification have been identified in patients with lung adenocarcinoma. The frequency of such mutations is less than 5%, and the frequency of such amplification is 5 to 10%. *HER2* kinase domain mutations (in-frame insertions in exon 20) and *EGFR* kinase domain mutations have similar associations with female sex, nonsmoking status, and Asian background in patients with adenocarcinoma. *HER2* amplification is associated with sensitivity to inhibitors of the EGFR tyrosine kinase; *HER2* mutations are associated with resistance to such inhibitors but also with sensitivity to HER2-targeted therapy. *HER3* kinase domain mutations have not been detected in patients with non–small-cell lung cancer. Mutations in the *HER4* kinase domain were found in 2 to 3% of Asian patients with this

disease, with a possible association with male sex and smoking. (1)

KRAS mutations. Ras proteins function downstream of the EGFR signalling pathway to mediate cell proliferation. Oncogenic missense mutations in *KRAS* result in the loss of intrinsic GTPase activity that is required to return Ras proteins to their inactive, GDP-bound form. Therefore, the intrinsic negative-feedback control of Ras activity is lost, leaving the mutated Ras constitutively activated. Several distinctive features characterize *KRAS* mutations in lung cancer. (3) Activating *KRAS* mutations are limited to non–small-cell lung cancer (predominantly adenocarcinomas), virtually mutually exclusive of mutations in the *EGFR* and *HER2* kinase domains, and associated with resistance to EGFR inhibitors (tyrosine kinase inhibitors and cetuximab) and chemotherapy. Most *KRAS* mutations in lung adenocarcinoma are smoking-related G→T transversions (substitutions of a purine for a pyrimidine) and affect exon 12 (in 90% of patients) or exon 13. Transversions (smokers) and transitions (nonsmokers) also have been reported for *p53* mutations in lung adenocarcinoma. *KRAS* mutations appear to be an early event (e.g., detectable in the

preinvasive lesions of atypical adenomatous hyperplasia and bronchoalveolar carcinoma) that precedes smoking-related lung adenocarcinoma. They generally mark a poor prognosis. (1) Further evidence supporting this gene's role in the pathogenesis of lung cancer comes from transgenic mice bearing a mutated *KRAS* and in which multifocal atypical adenomatous hyperplasia and adenocarcinoma develop. (7)

PI3K–Akt–mTOR. The pathway consisting of PI3K, Akt, and mammalian target of rapamycin (mTOR), which is downstream of EGFR, is activated early in lung carcinogenesis. (8) Akt is also overexpressed in bronchial dysplasia. Inhibition of Akt can induce apoptosis of human premalignant and malignant lung cells and prevent lung carcinogenesis in an animal model. An mTOR inhibitor can block malignant progression of atypical adenomatous hyperplasia lesions in the *KRas* mouse model. Since mTOR drives tumorigenesis in part through macrophages, a prominent component of the tumor microenvironment, the antitumor effect of

mTOR inhibition requires the tumor microenvironment. There is mutation or amplification of *PIK3CA*, which encodes the PI3K catalytic subunit, in a subgroup of non–small-cell lung tumors, especially squamous-cell carcinoma, in association with increased PI3K activity and Akt expression. (1)

TP53 *gene.* The tumour suppressor p53 (encoded by *TP53*) has multiple functions, but mainly acts as a transcription factor for a large number of target genes. Downstream effects include the regulation of apoptosis and DNA damage responses. Mutations in *TP53* are one of the most frequent changes identified in human tumour cells, and the common mutations (usually in the DNA binding domains of the gene) lead to the generation of mutant forms with altered amino acid sequences that lack DNA binding activity. (9)

Methylation, allelic loss and gene silencing. Aberrant methylation of promoter CpG islands might result in gene silencing (through chromatin remodelling), and is a frequent mechanism of tumour-suppressor gene inactivation in cancer. Inactivation of one allele of a tumour-suppressor gene is often accompanied by allelic loss of the other allele, resulting in the 'two-hit' loss needed to inactivate most tumour-suppressor genes. (10) For example, smoking status is positively associated with methylation of the promoter region of the fragile histidine triad (*FHIT)* gene and negatively associated with methylation of the promoter of the O6-methylguanine-DNA methyltransferase (*MGMT)* gene. (3)

Angiogenesis. VEGF levels in bronchial epithelial cells of smokers increase in association with the progression of bronchial dysplasia from low grade to high grade. Bronchial hyperplasia, metaplasia, and carcinoma in situ are associated with increased microvessel density, and a distinctive pattern known as angiogenic squamous dysplasia can occur. (11) Factors associated with increased tumor angiogenesis correlate with the development and prognosis of lung cancer. Circulating VEGF levels may predict the clinical benefit of VEGF inhibitors in patients with this disease. Many angiogenic factors are regulated at least in part

through the hypoxia-regulated pathways, such as hypoxia-induced factor (HIF) 1α and 2α. In addition to hypoxia, VEGF and other angiogenic factors are also regulated by EGFR through HIFdependent and independent mechanisms and by oncogenes such as *KRAS* and *p53*. (1)
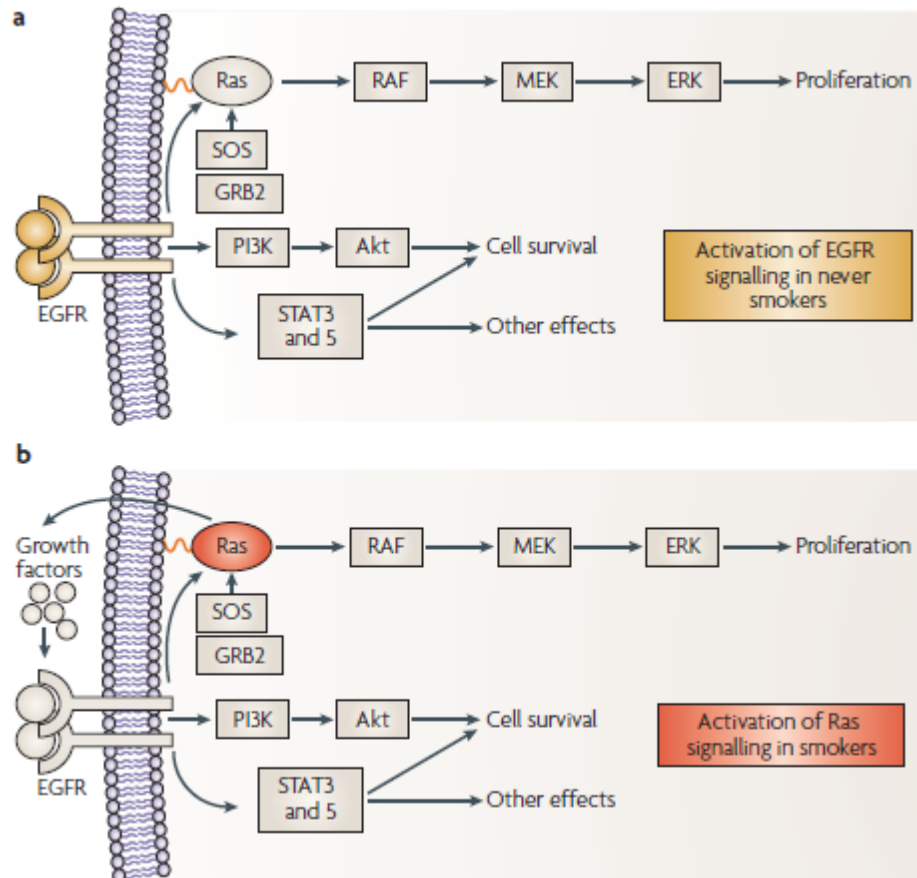
Figure 4. Two pathways to adenocarcinoma. Ligand binding to epidermal growth factor receptor (EGFR) induces homo- and hetero-dimerization of the receptor, resulting in activation of downstream effectors including the Ras–MAPK (mitogen-activated protein kinase), PI3K (phosphatidylinositol 3-kinase)–Akt, and signal transducer and activator of transcription (STAT) pathways that lead to cell proliferation, survival and many other effects associated with carcinogenesis. The EGFR pathway is frequently activated in never smokers by mutations in the EGFR gene. In smokers, mutations of the KRAS gene often occur, resulting in the release of growth factors, including transforming growth factor-α (TGFα), which is a ligand for EGFR. In addition, Ras directly activates the PI3K–Akt pathway. Thus, the end result of KRAS or EGFR mutations are virtually identical, and mutations of both genes in adenocarcinomas of the lung are rarely seen. Other methods of activation of these pathways include gene amplification and mutations in BRAF, PIK3CA (a subunit of PI3K), and ERBB2 (also known as HER2). (3)

Technical advances: molecular profiling. Molecular profiling, including the profiling of genes and proteins, to guide treatment may improve the clinical outcome in patients with non–small-cell lung cancer. Progress in the identification of markers, mutations, and genomic signatures far outstrips the modest improvement in treatments that are based on these molecular advances. Formidable obstacles to developing effective markers include tumor heterogeneity, the highly complex interplay between the environment and host and the complexity, multiplicity, and redundancy of tumor-cell signaling networks involving genetic,

epigenetic, and microenvironmental effects. Emerging high-throughput techniques for assessing genomic DNA, messenger RNA (mRNA), microRNA, methylation, and protein or phosphoprotein signaling networks should help address these obstacles. For the majority of patients with advanced or metastatic non–small-cell lung cancer, the most important potential effect of molecular markers is likely to be in predicting the response to specific therapies with the goal of "personalizing" treatment. Many exciting potential predictive markers have been developed in vitro and need validation in tumor samples and clinical trials. For example, gene-expression signatures have been developed for cisplatin and pemetrexed on the basis of in vitro sensitivity; the cisplatin in vitro signature predicted the likelihood of response. Recently developed in vitro profiles predicting the sensitivity of tumors to EGFR inhibitors and other therapies have yet to be assessed clinically. MicroRNA has recently emerged as an important regulator of gene expression. High-throughput analyses have shown that microRNA expression is commonly deregulated in lung and other cancers. Using real-time RT-PCR, investigators recently identified a five-microRNA signature that is associated with treatment outcome. Loss of microRNA-128b, a putative regulator of EGFR that is located on chromosome 3p, has been shown to correlate with the response to EGFR inhibition in patients with lung cancer. Studies suggest that information about tumor-specific genetic and epigenetic changes also may be obtained from the blood of patients with lung cancer. Circulating DNA can be detected in the plasma and serum of such patients, and levels of this DNA are associated with a poor prognosis. Tumor-specific DNA alterations (such as loss of heterozygosity), promoter methylation, and *KRAS* and *EGFR* mutations have also been detected in the blood of patients with lung cancer. New techniques for capturing circulating tumor cells allow the detection of EGFR-activating mutations and the drug-resistance allele T790M. Such techniques appear to be more sensitive than those for capturing circulating DNA. Furthermore, a decline in the number of circulating tumor cells was associated with tumor response on radiography. These studies suggest that blood profiling may provide useful information about genetic changes in tumors that could ultimately help detect lung cancer and guide therapy.

Profiling of genomic and mRNA expression provides an incomplete picture of the heterogeneity of non–small-cell lung cancer. Levels of mRNA do not always correlate with protein levels and do not provide information on protein–protein interactions or post-translational modifications such as phosphorylation that may be critical for regulating protein activity. Furthermore, most targeted therapeutic agents are designed to inhibit the activity of proteins such as tyrosine kinases. Therefore, protein-based profiling is likely to be essential in understanding the complexity of protein signaling networks and developing molecular signatures that predict a response to therapy. Immunohistochemical analysis remains the most widely applied method for assessing individual proteins and may be useful for estimating prognosis and predicting the response to therapy. Emerging high-throughput proteomic techniques, such as mass spectrometry and protein microarrays, have the potential to view signal transduction networks more globally than is possible with immunohistochemical analysis. Such techniques are feasible in small amounts of tumor tissue. Proteomic signatures for prognosis and predicting the response to chemotherapy or EGFR inhibitors have been developed in tumors and cell lines. Proteomic profiling from blood is also under study, allowing repeated measurements during treatment without the need for tumor tissue. Serum mass spectrometry profiles can distinguish patients with non–small-cell lung cancer from normal controls and patients with better outcomes from those with worse outcomes after treatment with EGFR tyrosine kinase inhibitors. New techniques also permit the multiplex analysis of dozens of cytokines and angiogenic factors in small amounts of serum or plasma. This approach is being used in developing predictive markers in non–small-cell lung cancer. Although promising, blood- and tissue-based proteomic approaches remain investigational and await prospective testing and validation in large, randomized trials before they can be applied clinically. (1)
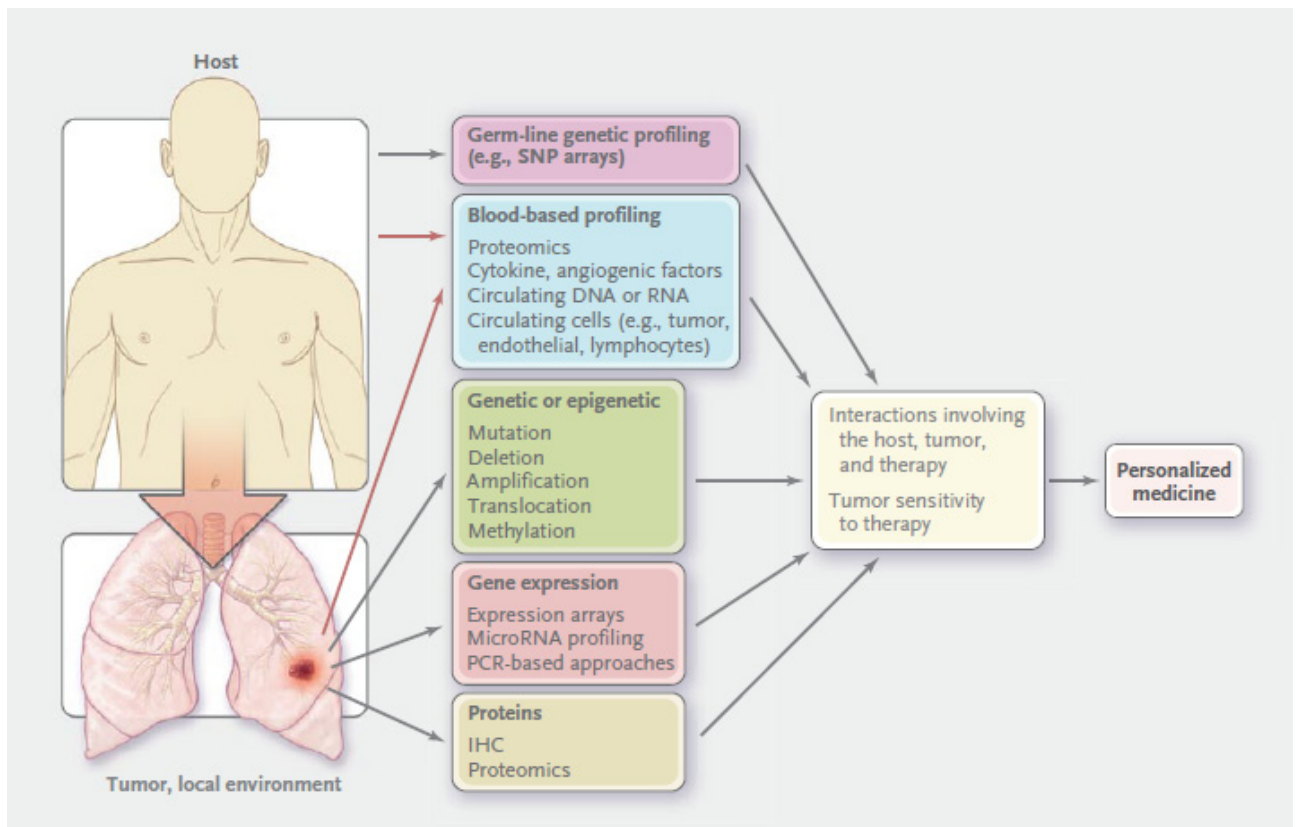
Figure 5. Development of Personalized Drugs for Lung Cancer, from Identification of Genomic Signatures to Prospective Trials of Personalized Therapy. Host profiling involves innate characteristics of the cancer patient. All markers that are involved in profiling lung cancer can apply to the tumor or its local environment. Predictive markers identify groups of patients who are likely to have increased sensitivity or resistance to a given therapy, a critical step in personalizing treatment. It has been traditional to assess individual genetic or protein prognostic or predictive markers (e.g., HER2 for breast cancer), but emerging techniques permit global analyses of the genomic, gene-expression, epigenetic, and protein profiles of the host (innate), including markers in blood and in tumor or nonmalignant lung tissue. These methods include single-nucleotide polymorphism (SNP) arrays to assess genomic alterations, bisulfite sequencing, and methylation-specific polymerase chain reaction (PCR) to assess epigenetic changes, microarrays for assessing gene expression or microRNA levels, and proteomic methods (such as mass spectroscopy, reverse-phase protein arrays, and multiplex beads) to assess intracellular signaling in tumor tissue and cytokines and angiogenic factors in blood. Blood-based profiling includes markers derived from the host (e.g., lymphocytes) and the tumor and local environment (e.g., circulating tumor cells and tumor-derived cytokines) (red arrows). IHC denotes immunohistochemical analysis. (1)

The molecular origins of lung cancer lie in complex interactions between the environment and host genetic susceptibility. Lung cancer then evolves through genetic and epigenetic changes, including deregulated signaling pathways, which are potential targets for chemoprevention and therapy. Emerging techniques for genomic, gene expression, epigenetic, and proteomic profiling could revolutionize clinical approaches across the spectrum of lung-cancer types and subtypes by identifying practical molecular markers of risk (in precancer), early detection and prognosis (in early-stage cancer), and treatment sensitivity (in early-stage and advanced stage cancer). Genomewide and other molecular

assessments are helping elucidate germ-line variations that may contribute to lung cancer risk, prognosis, and treatment sensitivity and somatic genetic alterations that occur in lung adenocarcinomas and in high-risk lung tissue associated with tumors or in smokers. (1)

APOPTOSIS

Apoptosis, or programmed cell death, is a normal component of the development and health of multicellular organisms. Cells die in response to a variety of stimuli and during apoptosis they do so in a controlled, regulated fashion. This makes apoptosis distinct from another form of cell death called necrosis in which uncontrolled cell death leads to lysis of cells, inflammatory responses and, potentially, to serious health problems. Apoptosis, by contrast, is a process in which cells play an active role in their own death (which is why apoptosis is often referred to as cell suicide). (12) Cells that undergo apoptosis are dismantled from within, in a controlled manner that minimizes damage and disruption to neighbouring cells. The resulting cellular debris is then removed, typically by professional phagocytes, and a new cell typically takes the place of the old one in a matter of hours. (13)
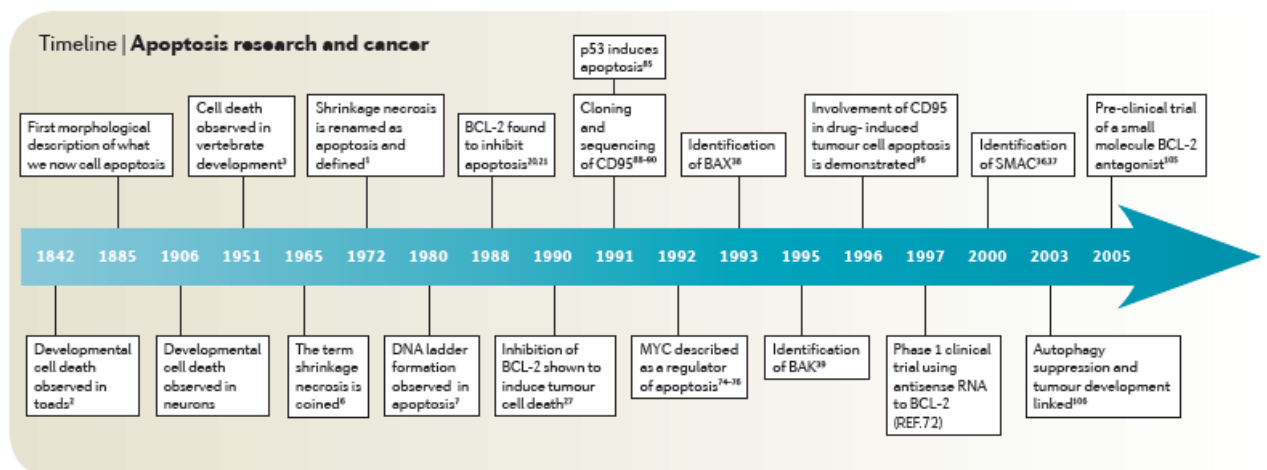
Figure 6. Timeline of the most important steps in apoptosis research. (14)

Morphological features. From the outside, it appears that cells that undergo this form of cell death initially become rounded and retract from neighbouring cells, which is reminiscent of what also happens when cells undergo mitosis. This is accompanied, or followed closely, by

a prolonged period of dynamic plasma membrane blebbing, which frequently culminates in the 'pinching off' of many of these blebs as small vesicles that have been named apoptotic bodies. Cells that undergo apoptosis are readily recognized as being different from their viable counterparts and are rapidly engulfed by phagocytes for recycling of their contents (1,2,5). This event is particularly remarkable when it is considered that phagocytes are normally engaged in the business of recognizing and removing foreign, or 'non-self', entities. However, in this instance, the dying cell becomes licensed for removal, despite having been a part of 'self' only minutes earlier. Indeed, for controlled cell elimination to operate, the minimum requirement seems to be for the chosen cell to undergo changes that attract the attentions of phagocytes. However, apoptotic cells also exhibit many other alterations to their internal architecture, which probably increase the efficiency of the disposal process and minimize activation of the immune system.

Looking inside the cell, one of the most noticeable features of apoptosis is condensation of the nucleus and its fragmentation into smaller pieces (1,2,6), a highly distinctive event that is not seen under any other circumstances. Another defining characteristic of this mode of cell death is the extensive hydrolysis of nuclear DNA into numerous fragments, often down to multiples of 200 bp8. Although more subtle, the Golgi, endoplasmic reticulum (ER) and mitochondrial networks also undergo pronounced fragmentation during apoptosis, and numerous proteins are released from the mitochondrial intermembrane space (9,10). (13)
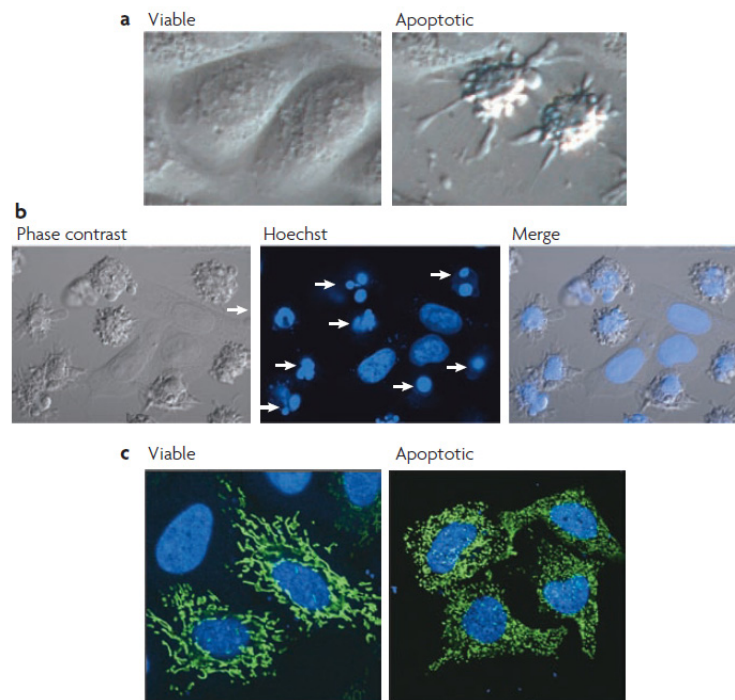
Figure 7. Morphology of apoptosis. **a** The morphology of apoptotic cells. HeLa cells were induced to die by exposure to daunorubicin (10 µM) for ~12 hours. The left panel shows cells after 2 h of exposure, when both cells in the field of view still appear healthy. By ~4.5 h (right panel), both cells display typical apoptotic morphology, with cell retraction and dynamic plasma membrane blebbing being evident. **b** Features of apoptosis-associated nuclear condensation and fragmentation. HeLa cells were induced to undergo apoptosis by treatment with actinomycin D (5 µM) followed by staining of nuclei (blue) with Hoechst dye. For comparison, a mixture of viable and apoptotic cells is shown. Apoptotic cells (arrows) exhibit extensive plasma membrane blebbing and contain nuclei that are condensed and/or fragmented into several pieces. **C** Fragmentation of mitochondrial networks. To visualize mitochondria, cells were transfected with a mitochondrially targeted green fluorescent protein construct, and then either left untreated (left panel) or treated with 5 µM actinomycin D for 12 h to induce apoptosis (right panel). Note that the mitochondrial network is extensively interconnected and appears filamentous in viable cells. By contrast, mitochondrial networks become highly fragmented in the early stages of apoptosis. (13)

Molecular features. At the molecular level, all pathways to apoptosis converge on the activation of caspases, which are cysteinyl aspartate proteases that coordinate the efficient dismantling and engulfment of doomed cells. (15) The caspases play an important role in apoptosis by activating DNases, inhibiting DNA repair enzymes and breaking down structural proteins in the nucleus.

- Inactivation of enzymes involved in DNA repair.

The enzyme poly (ADP-ribose) polymerase, or PARP, is an important DNA repair enzyme and was one of the first proteins identified as a substrate for caspases. The ability of PARP to repair DNA damage is prevented following cleavage of PARP by caspase-3.

- Breakdown of structural nuclear proteins.

Lamins are intra-nuclear proteins that maintain the shape of the nucleus and mediate interactions between chromatin and the nuclear membrane. Degradation of lamins by

caspase 6 results in the chromatin condensation and nuclear fragmentation.

- Fragmentation of DNA.

The fragmentation of DNA into nucleosomal units is caused by an enzyme known as CAD, or caspase activated DNase. Normally CAD exists as an inactive complex with ICAD (inhibitor of CAD). During apoptosis, ICAD is cleaved by caspases, such as caspase 3, to release CAD. Rapid fragmentation of the nuclear DNA follows. (12)

Two pathways of cell death can be distinguished by whether they require BCL-2 family proteins and by which caspases are crucial for their execution.

The intrinsic pathway. The intrinsic pathway — also called the BCL-2-regulated or mitochondrial pathway (in reference to the role these organelles play) — is activated by various developmental cues or cytotoxic insults, such as viral infection, DNA damage and growth-factor deprivation, and is strictly controlled by the BCL-2 family of proteins. This pathway predominantly leads to the activation of caspase-9 (Ref. 11) but, at least in certain cell types, the intrinsic pathway can proceed in the absence of caspase-9 or its activator, apoptotic protease-activating factor-1 (APAF1) (15).

Mitochondria play an important role in the regulation of cell death. They contain many pro-apoptotic proteins such as Apoptosis Inducing Factor (AIF), Smac/DIABLO and cytochrome C. These factors are released from the mitochondria following the formation of a pore in the mitochondrial membrane called the Permeability Transition pore, or PT pore. These pores are thought to form through the action of the pro-apoptotic members of the bcl-2 family of proteins, which in turn are activated by apoptotic signals such as cell stress, free radical damage or growth factor deprivation. Mitochondria also play an important role in amplifying the apoptotic signalling from the death receptors, with receptor recruited caspase 8 activating the pro-apoptotic bcl-2 protein, Bid. (12)
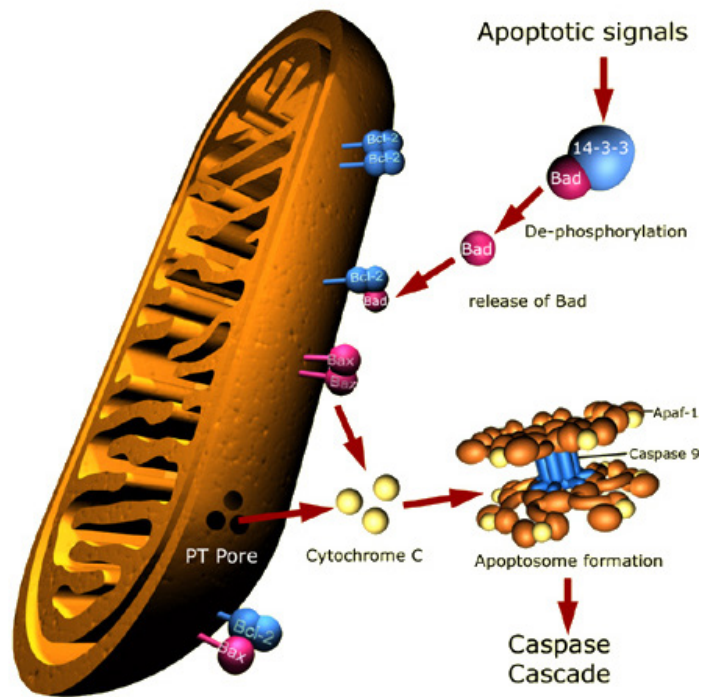
Figure 8. Illustration of the main apoptotic signalling pathways involving mitochondria (12)

The bcl-2 proteins are a family of proteins involved in the response to apoptosis. Some of these proteins (such as bcl-2, bcl-XL, blc-W) are anti-apoptotic, while others (such as Bad, Bax or Bid) are pro-apoptotic. The sensitivity of cells to apoptotic stimuli can depend on the balance of pro- and anti-apoptotic bcl-2 proteins. When there is an excess of pro-apoptotic proteins the cells are more sensitive to apoptosis, when there is an excess of anti-apoptotic proteins the cells will tend to be more resistant. An excess of pro- apoptotic bcl-2 proteins at the surface of the mitochondria is thought to be important in the formation of the PT pore. The pro-apoptotic bcl-2 proteins are often found in the cytosol where they act as sensors of cellular damage or stress. Following cellular stress they relocate to the surface of the mitochondria where the anti-apoptotic proteins are located. This interaction between pro- and anti-apoptotic proteins disrupts the normal function of the anti-apoptotic bcl-2 proteins and can lead to the formation of pores in the mitochondria and the release of cytochrome C and other pro-apoptotic molecules from the intermembrane space. This in turn leads to the formation of the apoptosome and the activation of the caspase cascade. The release of cytochrome C from the mitochondria is a particularly important event in the induction of apoptosis. Once cytochrome C has been released into the cytosol it is able to interact with a

protein called Apaf-1. This leads to the recruitment of pro-caspase 9 into a multi-protein complex with cytochrome C and Apaf-1 called the apoptosome. Formation of the apoptosome leads to activation of caspase 9 and the induction of apoptosis. (12)

The extrinsic pathway. Although there are differences in the signalling pathways activated by the different death receptors it is possible to outline a general apoptotic signalling pathway. Binding of the death inducing ligand to its receptor can lead to a the generation of ceramide, typically produced by acid sphingomyelinase. This ceramide release is thought to promote lipid raft fusion which results in a large scale clustering of the death receptors. The large scale receptor clustering is important because it helps to amplify the apoptotic signalling. In the absence of receptor clustering some cells, such as lymphocytes, are still able to trigger apoptosis but in most cases amplification of the signalling pathway is needed to activate the full apoptotic response.

The extrinsic or death-receptor pathway is triggered by ligation of so-called death receptors (members of the tumour necrosis factor (TNF) receptor family, such as Fas, TNF receptor-1 (TNFR1), TRAIL receptors DR4 and DR5), that contain an intracellular death domain, which can recruit and activate caspase-8 or -10 through the adaptor protein Fas-associated death domain (FADD; also known as MORT1) at the cell surface. This protein complex is often called the DISC, or Death Inducing Signalling Complex. This recruitment causes subsequent activation of downstream (effector) caspases such as caspase-3, -6 or -7, without any involvement of the BCL-2 family. In some cells, most notably hepatocytes, the extrinsic pathway can intersect the intrinsic pathway through caspase-8 cleavage-mediated activation of the pro-apoptotic BH3-only protein BID. The C-terminal truncated form of BID (tBID) translocates to mitochondria and promotes further caspase activation (caspase-9 and the effector caspases caspase-3, -6 and -7) through the intrinsic pathway. In these situations, loss of BID or overexpression of BCL-XL inhibits cell death. (12)
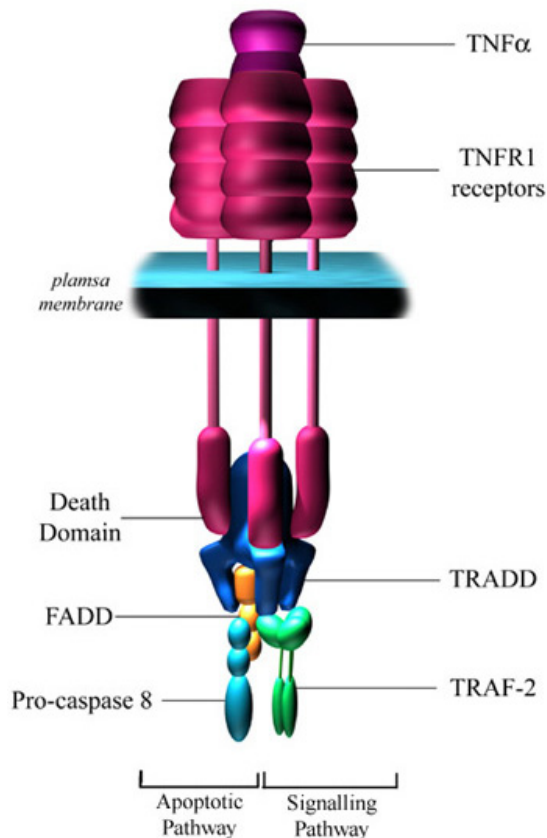
Figure 9. Illustration of the main TNF receptor signalling pathways. (12)

TNF receptor signaling. TNF is produced by T-cells and activated macrophages in response to infection. By activating its receptor, TNFR1, TNF can have several effects. In some cells it leads to activation of NF-kB and AP-1 which leads to the induction of a wide range of genes. In some cells, however, TNF can also induce apoptosis, although receptor ligation is rarely enough on its own to initiate apoptosis as is the case with Fas ligand binding. Binding of TNF alpha to TNFR1 results in receptor trimerisation and clustering of intracellular death domains. This allows binding of an intracellular adapter molecule called TRADD (TNFR-associated death domain) via interactions between death domains. TRADD has the ability to recruit a number of different proteins to the activated receptor. Recruitment of TRAF2 (TNF-associated factor 2) can lead to activation of NF-kB and the JNK pathway. TRADD can also associate with FADD, which leads to the induction of apoptosis via the recruitment and cleavage of pro-caspase 8. (12)

Signaling by Fas (CD95). The ligand for Fas (FasL or CD95L) activated apoptosis in a similar

way to the TNF receptor. Binding of the ligand promotes receptor clustering, DISC formation and the activation of the caspase cascade. However, signalling through the Fas receptor is slightly simpler than through the TNF receptor. The adapter protein FADD can be recruited directly to the death domain on the Fas receptor, without requiring the prior recruitment of TRADD. In addition the Fas receptor is generally though to only activate apoptosis and does not play an important role in other aspects of cell signalling like the TNF receptor.

Induction of apoptosis by TRAIL. In a number of ways TRAIL (TNF-related apoptosis inducing ligand) is similar in action to FasL. Binding of TRAIL to its receptors DR4 or DR5 triggers rapid apoptosis in many cells. Interestingly there are also decoy receptors that compete for binding of TRAIL with the DR4 and DR5 receptors. The decoy receptors are called DcR1 and DcR2. Both of these receptors are capable of competing with DR4 or DR5 receptors for binding to the ligand (TRAIL), however ligation of these receptors does not initiate apoptosis since DcR1 does not possess a cytoplasmic domain, while DcR2 has a truncated death domain lacking 4 out of 6 amino acids essential for recruiting adapter proteins. (12)
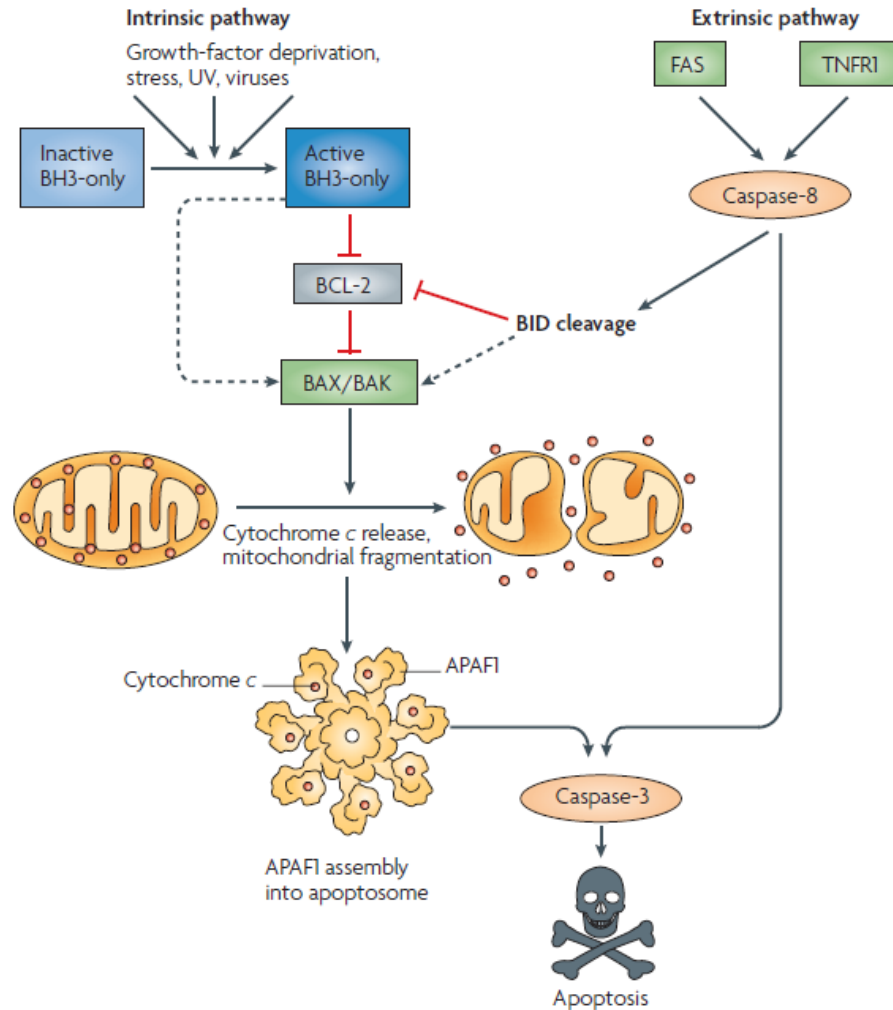
Figure 10. Scheme depicting intrinsic and extrinsic pathways of apoptosis. Apoptosis can be induced by cell surface receptors, such as Fas and tumour necrosis factor receptor-1 (TNFR1) (extrinsic pathway, right), or by various genotoxic agents, metabolic insults or transcriptional cues (intrinsic pathway, left). The intrinsic pathway starts with BH3-only protein induction or post-translational activation, which results in the inactivation of some BCL-2 family members. This relieves inhibition of BAX and BAK activation, which in turn promotes apoptosis. Some BH3-only proteins, such as BIM and PUMA, may also be able to activate BAX and/or BAK (as shown by the dotted line). Once activated, BAX and BAK promote cytochrome *c* release and mitochondrial fission, which leads to the activation of APAF1 into an apoptosome and activates caspase-9 to activate caspase-3. Caspases in turn cleave a series of substrates, activate DNases and orchestrate the demolition of the cell. The extrinsic pathway can bypass the mitochondrial step and activate caspase-8 directly, which leads to caspase-3 activation and cell demolition. The BCL-2 family regulates the intrinsic pathway and can modulate the extrinsic pathway when cleavage of BID communicates between the two pathways. (15)

Apoptosis in health and disease. Apoptosis occurs during the normal development of multicellular organisms and continues throughout adult life. The combination of apoptosis and cell proliferation is responsible for shaping tissues and organs in developing embryos. For example the apoptosis of cells located in-between the toes allows for their separation. Apoptosis is also an important part of the regulation of the immune system. T lymphocytes are cells of the immune system that are responsible for destroying infected or damaged cells in the body. They mature in the thymus, but before they can enter the bloodstream they are

tested to ensure that they are effective against foreign antigens and are also not reactive against normal, healthy cells. Any ineffective or self-reactive T-cells are removed through the induction of apoptosis.

Problems with the regulation of apoptosis have been implicated in a number of diseases. Cancer is a disease that is often characterized by too little apoptosis. Cancer cells typically possess a number of mutations that have allowed them to ignore normal cellular signals regulating their growth and become more proliferative than normal. Under normal circumstances damaged cells will undergo apoptosis, but in the case of cancer cells mutations may have occurred that prevent cells from undergoing apoptosis. In these cases there is no check on the cellular proliferation and consequently the disease can progress to the formation of tumors. In many cases these tumors can be difficult to kill as many cancer treatments rely on damaging the cells with radiation or chemicals and mutations in the apoptotic pathway often produce cells that are resistant to this type of attack. Understanding how apoptosis is regulated in cancer is therefore of major interest in the development of treatments for this disease. (12)

Many mechanisms are involved in resistance to induced apoptosis in cancer. Indeed some tumor suppressor genes can be altered or oncogenes expression can be upregulated. *p53* was the first tumor suppressor gene linked to apoptosis. *p53* mutations occur in the majority of human tumors and are often associated with advanced tumor stage and poor patient prognosis. In addition, several signal transduction pathways promote cell survival in response to growth and/or survival factors are upregulated in many tumors. One critical pathway involves signaling through PI-3 kinase, which can be activated by Ras and is downregulated by the PTEN tumor suppressor. Ras activation and PTEN loss are common in human tumors.

The cloning and characterization of the *bcl-2* oncogene established the importance of apoptosis in tumor development. *bcl-2* was first identified at the chromosomal breakpoint of t(14;18) in a human leukemia line and was later shown to be a common event in follicular lymphoma. At this time, oncogenes were classified as either `transforming' or `immortalizing'

oncogenes based on their properties in rodent cell transformation assays. However, *bcl-2* did not behave like a typical oncogene: instead of disrupting normal proliferation controls, Bcl-2 promoted cell survival by blocking programmed cell death. In addition to Bcl-2, Bcl-x$_L$ is a potent death suppressor that is upregulated in some tumor types. Conversely, Bax is a death promoter that is inactivated in certain types of colon cancer and in hematopoietic malignancies. (16) Moreover, overexpression of molecules such as cFLIP or PED/PEA15 in many human cancer can confer resistance to apoptosis induced by TNF, FasL or TRAIL.

If cancer is a disease where too little apoptosis occurs there are other diseases where too much apoptosis is thought to be part of the problem. For example in neurodegenerative diseases such as Parkinson's or Alzheimer's Diseases apoptosis is thought to account for much of the cell death and the progressive loss of neurons.

Apoptosis is also important for normal placental development. During pregnancy trophoblast cells from the placenta invade the uterine environment in order to remodel the maternal blood vessels and help establish and maintain a successful pregnancy. Strict control over cell proliferation and apoptosis is required to achieve this. In some cases this process can be compromised and excessive apoptosis of the trophoblast cells is thought to be implicated in the failure to fully remodel the maternal environment that is observed in complications of pregnancy such as preeclampsia.

Apoptosis is also thought to play a role in the progression of many auto-immune diseases. For example, in the case of rheumatoid arthritis excessive proliferation of synovial cells is thought to be due in part to the resistance of these cells to apoptotic stimuli. In other cases poor regulation of apoptosis in T-lymphocytes can result in auto-reactive T-cells entering the circulation and contributing to the onset of autoimmune diseases. (12)

MIGRATION

Cell migration is an essential process during, for instance, development and wound healing. Aberrations in signaling pathways involved in the regulation of cell migration, cell-cell and

cell-matrix interactions contribute to tumour invasion and metastasis. The regulation of cytoskeletal changes associated with migratory behaviour of cells has recently become focused on the family of small Rho-like GTPases. Cdc42,

Rac1 and RhoA regulate signal transduction pathways that mediate distinct cytoskeletal rearrangements required for cellular motility. Besides these direct effects on the cytoskeleton, Rho-like proteins are involved in transcriptional activation, endo and exocytotic pathways, cell-cycle progression, oncogenic transformation and metastasis formation.

Similar to Ras proteins, Rho-like GTPases function as molecular switches by cycling between an active GTP-bound state and an inactive GDP-bound state. The function of this switch is the regulated transmission of a signal perceived upon receptor stimulation of the cell to a downstream signaling pathway. This is achieved by the selective binding of the active GTPase to a downstream effector protein. Guanine nucleotide exchange factors (GEFs) stimulate the exchange of bound GDP for GTP leading to activation of the GTPases and binding of downstream effectors, thereby leading to transmission of the signal. GTPase-activating proteins (GAPs) promote inactivation of the GTPases by stimulating the intrinsic GTP-hydrolysis rate of Rho-like proteins. Guanine nucleotide dissociation inhibitors (GDIs) can block the exchange of GDP for GTP as well as the hydrolysis of GTP, as has been shown for Rho GDI. GEFs are characterized by the catalytic Dbl-homology (DH) domain, which is C-terminally flanked by a Pleckstrin-homology (PH) domain. PH domains have been implicated in binding to specific phosphoinositol lipids, as well as to proteins. In addition to the DH-PH combination, many GEFs contain other domains (e.g. SH2-, SH3-, PDZ domains) that are commonly found in signalling molecules, allowing them to assemble in multi-molecular signaling complexes. (17)
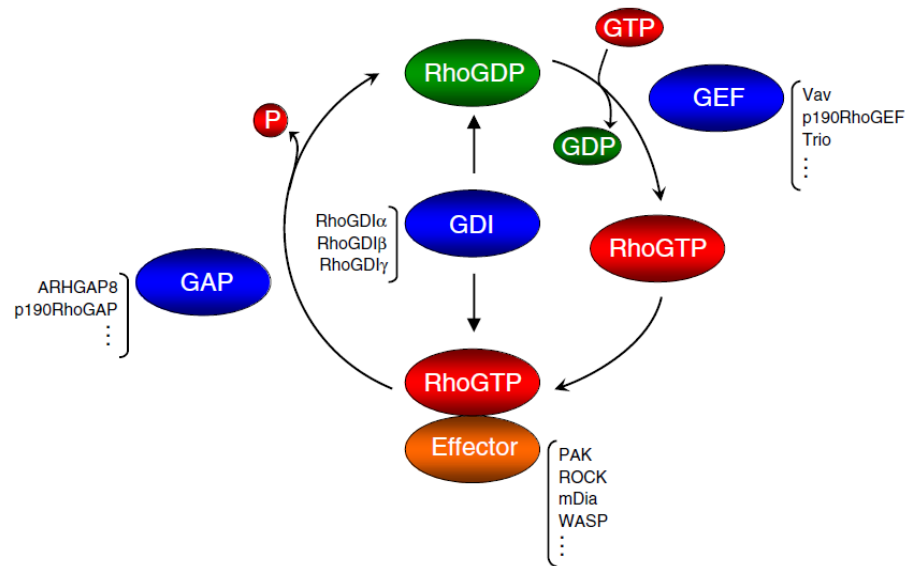
Figure 11. Basic Rho GTPase activation cycle. The loading of the Rho GTPases with GTP and subsequent activation is catalyzed by GEFs. In their GTP form they bind to different effectors to perform their functions. GAP proteins promotes the hydrolysis of GTP to inactivate the protein. RhoGDI proteins constitute an additional step of regulation by sequestering the protein in the cytoplasm impairing its function. Some examples of GEFs, GAPs and effectors are depicted. (18)

Formation of intercellular contacts depends on the activity of Rho-like proteins. Recently, family members of the Rho-like GTPases have been recognized to be required for the maintenance of the cytoskeletal organization of fully differentiated epithelia. In human keratinocytes and Madin-Darby canine kidney cells (MDCK), dominant-negative N17Rac as well as C3 transferase, which inactivates RhoA by ADP-ribosylation on Asn41, have been found to perturb the organization of actin filaments at sites of cell-cell adhesion. Inactivation of Rac or Rho results in dislocation of E-cadherin and its complex members from the adherens junctions. The efficiency of dominant-negative mutants of Rho-like GTPases in perturbing the architecture of adherens junctions varies with respect to the maturation state of cell-cell contacts and to the cell type. Rho-like GTPases play a role in the structural integrity of adherens junctions. Inhibition of endogenous Rac and Rho function affects the architecture of adherens junctions and their marker protein E-cadherin, but has no effect on desmosome morphology (desmoplakin) in keratinocytes. Functional activity of the Rac and Rho protein is thus required for the integrity of both tight junctions and adherens junctions. Rac-dependent actin polymerization in lamellipodia and membrane ruffles has been shown to require PI3-kinase. Tiam1-mediated activation of Rac and the induction of cell-cell

adhesion in transformed MDCK cells is also dependent on PI3-kinase activity, suggesting that similar regulatory mechanisms participate in actin polymerization at cell-cell contacts and in the formation of lamellipodia required for cell migration. (17)

Rho GTPases in cancer progression. Rho GTPases have been reported to contribute to most steps of cancer initiation and progression including the acquisition of unlimited proliferation potential, survival and evasion from apoptosis, tissue invasion and the establishment of metastases. Primary tumours generally arise as a consequence of multiple mutations and epigenetic changes affecting key genes that ultimately affect proliferation and survival. Activating mutations in the three Ras isoforms, Ki-Ras, N-Ras and Ha-Ras, are found in 15% of all human tumours. In contrast, Rho proteins are only rarely mutated in tumours, whereas their expression and/or activity are frequently altered. For example, several Rho GTPases are upregulated in some human tumours, including RhoA, RhoC, Rac1, Rac2, Rac3, Cdc42, Wrch2/RhoV and Rho. Uncontrolled proliferation, coupled to increased survival signals that permit tumour cells to escape from apoptosis, result in tumour growth. Some Rho GTPases stimulate cell cycle progression and regulate gene transcription, and this could in part explain their pro-oncogenic properties, for example in promoting Ras-induced transformation. The induction of tumour vascularisation is essential for tumours to grow beyond a certain size and malignant cells release factors that promote angiogenesis from nearby pre-existing blood vessels. Some Rho GTPases are thought to be able to regulate the release of pro-angiogenic factors to promote neovascularisation. Invasion of epithelial cancers is initiated when the integrity of the epithelium is disrupted and malignant cells disrupt the basement membrane and enter the underlying stroma. This normally implies loosening of epithelial cell–cell contacts and acquisition of a more motile phenotype in a process frequently referred as epithelial to mesenchymal transition (EMT). Invasive epithelial cancer cells often have reduced expression of the cell–cell adhesion protein E-cadherin and start expressing markers of mesenchymal origin such as vimentin and N-cadherin. Non-epithelial cancers also invade solid tissues. Degradation of the ECM by matrix

metalloproteases (MMPs) is essential for this kind of collective migration. To establish metastases in distant tissues, tumour cells have to enter the vascular or lymphatic system, then exit it and proliferate in the new tissue. The ability of Rho GTPase family members to regulate cytoskeletal dynamics, cell adhesion and cell migration points to a central role in cancer cell invasion and metastasis. (18)

Rho subfamily. The Rho subfamily consists of the highly conserved RhoA, RhoB and RhoC proteins. RhoA and RhoC expression and/or activity is frequently increased in human tumours, whereas RhoB is often downregulated. RhoA has been implicated in virtually all stages of cancer progression. RhoA might play a role during tumour cell proliferation and survival: for example, in vitro, constitutively active RhoA can stimulate transformation. In normal epithelia, RhoA contributes to the generation of epithelial polarity and junction assembly and function but also affects epithelial disruption during tumour progression. Rho activity can be inhibited downstream of cadherins leading to a more motile phenotype. Rho GTPases can also regulate the production of MMPs, affecting matrix remodelling and tumour cell invasion.

Increased RhoC expression has been claimed as the possible cause for the induction in invasion and metastasis and it can induce the production of angiogenic factors in breast cancer, and this could help promote entry into blood vessels and thereby metastasis. More extensive work is needed to elucidate the possible contribution of Rho GTPases to the extravasation of cancer cells. Unlike RhoA and RhoC, RhoB is often downregulated in human tumours and its expression inversely correlates with tumour aggressiveness. It has been proposed that RhoB can work as a tumour suppressor as it is activated in response to several stress stimuli including DNA damage or hypoxia, and it has been reported to inhibit tumour growth, cell migration and invasion and have proapoptotic functions in cells. (18)

Cdc42 subfamily. Cdc42 and the closely related RhoQ/TC10 and RhoJ/TCL form a distinct subfamily of Rho GTPases. Cdc42 expression is upregulated in some breast cancers, yet liver-specific knock-out indicates that loss of Cdc42 enhances liver cancer development,

suggesting that the contribution of Cdc42 to cancer progression may be tissue-specific. This could reflect the multiple roles of Cdc42 in regulating cell polarity as well as cell cycle progression. Both Cdc42 and RhoQ/TC10 stimulate transformation and contribute to Ras-induced transformation in vitro, and for Cdc42 this has been suggested to be due to its effect on receptor trafficking and degradation. RhoQ/TC10 is also implicated in receptor trafficking, particularly of the glucose transporter, but whether this accounts for its role in transformation is not known. Another mechanism whereby Cdc42 could affect cell cycle progression is by regulating chromosome segregation during mitosis: only Cdc42 knockdown out of all Rho GTPases was found to induce chromosome misalignment during cell division, leading to multinucleate cells. RhoJ/TCL and RhoQ/TC10 enhance this effect when suppressed in conjunction with Cdc42, pointing towards a possible redundancy in function of Cdc42 family proteins during spindle formation and cell division. Cdc42 is involved in the establishment of normal epithelial polarity as well as migratory polarity via its interaction with the Par3/Par6/aPKC polarity complex, which in turn regulates Rac via Tiam1. Cdc42 is thus predicted to inhibit invasion by promoting epithelial polarity, yet conversely also stimulate migration. Indeed, it contributes to cancer cell invasion in single cells in vitro with a mesenchymal morphology although probably not with an amoeboid morphology. It is also important for collective cancer cell invasion, where it acts through its target MRCK to stimulate actomyosin contractility. However, whether the Par3/Par6/aPKC complex is also involved in these processes is not yet known. (18)

Rac subfamily. The Rac subfamily of Rho GTPases comprises Rac1, Rac2, Rac3 and RhoG. Rac1 is over-expressed in various tumours and accumulating evidence indicates that Rac1-dependent cell signalling is important for malignant transformation. Rac1 is one of the few Rho GTPases mutated in some tumours, with mutations mainly affecting the effector domain that interacts with downstream targets. It was proposed that these mutations could increase the activity of the protein and the survival of the tumours. A splice variant of Rac1, Rac1b, has an extra intron close to the GTP-binding region. It was initially identified to be upregulated in colon cancers. It does not bind RhoGDI and thus is present predominantly in

the GTP-bound state. Although Rac1b is defective in activating several Rac1-regulated signalling pathways, in some cell types it stimulates cell survival and cell cycle progression through NFjB, and is less susceptible to ubiquitination and degradation, which could explain its increased expression in cancers. So far little is known about the role of Rac proteins in cancer progression in vivo. Rac1 knock-out in mice is embryonic lethal but conditional knock-out mice have been studied extensively. In a conditional lung cancer mouse model Rac1 function was required for K-Ras-driven proliferation and tumorigenicity. Rac1 could contribute to cancer cell proliferation via regulation of the cell cycle: for example, it stimulates expression of cyclin D1, and induces cell transformation in vitro. It is likely to inhibit cancer invasion through its ability to enhance epithelial cell-cell adhesion. However, active Rac can mediate the loss of adherens junction in some situations, promoting a more migratory phenotype, and thus Rac could promote or inhibit tumour cell invasion depending on the cell background. Rac is necessary for the generation of lamellipodial protrusions during mesenchymal migration, as well as for the amoeboid migration of Ras-transformed cells. Rac1 can also contribute to cancer cell invasion by regulating the production of MMPs and their natural inhibitors, the Tissue-specific inhibitors of MMP (TIMPs). Like Rac1, Rac2 and Rac3 are over-expressed in some tumours. Rac3 is hyperactive and/or deregulated in breast cancers. The contribution of different Rac isoforms to migration is likely to depend on the cell type and their relative expression levels. Rac2 is required for neutrophil migration but whether it acts similarly in tumours is not known. In contrast, Rac1 and Rac2 are dispensable for cell migration in macrophages, although Rac1 is required for invasion. Studies of Rac3-null mice indicate that Rac3 but not Rac1 or Rac2 specifically contributes to the development of Brc-Abl-induced lymphomas in vivo. However, in fibroblasts, Rac1 but not Rac3 suppression by RNAi affects lamellipodium formation although cell invasion is reduced in both cases. It is not yet clear how these results can be translated to cancer cell invasion in vivo. Little is known about the role of RhoG in cancer, although it induces actin reorganization and cell migration via Rac in vitro, and thus it will be interesting to determine its role in cancer cell invasion. (18)

Regulation of cell motility by Rho-like GTPases: implications for invasion. Migrating cells extend lamellipodia and filopodia at the leading edge—structures which are regulated by Rac and Cdc42. Indeed, numerous studies have demonstrated that Rho-like proteins are important in cell migration. Since migration is a component of the invasive phenotype, it is perhaps not surprising that disruption of function of Rho-like GTPases also influences invasiveness *in vitro*. Increased Rac activity due to expression of the Rac exchange factor, Tiam1, or expression of constitutively active Rac, promotes migration and invasion of T-lymphoma cells. However, expression of Tiam1 or active Rac actually inhibits the migration and invasion of epithelial cells. This is due to the ability of Rac to promote cadherin-mediated cell–cell adhesion, emphasizing the importance of the balance between cell–cell forces and migratory forces in determining the cellular response. In macrophages, migration is inhibited by both active and dominant negative mutants of Rac and Rho, suggesting that the right level of activity of Rho-like GTPases is critical. How Rac is involved in migration is not clear. One target of Rac is PIP 5-kinase, a phospholipid kinase which converts PIP to PIP2. PIP2 induces the uncapping of actin filaments, leading to increased polymerisation. Increased actin polymerization in the advancing lamellipodia may be causal in promoting migration and invasion. Another target of Rac (and also Cdc42) is the serine/threonine kinase Pak (p21 activated kinase). Active and inhibitory mutants of Pak can both stimulate and inhibit cell migration depending on the cell type and experimental conditions. The effects of Pak on motility and invasion may be due to effects on myosin-II light chain and/or heavy chain phosphorylation, which is enhanced by Pak. A model is emerging which suggests that Pak influences migration by promoting focal adhesion turnover, combined with stress fiber formation and contraction of the trailing edge. (19)

Cell–matrix interactions and Rho-like GTPases. Integrin-mediated adhesion to the extracellular matrix plays an important role in the organization of tissues and the behaviour of individual cells. Transformed cells show changes in the profile of integrin expression that correlate with increased invasiveness. Increased invasiveness may be due to the effects of

changes in cell adhesion on cell motility. However, in addition to mediating adhesion, integrin engagement also modulates a number of intracellular signalling pathways that may also contribute to the invasive properties of cells. Rho-like GTPases have been implicated both as regulators of integrin-mediated cell adhesion and as downstream effectors of integrin signalling; they thus have the potential to regulate tumour invasion. One intermediate between integrin engagement and activation of Rho-like GTPases is phosphoinositide 3-kinase (PI3K). PI3K is activated following integrin-mediated adhesion and its products promote activation of certain Rho-family exchange factors. Consistent

with these observations, integrin-mediated PI3K activation also promotes carcinoma invasion. Rho, Rac and Cdc42 can influence cell adhesion by driving the formation of integrin-containing focal complexes. These complexes also contain numerous signalling molecules including focal adhesion kinase (FAK) and paxillin and are therefore sites for intracellular signalling. The transient formation of these adhesion complexes combined with remodelling of the cytoskeleton may allow Rho-like GTPases to coordinate cell motility.

Adhesion to the extracellular matrix can also regulate the activity of Rho like GTPases. Adhesion to fibronectin induces Cdc42 and Rac activation, whereas adhesion to laminin induces the activation of Rho. Adhesion also regulates the targetting of growth factor-activated Rac to the plasma membrane and thus mediates the coupling of Rac with its downstream effectors. Indeed, a number of related proteins have been identified recently that form a complex with paxillin and Pak and may serve to target Rac to focal adhesions. The composition of the extracellular matrix and thus activation of specific integrins appears to determine the activation of Rho-like GTPases. Specific integrin signals also determine the phenotypic responses to Tiam1–Rac signalling. Thus, Tiam1-induced Rac activation induces the migration of Ras-transformed MDCK cells plated on collagen, but restores a polarized epithelial phenotype on fibronectin or laminin. Interestingly, expression of β1 integrins actively disrupts adherens junctions in β1-deficient epithelial cells and promotes migration, whereas α5 integrins promote cadherin-mediated adhesion in myoblasts, leading to a

suppression of migration. Specific integrin signals may therefore regulate the localisation of Rho-protein signalling complexes (e.g. Tiam1–Rac) to sites of cell–cell or cell–matrix interaction and thus promote either intracellular adhesion or migration, respectively. (19)
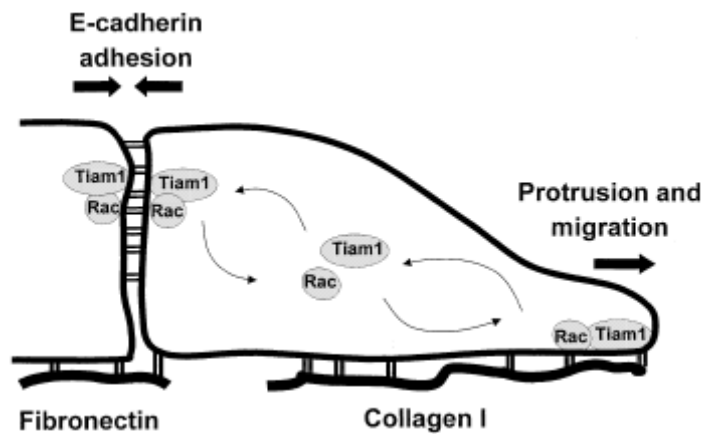

Figure 12. Rho-like proteins can influence both cell–cell adhesion and cell migration. Whether cells acquire an epithelial phenotype or an invasive mesenchymal-like phenotype depends on the balance between E cadherin mediated cell–cell contacts and pro-migratory forces. Tiam1/Rac signaling can promote either cell–cell adhesion or migration depending on the composition of the extracellular matrix, suggesting that integrin-mediated signalling may determine the localisation of Rho-protein signalling complexes, such as Tiam1/Rac. (19)

Cell–cell adhesion forces modulate invasiveness. The integrity of epithelial monolayers is maintained by adherens junctions, which link the actin cytoskeletons of adjacent cells. Disruption of these junctions leads to the loss of cell–cell contacts and allows cell motility and invasion. Adherens junctions are specialised structures in the plasma membrane where E-cadherin molecules from adjacent cells form homotypic associations. Cadherin–cadherin interactions are stabilised by the associated catenins (α-catenin, β-catenin and γ-catenin/plakoglobin), which link the cadherin molecules to the actin cytoskeleton. Indeed, adherens junctions are suppressed by mutations in the catenins, demonstrating the importance of this linkage with the actin cytoskeleton. In additionto stabilising existing adherens junctions, the actin cytoskeleton may play an active role in the formation of new cadherin-mediated cell–cell contacts by promoting the appositioning of adjacent cell membranes, allowing homotypic cadherin interactions to take place. Rho, Rac and Cdc42 have all been reported to influence the integrity of adherens junctions—effects which are probably due to both modulation of adherens junction components and of the actin cytoskeleton. Rac (and Cdc42) may also modulate the stability of the adherens junction. (19)

The microtubule cytoskeleton and polarity. Although the effects of Rho GTPases on the actin cytoskeleton have received most attention to date, it is now clear that they can also modulate the microtubule cytoskeleton. While it is unlikely that the microtubule cytoskeleton plays an essential role during cell migration or chemotaxis over short distances, efficient and persistent long range migration requires stabilization of cell polarity and this is achieved through reorganization of the microtubule cytoskeleton. The first clue for a link between Rho GTPases and microtubules was the observation that nocodazole (an inhibitor that disrupts microtubules) activates Rho, but when washed out of cells it leads to Rac activation. Later, Rho was shown to promote the stabilization of microtubules through its target mDia that directly interacts with microtubules and promotes their capping. Rac, on the other hand, may promote microtubule elongation through p65PAKdependent phosphorylation and inactivation of the microtubule destabilizing protein, stathmin. The polarized migration of many cells is reflected in the reorganization of the microtubule cytoskeleton and the centrosome, which usually (though not always) face the direction of migration. This facilitates cell migration by directing transport pathways to the leading edge and is particularly important to achieve efficient and persistent migration over longer distances. Efficient cell migration requires integrin-dependent matrix adhesion to generate traction forces at the front and in the cell body, but integrin adhesion complexes must be dynamic and disassembled at the cell rear to allow the cell to pass. Members of the WASp/SCAR/WAVE family of scaffold proteins are key regulators of actin polymerization. In their activated state, each of these proteins is able to stimulate the Arp2/3 complex, which can initiate actin polymerization either de novo or at the barbed end or sides of preexisting filaments. In this way, the dendritic morphology of lamellipodial actin is generated. WASp/WAVE can also bind to profilin, which acts synergistically with Arp2/3 to speedup actin polymerization. Cdc42 activates WASp and N-WASp directly, although the lipid PI(4,5)P2 is an essential cofactor. Rac activates the Scar/WAVE family indirectly and this involves an Nck-adaptor complex. (20)
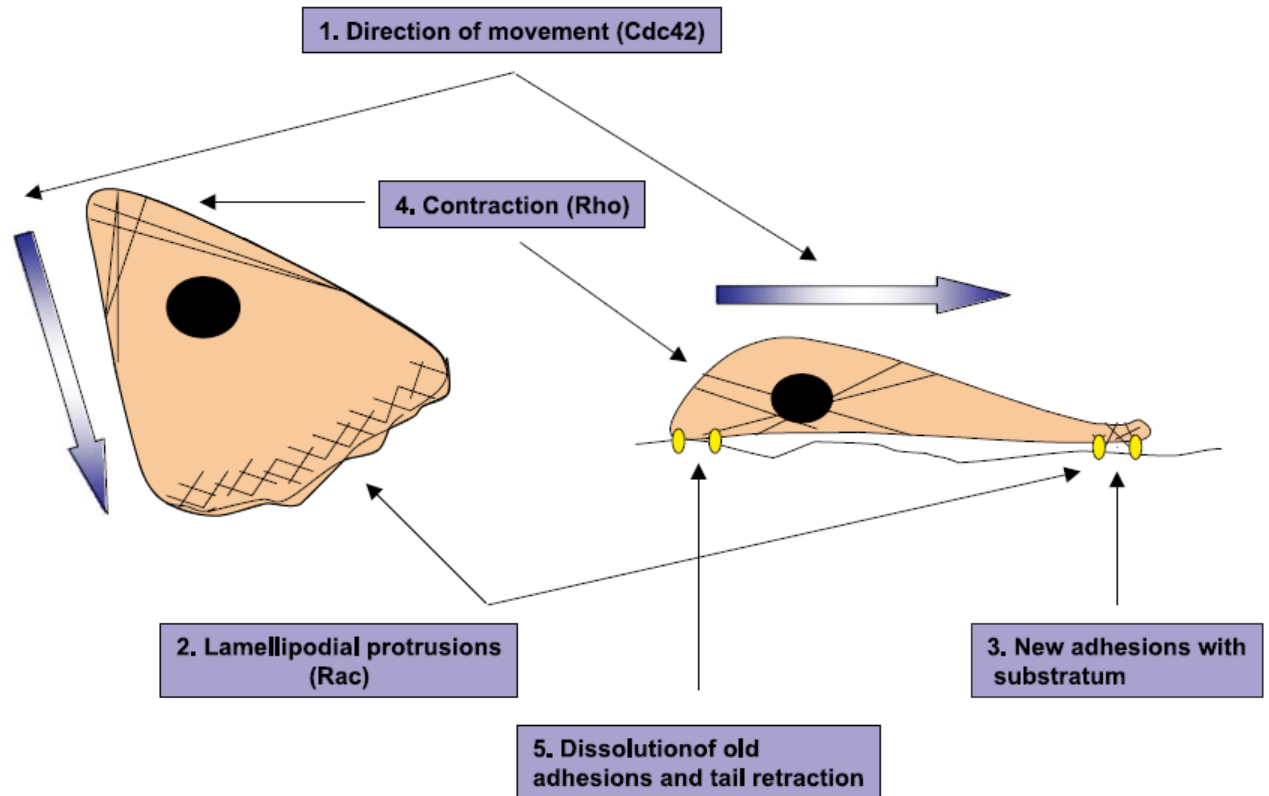
Figure 13. A migrating cell (seen from the top and side). A migrating cell needs to perform a coordinated series of steps to move. Cdc42 regulates the direction of migration, Rac induces membrane protrusion at the front of the cell through stimulation of actin polymerization and integrin adhesion complexes, and Rho promotes actin:myosin contraction in the cell body and at the rear. (20)

MAPK and cellular migration structures. The mitogen-activated protein kinase (MAPK) pathways that activate ERK, JNK and p38 kinases play important roles in modifying the morphogenetic and motile responses of cells. These pathways receive inputs from both soluble growth factors and extracellular matrix proteins to regulate the localization, amplitude and duration of MAPK signaling, and hence the spectrum of targets phosphorylated. Emerging data implicate MAP kinase signaling in the control of F-actin and focal adhesion formation and turnover required for cell morphogenesis and migration. Binding of growth factors to cognate receptor tyrosine kinases at the plasma membrane promotes activation of Ras. Ras recruits Raf family kinases to the membrane where they are activated by incompletely understood mechanisms including phosphorylation/dephosphorylation and lipid binding. Active Raf phosphorylates and activates the dual specificity tyrosine and threonine kinases MEK1&2, which are upstream kinases for ERK1&2. Activated ERK can be

translocated to the nucleus to regulate transcription or retained/routed within the cytoplasm to regulate diverse activities including cell motility, organelle structure, integrin signaling and cytoskeletal dynamics.

ERK is also implicated in the co-ordinate control of Rho and Rac activities in fibroblast models of transformation and human tumor cells. However, the precise mechanisms and targets through which ERK signals, and their spatiotemporal control, are not well understood. In these situations, ERK signaling does not acutely influence Rho function, but rather sustained ERK signaling selects for down-regulation of Rho or

Rho effector function.

The presence of activated MEK and ERK on cytoskeletal structures and their association with focal adhesions and microtubules is consistent with the hypothesis that localized MAPK signaling modulates Rho signaling. Indeed, considerable evidence indicates that the integration of Rho family GTPase and ERK signaling is important in the control of cell morphogenesis. Integrin activation of MAPK requires c-Src and FAK, and ERK activity is required for FAK stimulated focal adhesion disassembly to promote cell migration. Several studies have shown that FAK or v-Src can suppress the activities of Rho and its effector, ROCK, and this pathway requires ERK signaling to modulate actin and focal adhesion dynamics. (21)

PED/PEA15

PED, (phosphoprotein enriched in diabetes), also known as PEA15, (phosphoprotein enriched in astrocytes), is 15 kDa adaptor protein involved in many cellular pathways, among which are apoptosis, autophagy, survival, proliferation and migration (22-24). It was first identified as a phosphoprotein highly expressed in astrocytes and then found overexpressed in type II diabetic patients. PEA-15 exists in vivo as three isoforms, namely N, Pa and Pb, which correspond to the unphosphorylated, mono and diphosphate forms, respectively. Phosphorylation occurs on two seryl residues. The first one, Ser104, is located within the motif LTRIPSAKK, is a PKC target. The second site, Ser116, is included in the motif

DIRQPSEEEIIK, and is the target of the CaMKII and AKT. Membrane-permeant phosphatase antagonists were therefore used to determine the PEA-15 dephosphorylation pathway: okadaic acid (OK) that inhibits phosphatase 2A (PP2A) and, with a lesser efficacy, phosphatase 1 (PP1), Calyculin A (CalA) which is equipotent to inhibit PP1 and PP2A, and Tautomycin (Tau) that preferentially inhibits PP1. PEA-15 phosphorylation was rapidly enhanced following treatment of the striatal astrocytes with OKand CalA whereas Tau was poorly effective. These results suggest that PP2A is essentially involved in PEA-15 dephosphorylation. (23)

The ped gene and its transcriptional regulation. Two forms of mouse PED cDNA that differ in the length of the 3'UTR have been cloned. These likely represent transcripts generated by alternative polyadenylation. Northern blots indicate that expression of PED is predominant in the CNS. However, ped transcripts are also detected in several peripheral organs. This suggests additional functions for PED required in multiple cells and tissues, beside its specific role in astrocytes. The ped gene has now been cloned in several mammals and found to be highly conserved. Furthermore, computer analysis of the drosophila genome did not reveal any sequence related to ped. Thus, it might be possible that ped only appeared with mammals. The genomic sequence of pea15 is composed of four exons and spans approximately 10.2 kb of genomic DNA flanked upstream by a potentially expressed Alu element and downstream by the H326 gene. The human ped gene was mapped to 1q21–q22, between the markers D1S2635 and D1S484. A few diseases were mapped to this region, including type II diabetes in Pima Indians, autosomal dominant non-syndromic hearing impairement locus, DNFA7, hyperparathyroidism-jaw syndrom, familial hemiplegic migrane, MHP2, a non-Hodgkin lymphoma and the loop–tail mutation in mouse. A detailed gene scan didn't found any evidence for a ped mutation in type II diabetes or loop–tail mutation. In addition to the remarkable conservation of the PED protein sequence, three highly conserved regions are found within the 3'UTR of its cDNAs, each greater than 100 nucleotides in length. 3'UTRs are known to contain regulatory sequences that signal mRNA

localization, translational regulation and direct degradation. Conserved sequences found in mouse and human PED cDNA 3'UTR are good candidates for such roles. Indeed, several infrequent regulatory motifs were found in these regions, including JCV repeats. The human JC polyomavirus (JCV) is the etiologic agent of the neurodegenerative disease progressive multiple leukoencephalopathy, and replicates only in astrocytes. In good agreement with an important function of PED 3'UTR, is the presence within this region of the protooncogene MAT1. Indeed, it was demonstrated that MAT1 cDNA is a partial sequence of the PED 2.4 kb mRNA does not encode a protein. TheMAT1 sequence was isolated from a mouse mammary tumor induced in vitro with N-methyl-N-nitrosourea and lithium, and was reported to induce the oncogenic transformation of NIH- 3T3 cells. Accordingly, increased expression of PED transcripts was reported in numerous tumors, including gliomas, the main primary tumors of the brain. (23)

The molecular mechanisms that regulate PED expression in human cancer are still unclear. Recent studies revealed that PED expression can be regulated by several transcription factors. Hepatocyte nuclear factor 4 alpha (HNF-4α), which is involved in induction of apoptosis in pancreatic INS-1 beta-cell line, negatively regulates PED expression (25), while its expression is upregulated by Chicken Ovalbumin Upstream Promoter-Transcription Factor II (COUP-TFII) (25), by vitamin D receptor (VDR) upon vitamin D_3 treatment (26) and by IL-4 (interleukin-4) (27). More recently we demonstrated that PED levels may be regulated by microRNAs (Incoronato et al., personal communication, Cancer Research, submitted).

PED role in apoptosis. Membrane receptor-induced apoptosis results from an orderly cascade of cellular events. Upon binding to their respective ligands, Fas and TNFR1 receptors, FasL or TNF initiate apoptosis by recruiting the cytosolic adaptor molecule FADD to the plasma membrane to form a multiprotein complex named death inducing signaling complex (DISC). The N-terminal part of FADD contains a DED that binds to homologous domains located in the N-terminal part of caspase-8 allowing the activation of the caspase. Mutants of FADD lacking DED, or mutants of caspase-8 with only its DEDs can act as

43

dominant-negative inhibitors suggesting that endogenous inhibitors of the early steps of apoptosis could exist. (23) PED is member of Death Effector Domain (DED) containing protein family. These domains were described to regulate cell death through protein-protein interaction (24).
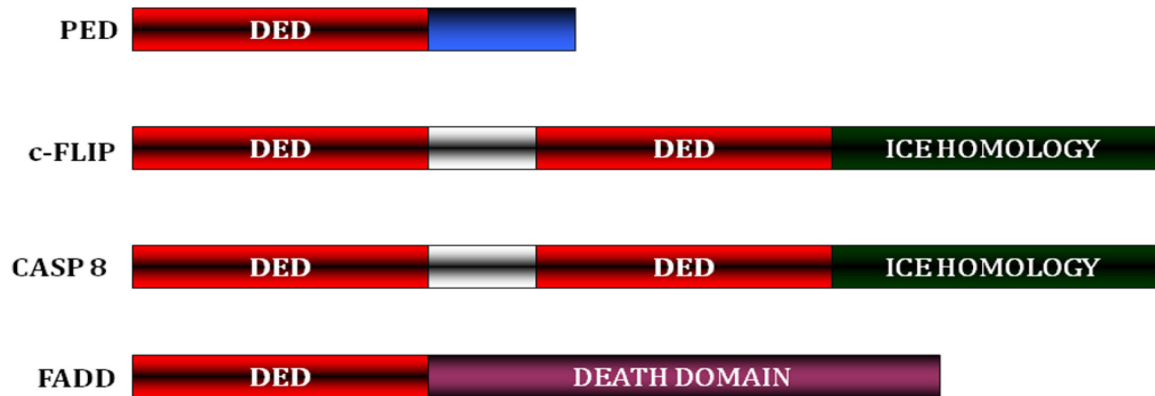

Figure 14. Apoptosis related molecole homology.

In particular, PED was described to inhibit DISC (Death Inducing Signaling Complex) formation and caspase 8 activation upon death cytokines stimulation (FasL, TNFα, TRAIL) in different cell types (22-24). PED molecules in the proximity of caspase-8 and caspase-10 in the DISC may prevent further cleavage of the caspases according to the induced proximity model. Indeed, PED can be recruited in the DISC. PED expression is required to divert astrocytes from the deleterious effects of TNF. This was demonstrated using astrocytes from wild type versus PED null mutant mice. Astrocytes lacking PED and exposed to TNF rapidly exhibited the classical signs of apoptosis including inversions of membrane lipids, evidenced by annexin V labeling, and nuclear fragmentation leading to the formation of DNA ladders. Re-expression of PEA-15 after transfection restored protection and survival. (23) Furthermore, Hao et al. found increased PED expression in primary human malignant glioma cell lines. (28) We recently demonstrated that PED expression is altered in B-CLL (B-cell chronic lymphocytic leukemia) (29) and non-small cell lung cancer (NSCLC) (30), where it mediates resistance to TRAIL (TNF-Related Apoptosis Inducing Ligand) induced apoptosis. Interestingly, PED needs to be double in its diphosphate form to be recuited to the DISC. Moreover, PED can contribute to apoptosis resistance to chemotherapies for breast cancer (31).
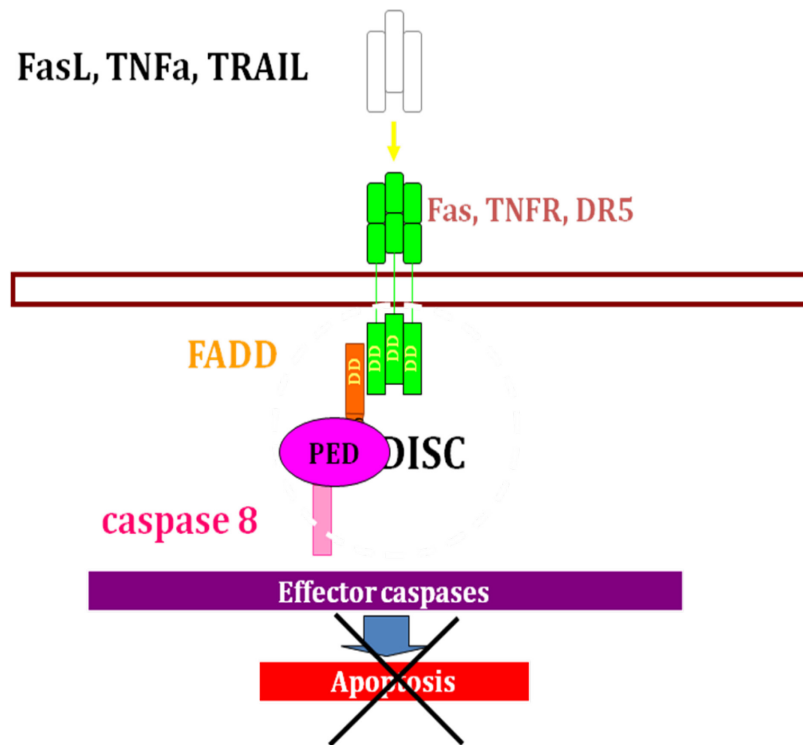
Figure 15. Extrinsic pathway inhibition by PED. Inhibition of caspase-8 and -10 cleavage and activation mediated by PED when it is recruited to the DISC.

PED affects MAPK signaling: effects on proliferation and migration. PED is particularly enriched in mature, non-dividing astrocytes. During development of the brain, PEA-15 expression begins relatively late at embryonic day 12 (E12) and reach the adult levels by postnatal day 10 (P10) when cell proliferation is strongly reduced in the CNS. Moreover, the levels of PED in proliferating astrocytes are lower than in non-proliferating astrocytes in cultures. Conversely, PED null mice exhibit a marked increase in cell proliferation in several lineages including astrocytes, lymphocytes and hepatocyte.

Thus, PED expression appears closely, and inversely, correlated with cell proliferation. The ERK1/2 p44/42 ERK MAP kinase cascade seems essential for entry into the cell cycle Multiple substrates of ERK1 and ERK2 have been characterized, located in different subcellular compartments such as the plasma membrane for the epidermal growth factor receptor, the cytosol for the microtubule destabilizing protein stathmin, or the nucleus for the transcription factor Elk1. The inactive ERK is essentially located in the cytosol. Its activation leads to its translocation into the nucleus, an event that seems to be essential for ERK action and signal termination. The first evidence for a link between PED and the MAP kinase signaling pathway came from the reversal of the H-Ras inhibition of integrin signaling by PED

45

expression, evidenced using expression cloning. Surprisingly, PED blocked Ras effect on integrin without affecting its stimulation of ERK activity. It was subsequently demonstrated a direct interaction between PEA- 15 and the MAP kinase cascade after a yeast two-hybrid screen, using PED as a bait, that allowed to characterized ERK1 and ERK2 as the PED partners. PED is not a substrate for ERK. Indeed, PED lacks the canonical proline-directed ERK phosphorylation sites and is not phosphorylated by ERK in vitro. PED alters the output of ERK signaling without blocking ERK activation. Indeed, we observed that PED does not interfere with ERK activation or activity. PED does not affect the phosphorylation of ERK cytosolic substrates, such as stathmin or p90RSK, but it blocks the phosphorylation of ERK nuclear substrates, such as Elk-1, with a consequent inhibition of ERK-dependent transcription. PED modifies ERK signaling by excluding ERK from the nucleus. PED contains a nuclear export signal (NES) that is required for ERK localization to the cytosol. (23)
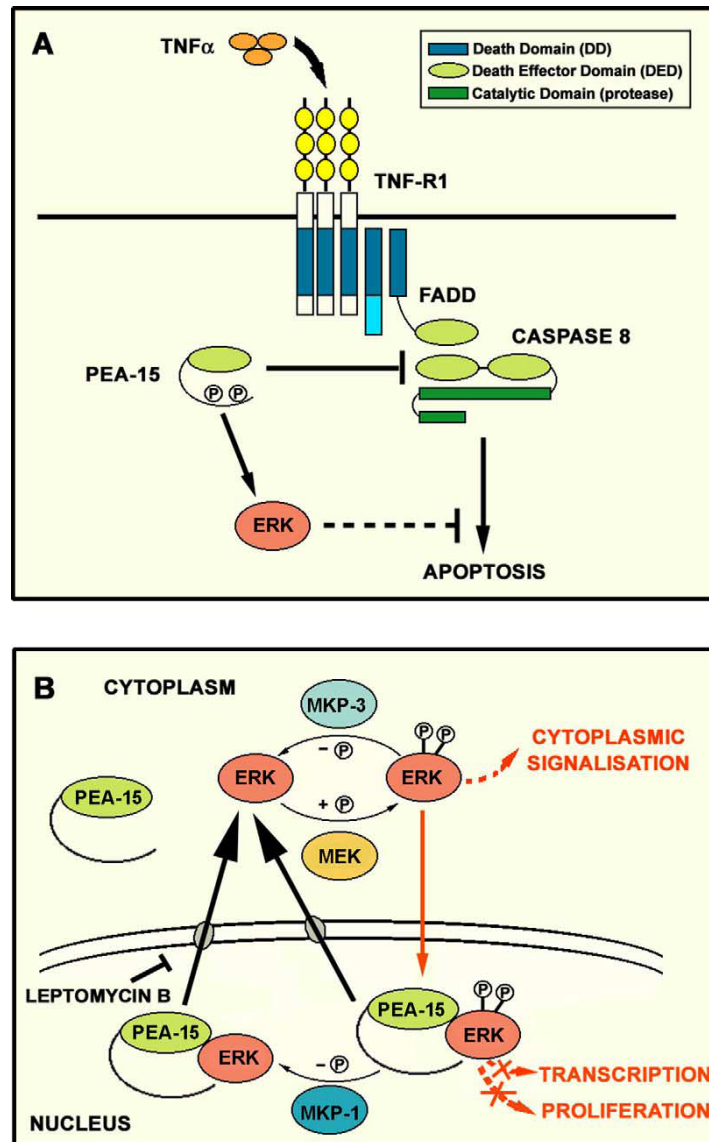
Figure 16. PEA-15 regulates both TNFalpha-induced apoptosis and ERK-dependent transcription. (A) PEA-15 participates in the formation of the DISC formed of the receptor, FADD, caspase-8 as mentioned in the text, where it may bind to FADD and/or pro-caspase-8, blocking the activation of the caspase. An indirect effect on ERK (dotted line) may also participate in the anti-apoptotic effect of PEA-15. (B) PEA-15 binds and exports ERK from the nucleus, redirecting the kinase activity toward its cytosolic substrates. (23)

Additional functions of PED. Using differential display to identify genes whose expressions are altered in tissues derived from type II diabetes mellitus patients compared with nondiabetic individuals, Condorelli et al. cloned cDNAs encoding PED, which they named PED for ''phosphoprotein enriched in diabetes''. They found that PED mRNA was overexpressed in fibroblasts, skeletal muscle, and adipose tissue from type II diabetics. The protein levels were also elevated in type II diabetic tissues. Furthermore, transfection of a PED cDNA into differentiating L6 skeletal muscle cells increased the content of glucose transporter-1 (GLUT1) on the plasma membrane and inhibited insulin-stimulated glucose transport and cell surface recruitment of glucose transporter-4 (GLUT4). These effects were

reversed by the inhibition of PKC activity, suggesting that the phosphorylation of PED might be involved. While the role of ERK in glucose transport is uncertain, based on our data it is reasonable to predict that PED overexpression could block glucose stimulated ERK translocation. This may partly explain the changes observed in glucose transport and cell surface recruitment of GLUT4 in type II diabetes. A two-hybrid search also evidenced an interaction of PED with PLD1, that was further confirmed in intact cells. Elevated levels of PLD1 activity were observed in vitro and in vivo after co-expression with PED. This enhanced PLD1 activity was correlated with elevated levels of PLD protein, leading to the conclusion that PED was affecting the accumulation or degradation rates of PLD1 rather than its activity per se. (23)

Tandem Affinity Purification (TAP)

The sequencing of complete genomes of several organisms provides an exceptional opportunity to analyze the all different functions governed by their genes. Insights into these complex biological systems can be gained by the analysis of gene regulatory networks and by determining the identity, modification, and expression levels of encoded protein as well as by defining interactions existing among proteins (proteomic analyses). Large-scale two-hybrid screening has been used for this latter purpose. However, false-positive and false-negative results, the lack of information about stoichiometry, and the limited set of conditions testable make it desirable identification vary from protein to protein, making it impossible to able to use additional strategies to easily detect interactions. Biochemical purification of proteins in combination with mass spectrometry allows identification of interacting partners.

The Tandem Affinity Purification (TAP) method is a purification procedure based on a fusion of a tag to the target protein and the final recovery of the target protein and its interacting partner through mass spectrometry analysis.

The TAP method involves the fusion of the TAP tag to the target protein and the introduction of construct into the host cell or organism. For optimal results, it is preferable to maintain expression of the the fusion protein at, or close to, its natural level. Indeed, overexpression of

the protein often induces its association with nonnatural partners (heat shock proteins, proteasome). Cell extracts are prepared and fusion protein as well as associated partners is recovered by two specific affinity purification/elution steps. The material recovered can be analyzed in several ways. For protein complex characterization, proteins are concentrated, and eventually fractionated on a denaturing gel before identification by mass spectrometry. Because the various TAP purification steps are performed in a gentle native manner, purified complexes may also be tested for their activities or used in structural analysis.

The TAP tag consists of two IgG binding domains of *Staphylococcus aureus* protein A (ProtA) and a calmodulin binding peptide (CBP) separated by a TEV protease cleavage site. Both affinity tags have been selected for highly is efficient recovery of proteins present at low concentration. ProtA binds tightly to an IgG matrix, requiring the use of the TEV protease to elute material under native conditions (Fig. 1B). The eluate of this first purification step is then incubated with calmodulin coated beads in the presence of calcium. After washing, which removes contaminants and the TEV protease after the first affinity selection, the bound material is released under mild conditions with EGTA conditions have been developed for the generic use of the TAP strategy. The TAP-tag is, however, very tolerant to buffer conditions changes and can easily be implemented to optimize recovery of specific complexes. (32)
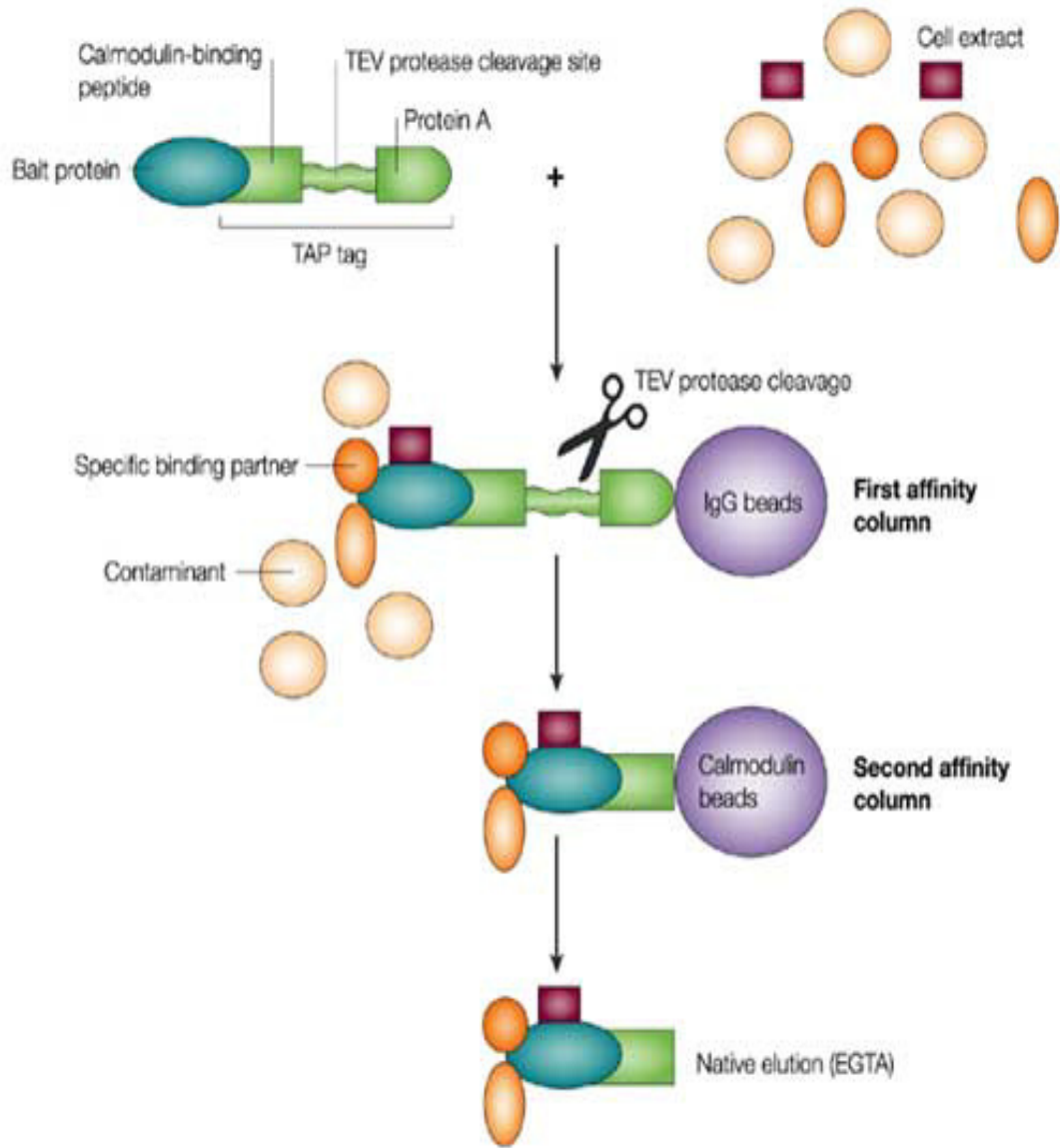
Figure 17. Schematic representation of the subtraction strategy. (40)

Methods (I)

Materials. Media, sera and antibiotics for cell culture were from Life Technologies, Inc. (Grand Island, NY, USA). Protein electrophoresis reagents were from Bio-Rad (Richmond, VA, USA), and Western blotting and ECL reagents were from Amersham (Aringhton Heights, IL, USA). All other chemicals were from Sigma (St. Louis, MO, USA) unless otherwise stated. The following primary antibodies were used: anti-PED antibody (33); anti-β-actin antibody (Ab-1, mouse IgM, Oncogene, Darmstadt, Germany); anti-caspase 8 antibody (1C12) Cell Signaling Technology, Inc. (Danvers, MA, USA), anti-caspase 3 antibody (Abcam, Cambridge, USA); anti-caspase 10 antibody (StressGene, Victoria, BC Canada); anti-cFLIP (NF6) antibody (Alexis, Lausen, Switzerland); anti- FADD antibody (BD Transduction Laboratories, San Jose, CA, USA); anti-TRAIL receptor antibodies (R&D Systems, Minneapolis, MN, USA); anti PARP antibody (SC7150) (Santa Cruz Biotechnology, Inc., Santa Cruz, CA, USA).

Cell culture. Human CALU-1 and A459 NSCLC cell lines were grown in DMEM; H460 and A549 cell lines were grown in RPMI. Media were supplemented with 10% heat-inactivated FBS, 2mM L-glutamine and 100U/ml penicillin-streptomycin.

Protein isolation and Western blotting. Lung tissue specimens (neoplastic and adjacent normal tissue) were collected during surgical intervention on 27 patients affected with lung tumor, in accordance with the ethical standards of the institutional responsible committee on human experimentation. The clinical and pathological characterization (including TNM staging) of these patients, which were not receiving medical treatment at the time of the operation, is shown in Table 1. The collected samples were homogenized in 1ml PBS (0.14M NaCl, 2.7mM KCl, 8mM Na2HPO4, 1.5mM KH_2PO_4) containing 1% Triton X-100 and Proteinase Inhibitor Cocktail, with a tissue homogenator. Cultured cells were pelleted, washed twice with cold PBS and lysed in the same harvest buffer. Solubilized proteins were incubated for 30 min on ice, and after centrifugation at 10,000 g for 30 min at 4°C,

supernatants were collected. Fifty µg of sample extract were resolved on 12% SDS-polyacrylamide gels using a mini-gel apparatus and transferred to Hybond-C extra nitrocellulose. Membranes were blocked for 1 h with 5% non-fat dry milk in TBS containing 0.05% Tween-20, incubated for 2 h with primary antibody, washed and incubated with secondary antibody, and visualized by chemiluminescence.

Cell death and cell proliferation quantification. Cells were plated in 96-well plates in triplicate and incubated at 37°C in a 5%CO2 incubator. To induce apoptosis, Superkiller TRAIL (Alexis Biochemicals, Lausen, Switzerland) was used for 24 h at 10ng/ml. Cell viability was evaluated with the CellTiter 96® AQueous One Solution Cell Proliferation Assay (Promega, Madison, WI, USA), according to the manufacturer's protocol. Metabolically active cells were detected by adding 20 µl of MTS to each well. After 2 h of incubation, the plates were analyzed in a Multilabel Counter (Bio-Rad, Richmond, VA, USA). Apoptosis was also assessed using annexin V–FITC Apoptosis Detection Kits followed by flow cytometric analysis. Cells were seeded at 1.8 106 cells per 100-mm dish, grown overnight in 10% FBS/RPMI, washed with PBS, then treated for 24 hours with 200 ng/ml TRAIL. Following incubation, cells were washed with cold PBS and removed from the plates by very mild trypsinization conditions (0.01 % trypsin/EDTA). The resuspended cells were washed with cold PBS and stained with FITC-conjugated annexin V antibody and propidium iodide (PI) according to the instructions provided by the manufacturer (Roche Applied Science, Indianapolis, IN). Cells (50,000 per sample) were then subjected to flow cytometric analysis. Propidium iodide staining and flow cytometry analysis were done as described [19].

Flow cytometry. The relative level of surface TRAIL receptors was assessed by FACS analysis. To this end, 1 million cells were collected and washed twice in PBS, incubated with PE-conjugated purified monoclonal antibodies against TRAIL receptors or with mouse isotype control phycoerythrin IgG2b for 1 hour on ice, and then washed once with 3 ml PBS. After centrifugation, the cell pellet was resuspended in 1 ml PBS and analyzed with a

FACSsort (Becton Dickinson, Franklin Lakes, NJ, USA).

Small interfering (si) RNAs. The Dharmacon siDesign Center software program was used to design a duplex siRNA targeting PED mRNA (siPED). This duplex consisted of a 21 nt doublestranded RNA, comprised of 19 base pairs with two T, 3' overhanging ends, synthesized by Invitrogen (Invitrogen Corporation, Carlsbad, CA, USA) (UCACUAUGGUGGUUGACUATT). c-FLIP siRNA was purchased from Santa Cruz Biotechnology, Inc. (Santa Cruz, CA, USA) (sc-35388). siCONTROL Non-Targeting siRNA Pool #2 (D-001206-14-05) was from Dhamarcon (Lafayette, CO, USA) and comprised four siCONTROL Non-Targeting siRNAs. Each individual siRNA within this pool was characterized by genome-wide microarray analysis and found to have minimal offtarget signatures.

Transfection experiments. CALU-1 or H460 cells were cultured to 80% confluence in p60 plates. 100 nM of control, PED or c-FLIP siRNA were transiently transfected in cells kept in antibiotic-free, serum-containing medium, using LIPOFECTAMINE 2000, according to the manufacturer's instructions. Cells were incubated with siRNAs for the indicated times. PED protein levels were upregulated where indicated by transfecting cells with 5 µg of pcDNA3-Myc PED.

Tissue microarray (TMA) construction and immunohistochemistry (IHC). 0.6 mm-diameter cylinders were punched from donor blocks in areas identified as neoplastic after analysis of hematoxylin/eosin (H&E) stained sections. The tissue cylinders were inserted into a recipient paraffin block using a precision instrument (Beecher Instruments, Sun Prairie, WI, USA). Standard indirect staining procedures were used for IHC (ABC-Elite-Kit, Vector Laboratories, Burlingame, CA, USA). After heat-induced pre-treatment (in citrate buffer, pH6, water bath at 90° for 30 min) for antigen retrieval, a rabbit polyclonal anti-PED antibody was applied for 2 h at adilution of 1:5000 at 37°C. The slides were then incubated with the secondary,

biotinylated antibody. Osmium-enhanced diaminobenzidine was used as the chromogen. Counterstaining was carried out with Harris' hematoxylin. Only fresh cut sections were stained to minimize the influence of slide ageing and maximize repeatability and reproducibility of the experiment. For negative controls, the primary antibody was omitted; as positive control, normal tissue with known PED positivity was used. For each sample, percentage of positive tumor cells and staining intensity (0,faint, moderate or intense) were recorded. A case was graded: a) negative, if no cells were stained; b) weakly positive (mild), if up to 33% of cells were stained; c) moderately positive if 34-66% of cells were stained; or d) strongly positive if 67% 100% of cells were positive. Staining intensity was not used for correlation with clinical findings, as it can vary depending on the manner of tissue fixation. The slides were all evaluated in one day by one experienced pathologist (DB).

Methods (II)

*Cell culture, treatments***.** The human neuronal stem cell line (HNSC.100) was propagated in DMEM:F-12 (1:1) medium, supplemented with 0.5% FCS (Life Technologies, Inc. Grand Island, NY, USA), 1% N2 (Life Technologies, Inc., Grand Island, NY, USA), 1% BSA (Sigma), 1% Penicilin/Steptomycine and human recombinant growth factors EGF and FGF-α (Tebu Biochem, 20nM each). For differentiation, the mitogens were removed and replaced with CNTF (100nM) for about 2 weeks. Differentiated HNSC.100 were treated for 24h with ethanol vehicle, or 10^{-7}M vitamin D3 (Biomol, CA) and lysates were prepared with ice-cold lysis buffer (20mM MOPS, pH 7.2, 2mM EGTA, 3.5mM EDTA, 30mM sodium fluoride, 60mM glycerophosphate pH 7.2, 20mM sodium pyrophosphate, 1mM sodium orthovanadate, 1mM phenylmethylsulfonylfluoride, 3mM benzamidine, 5μM pepstatin A, 10μM leupeptin, 1% Triton X-100).

Real-time PCR. Total RNA was extracted from A549 cells using the TRIZOL reagent protocol (InVitrogen). Quality and quantity of the RNA were determined by measuring the absorbance at 260 and 280 nm, and by 1% agarose gel electrophoresis under denaturing conditions. RNA (1μg) from each sample was reverse transcribed and one-step RT-PCR was performed

by using SuperScript® III First-Strand system (Invitrogen) according to manufacturer's instructions. Primers for PEA-15 were: 5'-GCAGTGCCTGGTTTAGCTTC-3' (forward), 5'-TACGGGTTAGCTTGGTGTCC-3' (reverse) and were synthesized commercially (PRIMM, Milan, Italy). Real-time PCR was performed by using iQ^{TM} SYBR$^®$ Green Supermix (BIO-RAD). Reactions were performed in triplicate and β-Actin used as an internal reference cycling (conditions are available upon request).

Methods (III)

Plasmids. Expression vectors for Rac wild type, RacQL, Rac12V and Vav1 were kindly provided by Dr. Mario Chiariello. PED-MYC expression plasmid was previously described (33). PED-MYC S104G was realized through AGT-GGT single nucleotide substitution (QuikChange Site-Directed Mutagenesis Kit, Stratagene, La Jolla, CA, USA). ShRNAi-PED and shRNAi-scrambled were from Open Biosystems (Huntsville, AL, USA), GST-CRIB has been previously described (34).

Tandem Affinity Purification. A459 cells were lysed in TEB buffer (50 mM Tris-HCl, pH 8, 150 mM NaCl, 5% glycerol, 1% Triton X-100, 1.5 mM MgCl$_2$, 2 mM EGTA and protease inhibitors from Roche) for 2 h under gently mix and cleared by centrifugation for 30 min at 13000 rpm. The lysate was incubated with rabbit-IgG agarose beads (Sigma, St. Louis, MO, USA) overnight at 4°C. Beads were collected by centrifugation (3000 rpm for 5 min), and then extensively washed firstly with TEB buffer and then with TEV-protease cleavage buffer (TCB: 10 mM Tris-HCl (pH 8), 150 mM NaCl and 0.1% Triton X-100, 0.5 mM EGTA). Beads were then incubated with 150 µl TEV protease in 1.5 mL of TCB overnight at 4°C. The TEV-protease cleavage products were colleted and then loaded onto calmodulin sepharose beads (GE Healthcare, Piscataway, NJ, USA) in Calmodulin Binding Buffer (CBB: 10 mM Tris-HCl, pH 8, 150 mM NaCl, 0.1% Triton X-100, 1 mM MgAcetate, 1mM Imidazole, 2 mM CaCl$_2$) supplemented with 250 mM CaCl$_2$ at 4°C for 1.5 h. Beads were recovered by centrifugation at 3000 rpm for 5 min and then extensively washed with CBB. Proteins retained on the beads

were eluted by incubation with Calmodulin Eluition Buffer (CEB:10 mM Tris-HCl, pH 8, 150 mM NaCl and 0.1% Triton X-100, 1 mM MgAcetate, 1 mM Imidazole) with three different $CaCl_2$ concentrations (2, 10 and 20 mM). The eluate was collected and concentrated by methanol/chloroform precipitation before loading onto a 12% SDS– PAGE.

Mass spectrometry analysis and protein identification. The gel was stained with colloidal Coomassie blue (Sigma, St. Louis, MO, USA). Protein bands were excised from the gel, reduced, alkylated and digested with trypsin (35). Peptide mixtures were extracted from the gel and analyzed by nano-chromatography tandem mass spectrometry (nanoLC–MS/MS) on a CHIP MS Ion Trap XCT Ultra equipped with a capillary 1100 HPLC system and a chip cube (Agilent Technologies, Palo Alto, CA, USA). Peptide analysis was performed using data-dependent acquisition of one MS scan (mass range from 400 to 2000 m/z) followed by MS/MS scans of the three most abundant ions in each MS scan. Raw data from nanoLC–MS/MS analyses were employed to query a non-redundant protein database using in house MASCOT software (Matrix Science, Boston, MA, USA).

Virus production. We produced vector stocks by calcium phosphate transient transfection, cotransfecting three plasmids in 293 T human embryonic kidney cells, since these cells are good DNA recipients. The three plasmid are: the packaging plasmid, pCMVDR8.74 designed to provide the HIV proteins needed to produce the virus particle; the envelope-coding plasmid, pMD.G, for pseudotyping the virion with VSV-G and TWEEN PED-TAP vector, the transgene coding plasmid. The calcium phosphate–DNA precipitate was allowed to stay on the cells for 14–16 h, after which the medium was replaced, collected 48 h later, centrifuged at 1000 rpm for 5 min at room temperature and filtered through 0.22 mm pore nitrocellulose filters.

Generation of lentiviral vectors and gene transfer. For PED-TAP plasmid, we PCR-amplified PED cDNA from PED-MYC expressing vector and subcloned into the pBS1761 plasmid for TAP-tagging of proteins at the N-terminus. For TWEEN PED-TAP vector, we PCR-amplified PED-TAP cDNA from PED-TAP expressing vector and subcloned into the lentiviral vector TWEEN17 under control of them cytomegalovirus promoter. On the day of infection, the medium was removed and replaced with viral supernatant to which 4 mg/ml of Polybrene had been added. Cells were then centrifuged in their plate for 45 min in a Beckman GS-6KR centrifuge, at 1800 rpm and 32°C. After centrifugation, cells were kept for either 1 h 15 min or ON in a 5% CO2 incubator at 32 or 37°C, respectively. After exposure, cells were washed twice with cold PBS and fresh medium added. At either 12 or 48 h after the infection, cells were washed with PBS, harvested with trypsin/EDTA and analyzed by FACS for GFP expression.

Cell culture. Human A459, A459 TWEEN, A459 TWEEN PED-TAP and HeLa cell lines were grown in DMEM containing 10% heat-inactivated FBS and with 2 mM L-glutamine and 100 U/ml penicillin-streptomycin. PEDshRNA A459 clones (#1 and #2) and SCRAMBLEDshRNA A459 clone were grown in DMEM medium containing 10% heat-inactivated FBS, with 2 mM L-glutamine and 100 U/ml penicillin-streptomycin and selected with 2.5 μg/ml puromycin from Sigma (St. Louis, MO, USA).

Western blotting. Total proteins from A459 and HeLa cells were extracted with RIPA buffer (0.15 mM NaCl, 0.05 mM Tris-HCl, pH 7.5, 1% Triton, 0.1% SDS, 0.1% sodium deoxycolate and 1% Nonidet P40). Fifty μg of sample extract were resolved on 10 –15% SDS-polyacrylamide gels using a mini-gel apparatus (Bio-Rad Laboratories, Richmond, CA, USA) and transferred to Hybond-C extra nitrocellulose. Membranes were blocked for 1 hr with 5% non-fat dry milk in TBS containing 0.05% Tween-20, incubated over night with primary antibody, washed and incubated with secondary antibody, and visualized by chemiluminescence. The following primary antibodies were used: anti- PAP (Peroxidase-

Anti-Peroxidase Soluble Complex), anti-β-Actin antibodies from Sigma (St. Louis, MO, USA), anti- Rac1 antibody from Abcam (Cambridge, MA, USA); anti- phospho ser71 Rac1, anti- phospho ser104 PED, anti- ERK 1/2, anti- phospho ERK 1/2, anti- ELK1, anti- phospho- ELK1, anti- MYC-tag antibodies from Cell Signalling (Danvers, MA, USA), anti- phospho ser116 PED antibody from Biosource International Inc. (Camarillo, CA, USA), anti- PED antibody (33), anti- AU5, anti- HA antibodies from Covance (Emeryville, CA, USA).

Immunoprecipitation. Cells were cultured at a final concentration of 90% in p100 plates. The cells were harvested with RIPA Buffer on a shaker for 30 minutes. 1 mg of total extract was immunoprecipitated using the indicated antibodies (4 µg/ml Anti-Rac1, 4 µg/ml Anti-PED), for 16 hrs on shaker. Then, A/G beads (Santa Cruz Biotechnology Inc., Santa Cruz, CA, USA) were added for two hrs. The beads were washed for three times with washing buffer (50 mM Tris Hcl pH 7.5, 150 mM NaCl, 0.1% Triton, 10% glycerol), and then 20 µl of sample buffer was added; the samples were boiled at 100°C for 5 minutes and then the supernatants resolved by SDS-PAGE.

siRNA and plasmid transfection. A459 cells were cultured to 80% confluence and transiently transfected using LIPOFECTAMINE 2000 (Invitrogen, Carlsbad, CA, USA) with 150 nM anti- PED siRNAs and anti-Rac1 siRNAs (Dharmacon, Lafayette, CO, USA), or with control vector, PED, PED S104G, Rac, RacQL, Rac12V, Vav1 cDNAs as reported in the paper, as described in the manufacturer's protocol.

Rac1 pull-down assay. Plates were starved for 24 h and then treated as indicated. After a quick wash with iced-cold PBS, cells were lysed with GST-Fish buffer (50 mM Tris/HCl ph 7.4, 2 mM $MgCl_2$, 1% NP-40, 10% glycerol, 100 mM NaCl, 1 µg/ml leupeptin, 1 µg/ml pepstatin, 1 µg/ml aprotinin, 1 mM PMSF and 2 mM DTT). After 10 min at 4°C under

agitation, cells were scraped and lysates were cleared by centrifugation in a precooled rotor. 150 µg of total protein extract was mixed with 10 µg of GST-PAK-CRIB domain coupled to glutathione-sepharose beads and incubated 30 min at 4°C under agitation. Beads were the rinsed three times rapidly with 1 ml of iced-cold GST-Fish buffer. The amounts of total Rac and Rac-GTP were estimated by immunoblot against Rac1.

Migration assay. Transwell Permeable Supports, 6.5 mm diameter inserts, 8.0 µM pore size, polycarbonate membrane (Corning Incorporate, Corning, NY, USA) were used to perform migration assay. A459 and HeLa cells were grown as indicated above, then harvested by TrypLE^{TM} Express (Invitrogen, Carlsbad, CA, USA) and 10^5 cells were washed three times and then resuspended in 1% FBS containing DMEM medium and seeded in the upper chamber. Lower chamber of the tranwell was filled with 600 µl of culture medium containing 10% FBS, 5 µg/ml fibronectin, as an adhesive substrate. Cells were incubated at 37°C for 24 h. Transwell were then removed from 24-well plates and stained with 0.1% Crystal Violet in 25% methanol. Nonmigrated cells were scraped off on the top of the transwell with a cotton swab. % of migrated cells was evaluated by eluiting crystal violet with 1% SDS and reading the absorbance at λ 570 nm.

Invasion assay. A similar procedure as in migration assay was used. The upper chamber of the transwell was filled with 100 µl of BD Matrigel^{TM} (BD Biosciences, San Jose, CA, USA). BD Matrigel^{TM} was diluited to 1mg/ml in serum free culture medium and put into the top of the traswell. Then it was incubated for 4 h for gelling. Cells were counted and treated as indicated above. Invaded cells were measured as % over control cells, transfected with empty vector.

Wound healing. Cells were cultured as confluent monolayers, synchronized in 1% FBS for 24

h, and wounded by pipette tip. Wounded monolayers were washed twice with PBS to remove nonadherent cells. Wound healing was followed up to 24 hours. For these studies, cells were seeded in 35 mm Petri dishes and kept at 37°C in a humidified atmosphere with 5% CO_2.

Results (I)

PED expression in NSCLC tissue. Specimens were collected from 27 NSCLC-affected patients (clinical features are summarized in Table 1) and processed for Western blotting. PED was increased in the tumor tissue of all the patients analyzed and only rarely expressed in the adjacent normal tissue (Figure 18a). The mean PED expression level was six-fold higher in the transformed areas compared to normal tissue (Figure 18b). Furthermore, analysis of TNM staging revealed that the expression of PED was greater during the initial stages of the disease (T1 and N0) than in T2 and N1 lesions (Figure 18c). We also analyzed PED expression on a TMA constructed from 160 different histological lung cancer samples. As shown in Table 2, PED expression was considered high in the majority of cases and in all the types of lung tumor present, with only 4% of the tumors analyzed resulting negative for PED staining. Immunohistochemical analysis of PED expression is depicted in Figure 19 where it is possible to evaluate the different PED staining intensity. Panel A represents an example of PED negative staining; panel B, of mild, panel C of moderate and panel D of strong PED staining. The majority of samples showed strong staining for PED.

Clinical features of the patients

P #	Sex	Age	Histology	TNM
1	M	49	ADENO	T1N0MX
2	M	61	ADENO	T2N2MX
3	M	68	ADENO	T3N0MX
4	M	64	ADENO	T1N0MX
5	M	63	ADENO	T2N1MX
6	M	55	ADENO	T2N2MX
7	M	56	ADENO	T2N0MX
8	M	56	SQUAM	T1N1MX
9	M	63	ADENO	T3N2MX
10	M	66	ADENO	T1N1MX
11	M	77	ADENO	T1N0MX
12	M	69	SQUAM	T2N0MX
13	M	61	SQUAM	T2N0MX
14	F	52	ADENO	T2N0MX
15	M	57	ADENO	T2N2M1
16	M	80	SQUAM	T2N0MX
17	M	63	ADENO	T1N2MX
18	M	55	ADENO	T1N2MX
19	M	63	SQUAM	T2N0MX
20	M	67	SQUAM	T1N0MX
21	M	63	SQUAM	T1N0MX
22	M	70	SQUAM	T3N0MX
23	M	68	SQUAM	T1N0MX
24	M	55	ADENO	T1N0MX
25	M	64	ADENO	T1N0MX
26	M	69	SQUAM	T2N0MX
27	M	68	ADENO	T1N0MX

Table 1. Age (years), sex and TNM (tumor, node, metastasis) staging [30] of patients (P) are reported. All patients were smokers. Histology of the tumors indicated that most were adenocarcinoma (ADENO) and the remaining squamous cell carcinomas (SQUAM).

Histological type	PED expression				Total
	Negative	Mild	Moderate	Strong	
Adenocarcinoma	1 2.3%	8 18.6%	10 23.2%	24 55.8%	43
Large cell carcinoma	1 2.4%	2 4.8%	15 36.5%	23 56.1%	41
Small cell carcinoma	2 6.6%	5 16.6%	7 23.3%	16 53.3%	30
Squamous cell carcinoma	2 4.3%	11 23.9%	13 28.2%	20 43.4%	46

Table 2: PED expression analyzed in the lung cancer TMA. Top number indicates number of cases present in the TMA; the bottom number indicates its relative percentage. PED expression was graded: **negative:** no staining; **mild:** 0-33% positively staining cells; **moderate:** 34-66% positively staining cells; **Strong:** 67-100% positively staining cells.
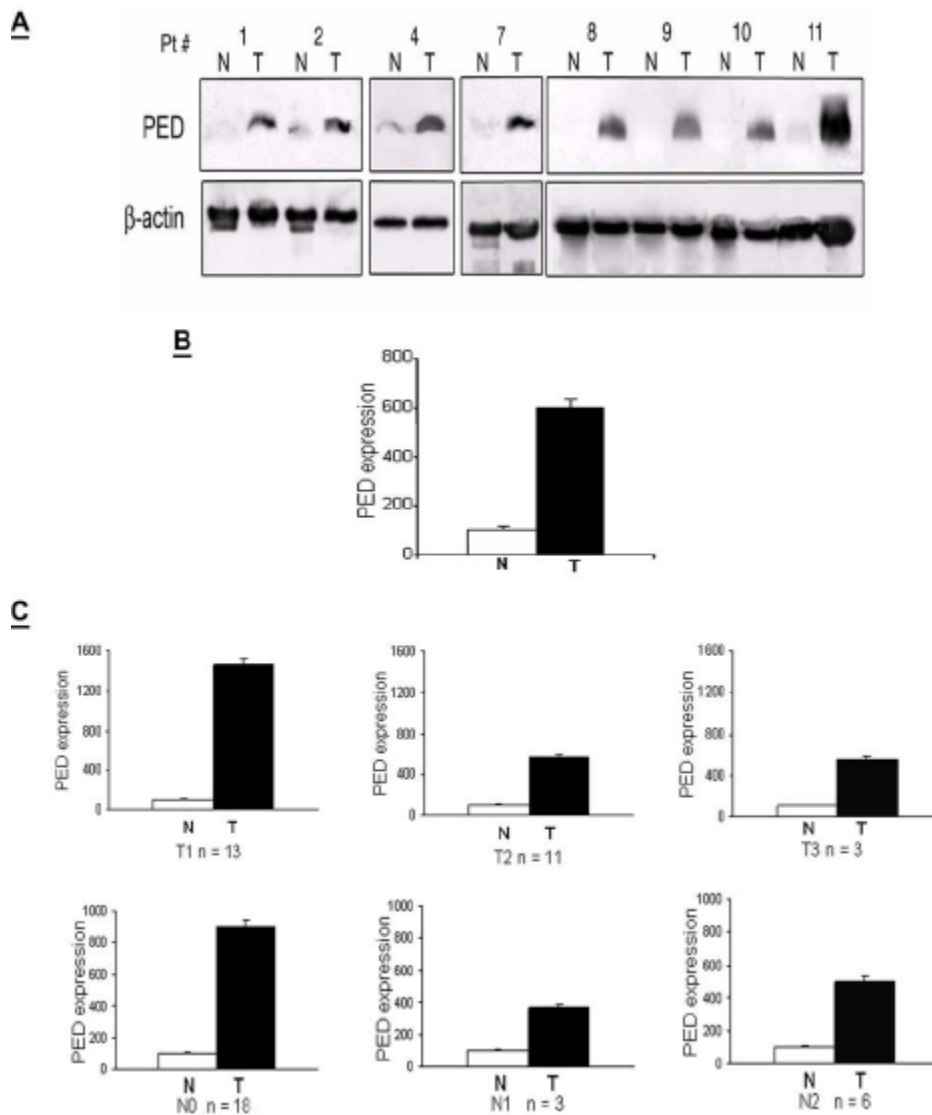
Figure 18. PED expression is increased in human lung cancer. **(a)** Western blots showing expression of PED in tumor (T) and adjacent normal (N) lung tissue from some of the 27 NSCLCaffected patients (Pt). β-Actin was used for the loading control. **(b)** Graph of densitometric analysis. Mean ± SD PED expression of all the tumor samples (T) normalized to β-actin and expressed as % respect to the adjacent normal tissue (N). PED was >6-fold higher in cancer tissue compared to normal areas. **(c)** PED expression during T1, T2, T3 and N0, N1 and N2 stages of the disease. PED expression is greater during the initial stages (T1 and N0) of the disease compared with the T2 and N1 lesions.
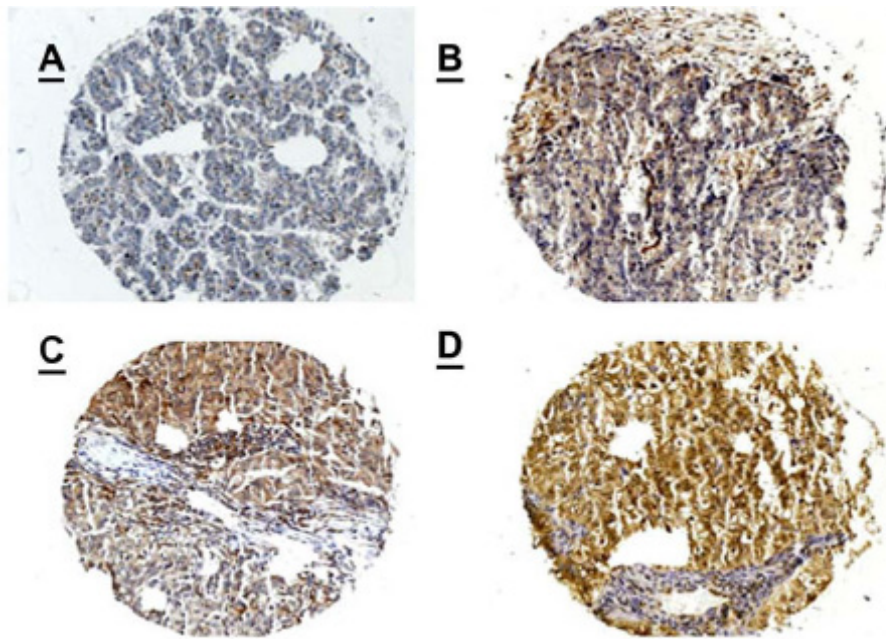
Figure 19. PED expression levels in NSCLC cancer samples. Immunohistochemical analysis of paraffin-embedded NSCLC sections labeled with anti-PED antibody (1:5000) and revealed by secondary, biotinylated antibody. **(a)** negative **(b)** mild; **(c)** moderate; **(d)** strong staining.

PED expression correlates with resistance to TRAIL in NSCLC cell lines. PED is a DED-containing protein that inhibits the formation of a functional DISC following treatment with different apoptotic stimuli, including TRAIL, in several cell types. We therefore, investigated whether PED expression correlated with resistance to TRAIL in different NSCLC cell lines. As shown in Figure 20a, PED is expressed at higher levels in CALU-1 cells compared to H460 cells. Intermediate levels of expression were observed in A459 and A549 cells. When exposed to TRAIL, H460 cells underwent TRAIL-induced cell death, whereas CALU-1 cells were completely resistant (Figure 20b and c). A459 and A549 cells exhibited intermediate sensitivities to TRAIL (Figure 20b and c). Therefore, PED expression levels correlated with TRAIL resistance in the NSCLC cell lines

analyzed. We also studied several components of the extrinsic cell death signaling pathway. As shown in Figure 20a, the expression of these TRAIL signaling molecules was comparable in the four cell lines, although c-FLIP expression was slightly lower in H460 cells.

TRAIL resistance in NSCLC cells does not depend on the expression of TRAIL receptors. TRAIL resistance could be correlated with different expression levels of TRAIL receptors. In

order to exclude this possibility, we investigated the cell surface expression of all four TRAIL receptor subtypes in NSCLC cells. As shown in Figure 21, expression of functional and decoy TRAIL receptors was comparable in all cell lines.
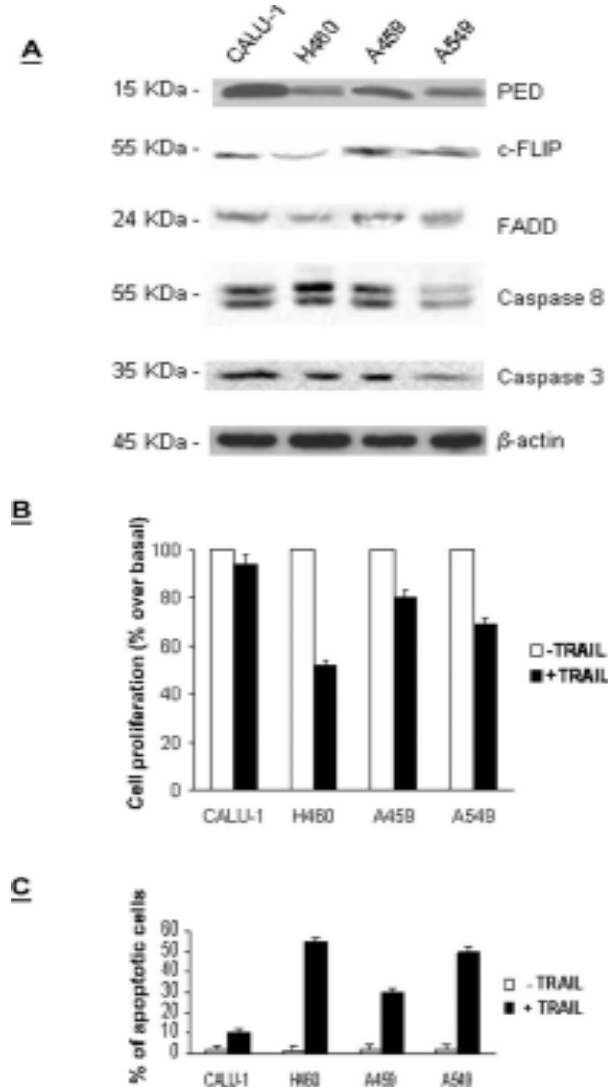

Figure 20. PED expression correlates with TRAIL resistance in NSCLC cell lines. **(a)** Fifty µg of total cell extract from CALU-1, H460, A459 and A549 cells were analyzed by Western blotting for the expression of PED and other TRAIL signaling molecules. β-actin was used as the loading control. Representative blots are shown. **(b)** Viability after treatment with TRAIL. Cells were incubated with superKiller-TRAIL (10 ng/ml) for 24 hrs and viability evaluated as described in the methods section. Mean ± SD of three independent experiments in triplicate. **(c)** Annexin V and propidium iodide (PI) staining of NSCLC cells after TRAIL treatment. Mean ± SD of four independent experiments in duplicate.
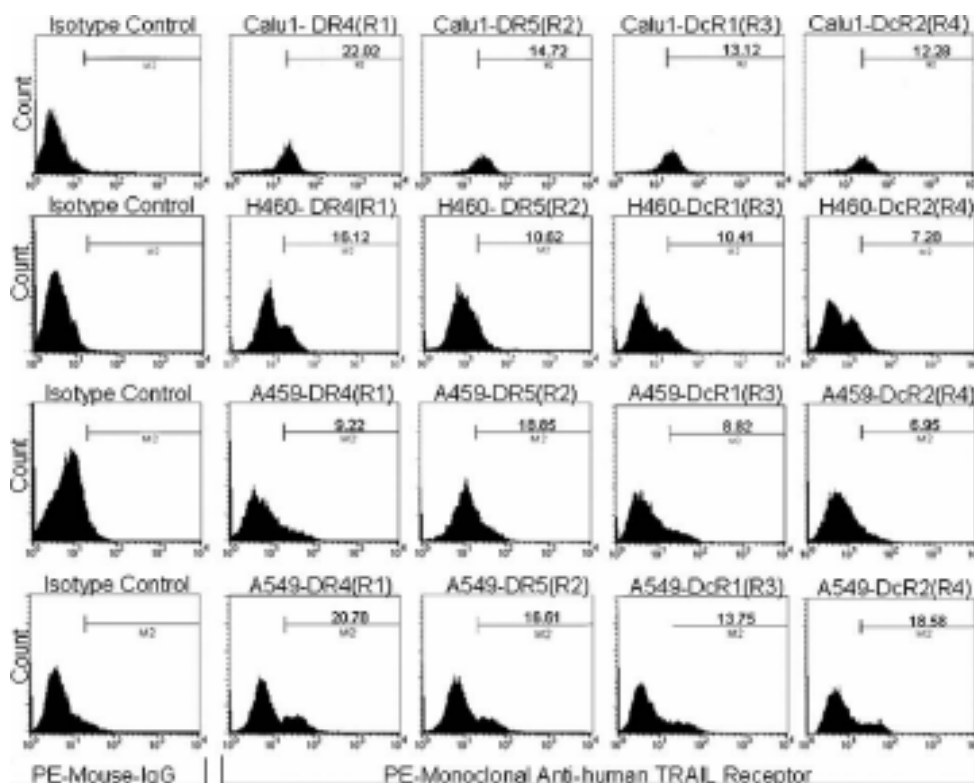
Figure 21. Surface expression of TRAIL receptors does not differ in TRAIL-resistant and TRAIL-sensitive cells. Surface expression of the four TRAIL receptor isotopes (R1, R2, R3 and R4) was analyzed by flow cytometry with specific PE-conjugated antibodies. Isotype-matched antibodies were used as control for unspecific binding. Receptor expression levels were comparable in CALU-1 and H460 cells.

Effect of the down regulation of PED and c-FLIP on insensitivity to TRAIL in CALU-1 cells. To better clarify the role of PED in TRAIL resistance in lung cancer cells, we transfected CALU-1 cells with PED siRNA. PED siRNA specificity was tested in CALU-1 cells by the co-transfection of PED siRNA with Myc-tagged PED cDNA. The PED siRNA duplex suppressed both endogenous (15 kDa) and exogenous (20 kDa) PED expression, while a control siRNA was not effective in reducing PED protein levels (Figure 22a). This silencing effect was evident at 48 hrs and more marked at 72 hrs. We found that also other in cell lines (HeLa, Human embryonic kidney 293) PED siRNA was able to knock down PED expression (data not shown). Transfected cells were then exposed to TRAIL. As expected, siRNA-mediated knock-down of PED was responsible for sensitization of CALU-1 cells to TRAIL-induced cell death (Figure 22b). Interestingly, comparable results were obtained when we knocked-down PED expression in A459 and A549 cells (Figure 22b). The treatment of CALU-1 cells with a specific c-FLIPL siRNA down-regulated c-FLIPL expression but did not increase sensitivity to

TRAIL-induced cell death (Figure 22c). These data further confirm that PED protects lung cancer cells from TRAIL-induced apoptosis, and that inhibiting PED expression results in increased TRAIL sensitivity.
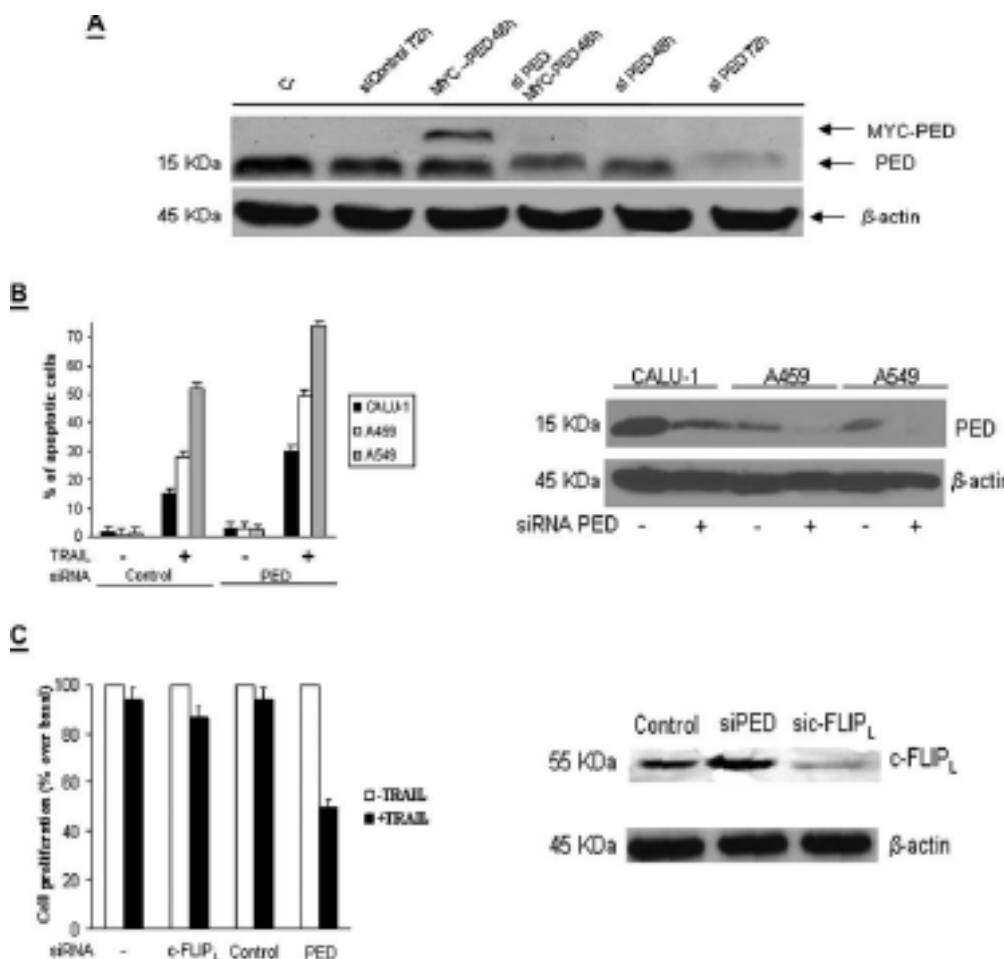

Figure 22. Down regulation of PED restores TRAIL sensitivity in CALU-1 cells. **(a)** PED siRNA or a control oligo were transiently transfected in CALU-1 cells in the presence or absence of PEDMyc cDNA. Cells were incubated for 48 or 72 hrs and analyzed by Western blotting. The PED siRNA duplex suppressed both exogenous and endogenous PED expression, whereas control siRNA had no effects. (b) PED siRNA effects in A459 and A549 cells. PEDsi RNA, transfected in NSCLC cells was able to reduce PED expression levels (right panel) and induce an increase in TRAIL sensitivity (left panel), as assessed by flow cytometry. Mean ± SD of two independent experiments in duplicate. (c) c-FLIPL siRNA or PED siRNA were transfected as described in Methods. Cells were analyzed for c-FLIP expression after 72 hrs incubation. c-FLIPL siRNA but not PED siRNA was able to reduce c-FLIPL expression Effects of silencing PED and c-FLIPL on TRAIL-induced cell death: CALU-1 cells were transfected with siRNA for PED, c-FLIPL or control for 48 hrs, after which cells were trypsinized, plated in 96-well plates in triplicate and further incubated with superKiller-TRAIL for 24 hrs. Metabolically active cells were then detected asindicated in the Methods. Mean ± SD of four independent experiments in duplicate. Downregulation of PED, but not cFLIPL, was responsible for increased sensitivity of CALU-1 cells to TRAIL-mediated cell death.

Effects of silencing PED on caspase activation in CALU-1 cells. We then examined the activation of caspase 8 and PARP upon exposure to TRAIL in CALU-1 cells treated with PED siRNA. As shown in Figure 23a, TRAIL-induced caspase 8 and PARP activation was greater in CALU-1 cells following PED siRNA transfection.

Effect of increasing PED expression on TRAIL sensitivity in H460 cell. In order to further evaluate the role of PED in apoptosis resistance, TRAIL-sensitive H460 cells were transfected with PED cDNA to up-regulate PED protein levels and then analyzed for their susceptibility to TRAIL-induced cell death. Increasing the expression of PED in these cells (Figure 23c) rendered them resistant to TRAIL, as assessed by Western blotting for caspase 8 and PARP (Figure 23b) or by a cell viability assay (Figure 23d).
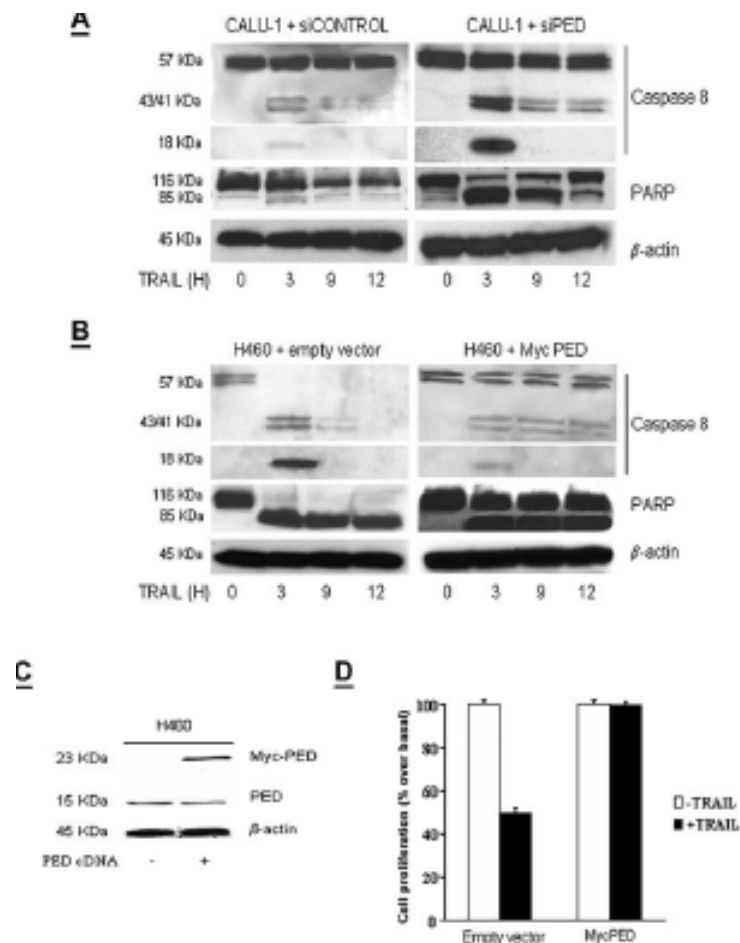

Figure 23. Effects of PED on caspase activation. (a) CALU-1 cells were transfected with PED or control siRNA for 72 hrs and then treated with superkiller TRAIL for the indicated times. Lysates were examined by Western blotting with anti-caspase 8 or anti PARP antibodies. Cleavage of caspase 8 and PARP was detected at a greater amount in CALU-1 cells transfected with PED siRNA. β-actin was used as the loading control. (b) PED cDNA (PED-Myc) was transiently transfected in H460 cells and cells were analyzed for caspase 8 and PARP activation as previously described or for or for cell viability (d) as indicated. (c) Western blot analysis of PED expression revealed that transfection increased PED expression levels in H460 cells. β-actin was used as the loading control. Representative blots are shown.

These results were published on *J Cell Mol Med*. 2008 Dec;12(6A):2416-26. Epub 2008 Feb 15

In collaboration with the group of Theo Rein, Max Planck Institute of Psychiatry, Munich,

Germany, we analyzed PED transcriptional regulation. This study aimed to investigate targets of vitamin D3 in a human brain stem cell line. We employed arrays with antibodies directed against more than 600 structural and signalling proteins including phospho-variants. Over 180 proteins responded to vitamin D3, such as cyclin-dependent protein-serine kinase 1/2, epidermal growth factor receptor-tyrosine kinase, protein kinase A, protein-serine kinase Bγ and proteinserine kinase Cα. PED resulted strongly up-regulated. In silico promoter analysis revealed conserved binding sites for vitamin D3 receptor, suggesting a strong vitamin D3 dependency of the PEA-15 promoter. The results shown here are those made in our laboratory.

Results (II)

We chose the human neuronal stem cell line HNSC.100 as a model. This cell line is derived from a 10-10.5 weeks gestational age human Caucasian embryo and has been immortalised by stable v-myc expression. These cells can be differentiated and up-regulate markers of three lineages (astrocytes $\geq$85%, neurons 10 -15% and oligodendrocytes $\leq$1%;). We employed antibody microarrays to detect proteins that were changed in their expression or modification/activation upon treatment with vitamin D in our cellular model. Several structural and signalling proteins were identified. These targets were tested for reproducibility by Western-blot analysis using an independent set of HNSC.100 protein extracts. Several candidate proteins were confirmed, with a particularly strong effect (up-regulation) for PED.

PED promoter analysis and mRNA induction by vitamin D3. Given the strong response of PED to vitamin D3 indicated by two independent samples/methods and its prominent expression in the CNS (particularly abundant in astrocytes), we focused our further experiments on this candidate. First, we searched by bioinformatics tools for VDR binding sites in the PED promoter of the human, mouse and rat genomes. The sequence upstream

of the transcription site contains several transcription factor binding motifs, including those for NFκB, EGRF, EKLF and SP1 (Figure 24a). One of these sites is conserved between human, mouse and rat promoter, thus strongly indicating a functional vitamin D3 – dependency of the PED gene promoter. To experimentally test the up-regulation of the PED gene promoter by vitamin D3 we treated cells with vitamin D3 and measured the mRNA of PED by real time PCR. We observed indeed a rise of the PED mRNA already after 3h and 6h (Fig. 24b). Using an antibody that recognises PED irrespective of its phosphorylation status we also detected an up-regulation of the total amount of PEA protein after 12h (Figure 24c).
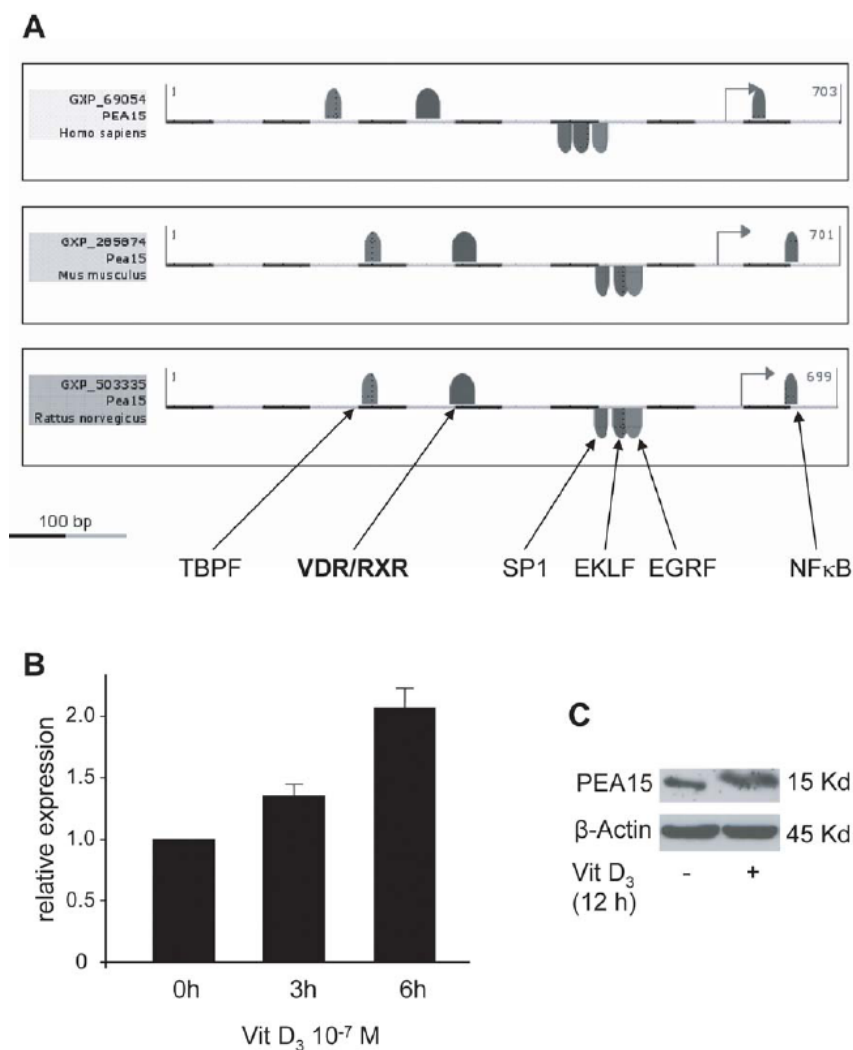

Figure 24. Conserved transcription factor binding sites in the promoter of PED and up-regulation of PED mRNA and protein. A. Several transcription factor binding motifs were identified, including those for VDR, NFκB, EGRF, EKLF and SP1. B. Effect of vitamin D3 on PEA15/PED mRNAlevels. A549 cells were treated with vitamin D3 (10^{-7}M) and the mRNA levels were determined by real time PCR at the times indicated. C. Verification of induction of total PED after 12h by Western blot.

Vitamin D$_3$ regulates PED function. We investigated whether the effect of vitamin D$_3$ on PED

expression changes cellular processes that depend on the function of PED. Numerous studies suggest the involvement of PED in a broad range of antiapoptotic processes in cultured cells. TRAIL (tumor necrosis factor apoptosis-inducing ligand) is an efficient inducer of apoptosis and in TRAIL-sensitive cells; transfection of PED cDNA resulted in cell resistance, whereas inhibition of PED expression changed the TRAIL-resistant phenotype to sensitive. Given that normal astrocytes are generally TRAIL-resistant, we chose the TRAIL-sensitive cell line A549 to examine VDR and PED expression in the presence and absence of vitamin D_3. First, we verified by Western blot that A549 cells express VDR (not shown). To test whether vitamin D_3 influences TRAIL-induced apoptosis, we pre-treated A549 cells with vitamin D_3 (10^{-7}M) for 12h before apoptosis was induced with TRAIL (100 ng/ml for the next 24h). Cell nuclei were visualized with propidium iodide and subjected to FACS analysis to monitor late stage apoptosis and MTS proliferation assays were performed to measure cell viability. Treatment with vitamin D_3 alone did not have a significant effect on apoptosis, as compared to vehicle-treated cells, whereas treatment with TRAIL resulted in 50% apoptotic cells, as expected. Notably, cells pre-treated with vitamin D_3 prior to TRAIL administration exhibited markedly decreased levels of TRAIL-induced apoptosis. MTS assays paralleled the observed changes, indicating that a decrease in cell proliferation/viability induced by TRAIL could be significantly reverted by pre-treating cells with vitamin D_3. To answer the crucial question of whether the effect of vitamin D_3 is dependent on PED, we silenced the PED gene with siPEA RNA, prior to treating cells with vitamin D_3 and TRAIL (reduced PED expression level are documented below the graphs of Figure 25b). Interestingly, the attenuating effect of vitamin D_3 on the actions of TRAIL in apoptosis and cell viability was completely abolished in PEA15 silenced cells (Figure 25b, dark grey bars). These data suggest that PED is mediating the effects of vitamin D_3 in cell survival.
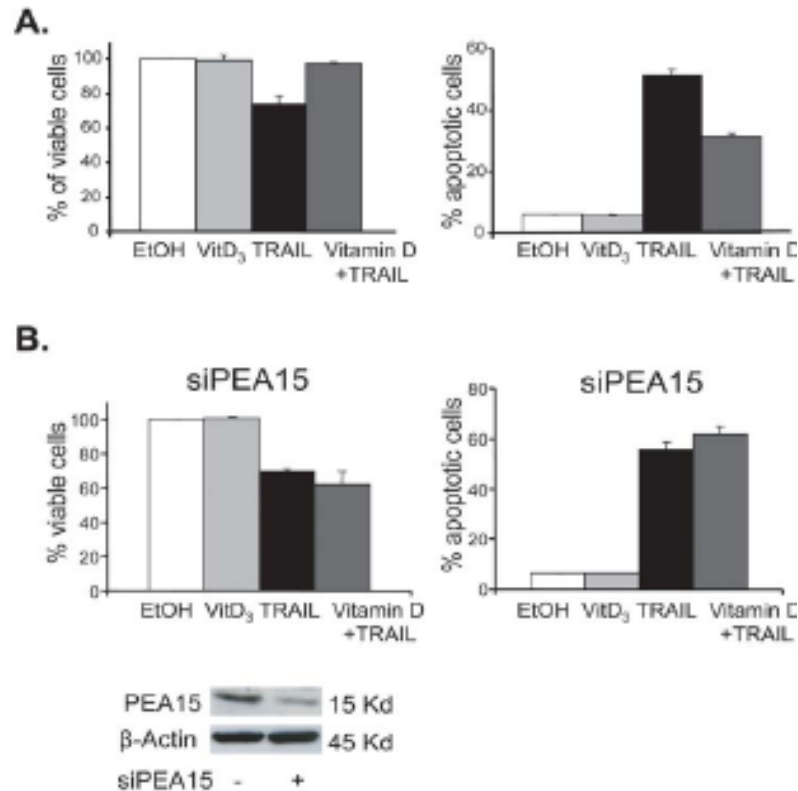
Figure 25. Effect of vitamin D_3 on TRAIL-induced apoptosis and cell survival in A549 cells. A. Cells were treated with vehicle, vitamin D_3 and TRAIL in the combinations indicated. Metabolic activity (as a measure of cell viability and apoptosis (FACS analysis) were determined. B. Same treatment as in A, but in the presence of RNAi directed against PEA15/PED. Data represent mean values + SEM of three independent experiments performed in triplicates each. Panel below B, verification of the efficacy of the siRNA directed against PED by Western blot using an antibody detecting total PED.

Vitamin D_3 increases phosphorylation of AKT1 and PED. The strong up-regulation observed using an antibody directed against PED phosphorylated at serine 116 raised the question of whether the increase in the level of total protein is achieved in part by increasing protein stability. It has been reported that PED is phosphorylated by protein kinase B/AKT1 which leads to stabilisation of the protein. Therefore, we used Western blot analysis to measure the levels of phosphorylated AKT1, total AKT1, phosphorylated PED, and total PED after treatment of the cells with vitamin D_3. Phosphorylation of AKT1 is a measure of the activity of this kinase. We observed an activation of AKT1 3h and 6h after addition of vitamin D_3, while the level of total AKT1 protein was unchanged (Figure 26). Interestingly, 6h after addition of vitamin D_3 we found an increase in phosphorylation of PED, but no change in the level of total PED yet (Figure 26), which rises only after 12h (Figure 24). This data supports the view that vitamin D_3 uses two mechanisms to increase the function of PED, stimulation of gene

transcription and stabilisation of the protein through phosphorylation, possibly via activation
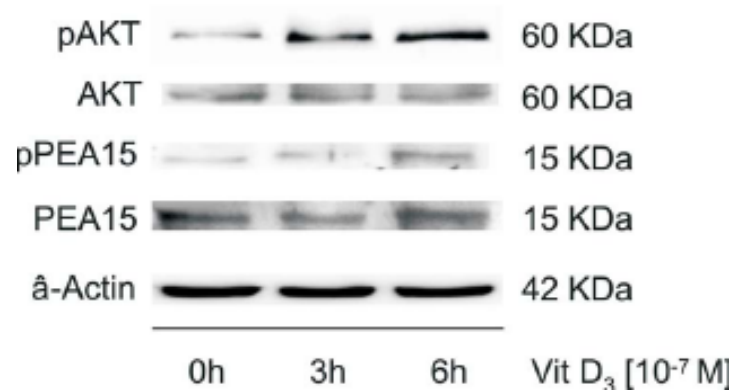
of AKT1.

Figure 26. Effect of vitamin D_3 on AKT and PED. A549 cells were treated with vitamin D_3, and harvested at the times indicated. Western analysis was performed to detect the levels of total AKT (AKT), phosphorylated AKT (pAKT), total PEA15/PED, phosphorylated PED (pPEA15), and α-actin.as loading control.

These results were published on *J Cell Mol Med*. 2009 Mar 27. [Epub ahead of print]

To better understand PED role in cancer, we focused on PED interactome characterization in Non Small Cell Lung Cancer (NSCLC) cell line A459. By the Tandem Affinity Purification (TAP), we identified Rac1, member of mammalian Rho GTPase proteins family, as PED-interacting protein. a member of mammalian Rho GTPase proteins family which switches between an active GTP-bound state and an inactive GDP-bound state. Rac1 binds to a variety of effector proteins thus regulating a wide range of cellular effects such as secretory processes, phagocytosis of apoptotic cells, epithelial cell polarization, growth factor-induced formation of membrane ruffles, ROS generation, lamellipodia formation and cell migration.

Results (III)

PED interacts with Rac1. Tandem Affinity Purification was used in order to discover new PED interactor. A459 cells were infected with tween-PED-TAP construct or with tween empty vector as control. The total protein lysate was incubated with immunoglobulin derivatised agarose beads and the retained sample eluted by hydrolysis with TEV protease. PED containing complexes were finally purified onto Calmodulin derivatised beads. After these

two purification steps, the sample and the control were fractionated by SDS-PAGE, the entire lanes from the gel were cut in slices and each gel slice was submitted to the identification procedure (fig. 27A and 27B). The resulting peptide mixtures were directly analyzed by mass spectrometry (LC-MS/MS) and identified by MASCOT protein database search. Common proteins identified in both the control and the sample lanes were discarded and only those proteins solely identified in the sample and absent in the control were selected as putative PED interactors. Several new candidate proteins were identified and among these we focused our attention on Rac1, because of its involvement in cancer signaling pathways. PED and Rac1 interaction was also confirmed by immunoprecipitation experiments from A459-tween PED-TAP cells (fig. 27C), from A459 transfected with Rac1 (fig. 27D) and from wild type A459 cells (fig. 27E). PED and Rac1 co-immunoprecipitation was evident either with exogenous or with endogenous proteins.
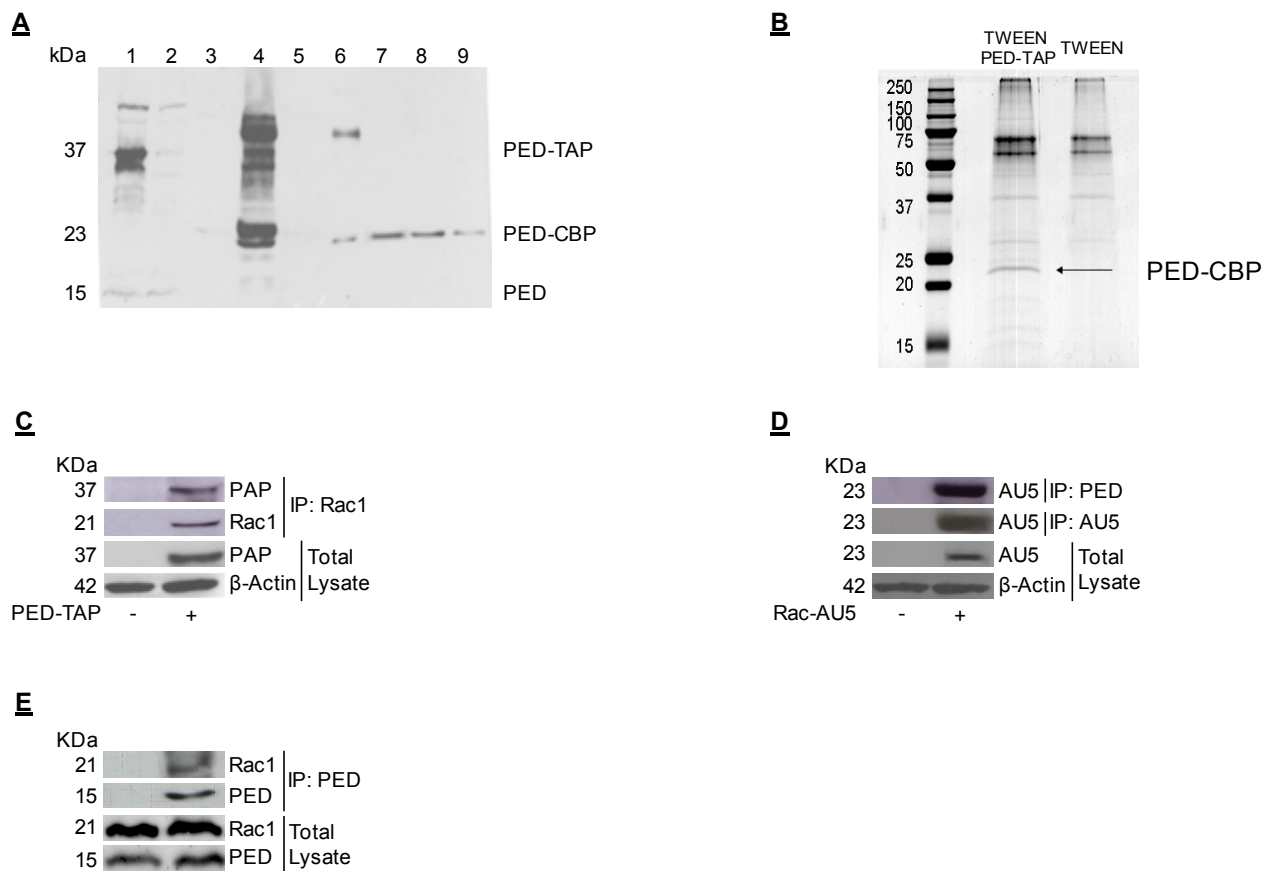

Figure 27. PED interacts with Rac1. (A) Samples from Tandem Affinity Purification collected at each step of the protocol. Lanes: (1) 40 µg of total extract; (2) 40 µg of supernatant after IgG incubation; (3) TEV cleavage control; (4) IgG beads after TEV cleveage; (5) supernatant after Calmodulin beads; (6) Calmodulin beads before final eluition; (7,8,9) eluition with 2, 10 and 20 mM EGTA. (B) Comassie staining of preparative polyacrilammide gel. Our PED-CBP bait is indicated at 23 KDa. A459 cells infected with TWEEN vector were used as negative control. (C) Co-immunoprecipitation of endogenous Rac1 with exogenous PED-TAP. 1 mg of total extract

immunoprecipitated using an anti-Rac1 antibody. Immunoprecipitated and input samples were loaded on 12% SDS polyacrilamide gel and blotted with an anti-Peroxidase Anti Peroxidase (PAP) antibody to identify the external part of the TAP tag. As negative control (C-), proteins were incubated with beads without antibody. (D) Co-immunoprecipitation of endogenous PED with exogenous Rac-AU5 tagged. The experimental procedure is indicated above. (E) Co-immunoprecipitation between endogenous PED and Rac1. Samples from A459 wild type cells were immunoprecipitated with anti-PED antibody.

PED affects Rac1 activation. In order to investigate the effects of PED on Rac1 activation, A459 cells were transfected with PED-MYC cDNA or control vector. After 24 h cells were serum starved for 16 h and then treated with 20% FBS for 5 or 15 min. The activity of Rac1 was assessed using the p21-binding domain (CRIB) of p21-activated kinase 1 (PAK1) in a GST-pull down assay. As shown in fig. 28A, after 5 min of stimulation a larger amount of Rac1-GTP could be observed in PED overexpressing cells, compared to the control cells, transfected with an empty vector. This activation decreased after 15 min. Similar results could be obtained upon EGF stimulation, a Rac1 specific activator, with a similar kinetics (data not shown).

Mechanisms of PED-mediated Rac1 activation. The removal of bound GDP and the subsequent loading of GTP are catalyzed by guanine nucleotide exchange factors (GEFs proteins). We therefore asked whether PED could act as a scaffold protein in Rac1 activation by promoting the interaction between Rac1 and its GEFs. A459 cells were transfected with PED-MYC cDNA, starved for 24 h and then incubated for 16 h with 100 µM of NSC23766, a Rac1 GTPase specific inhibitor that inhibits GEFs binding to Rac1 (35). Subsequently cells were treated with 20% FBS for 5 min and Rac1-GTP pull down assay was performed. As observed above, PED overexpression increased Rac1 activation upon serum stimulation. However, this effect was inhibited by pretreating cells with NSC23766 (fig. 28B), suggesting that Rac1 is activated by PED through a mechanism involving GEFs action.

Role of PED in AKT-mediated Rac1 phosphorylation. AKT is serine/threonine kinase downstream PTEN/PI3K pathway involved in many cellular processes, e.g. survival, apoptosis and migration. AKT phosphorylates Rac1 on Ser[71] and this process inhibits its GTP-loading. Because PED interferes with Rac1-GTP loading, we asked whether this effect was mediated through the regulation of Rac1 phosphorylation on Ser[71]. To this aim, A459 cells were transfected with control vector or PED-MYC cDNA. After 24 h, the cells were serum starved and then treated for 5 min with 20% FBS. As shown in fig. 2C, PED overexpression resulted in a strong reduction of serum mediated Rac1 phosphorylation in Ser[71]. Similar results were obtained with EGF stimulation (data not shown). To further confirm this observation, we evaluated basal Rac1 phosphorylation levels in A459 cells transfected with a constitutive active AKT (AKT D+) and PED-MYC cDNAs (fig. 28D). AKT D+ increased Rac1-Ser[71] phosphorylation, while co-transfection of AKT D+ and PED-MYC cDNAs resulted in a reduction of Rac1 phosphorylation levels. These results suggest that PED can enhance Rac1-GTP bound state by interfering with AKT-mediated Rac1 phosphorylation.
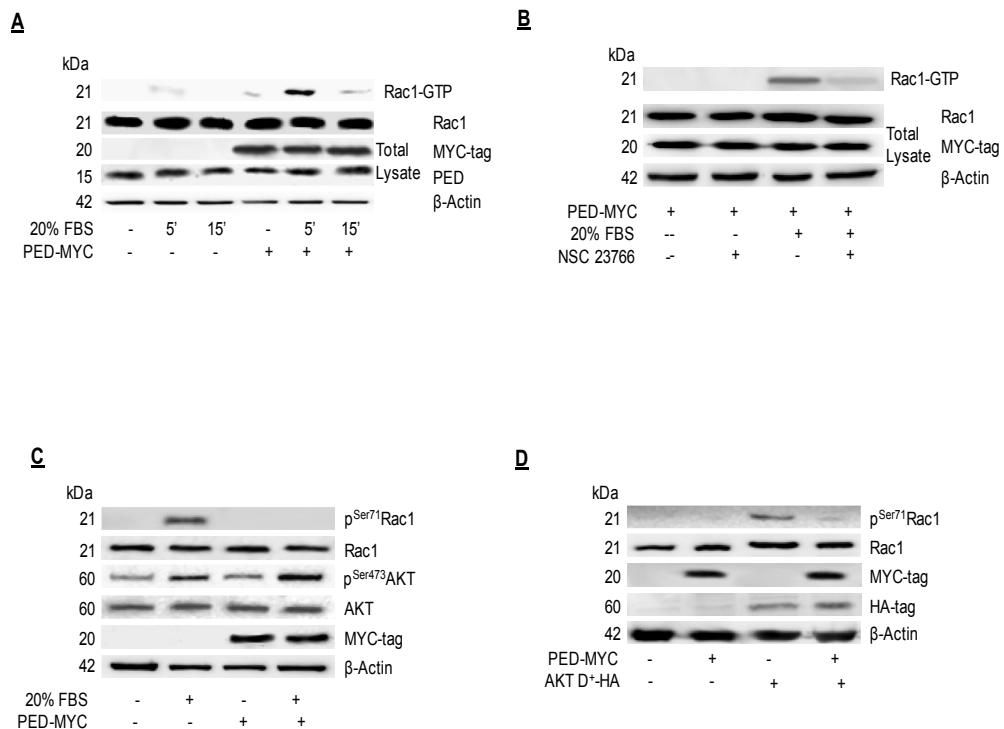

Figure 28. PED regulates Rac1-GTP loading. (A) A459 cells were transfected with 2 µg empty vector as control or 2 µg PED-MYC cDNA as indicated. After 24 h cells were serum starved and then treated for 5 and 15 min with 20% FBS respectively. Rac1-GTP pull down assay was performed as described in the methods section. The

amounts of total Rac1 and Rac1-GTP were estimated by immunoblotting with Rac1. (B) Rac1-GTP pull down assay with PED cDNA overexpression and 20% FBS stimulation or 100 μM NSC23766 pretreatment for 16 h. (C) PED cDNA expression inhibits AKT-induced Ser[71] Rac1 phosphorylation upon serum stimulation. A459 cells were transfected with 2 μg of PED cDNA or control vector, then starved for 16 h and treated as indicated. (D) Evaluation of Rac1 phosphorylation levels upon transfection with 2 μg of PED-MYC or AKT D+. The total amount of transfected plasmids is normalized with co-transfection of empty vector.

Effects of Rac1 activation on PED phosphorylation status. PED needs to be phosphorylated in Ser[104] and Ser[116] to be recruited to the DISC and to inhibit the apoptotic process. Furthermore, PED in its non-phosphorylated status can bind and sequester ERK 1/2 into cytosol . We asked whether Rac1 could alter PED phosphorylation status and thus its function. To this aim, we transfected A459 cells wild type Rac or constitutively active Rac (RacQL) cDNAs. Interestingly, PED-Ser[104] phosphorylation was increased upon transfection of wild type Rac and more strongly by RacQL compared to control (fig. 29A). Serine[116] phosphorylation was not modified (data not shown). Furthermore, Ser[104]-PED phosphorylation was also upregulated by transfection with another constitutively active Rac (Rac12V) and with Vav1 overexpression, one of Rac1 GEFs (fig. 29B). Because PKC is the major kinase involved in PED-Ser[104] phosphorylation, we investigated whether Rac1 may regulate PED phosphorylation through PKC. To this aim, A459 cells were transfected with constitutively active Rac and then treated with 108 nM Ro-32-0432, a cell-permeable and selective PKC inhibitor. PED phosphorylation levels on serine 104 were evaluated by blotting with specific anti-phospho-serine 104 PED antibody. As shown in figure 29C, RacQL-mediated PED phosphorylation was completely abolished when cells were treated with the PKC inhibitor. These results suggest that Rac1 augments PED phosphorylation on serine 104 by regulation of PKC activity.

Role of PED and Rac1 interaction on ERK 1/2 activation. In order to investigate the downstream effects of PED and Rac1 interaction, we investigated ERK 1/2 pathway. PED can promote ERK 1/2 phosphorylation and activation, but retaining them into cytosol avoiding their nuclear translocation. The mechanism by which PED allows ERK 1/2 phosphorylation is

not clear yet. Rac1 activation leads to ERK 1/2 phosphorylation through a pathway involving PAK1-MEK1-ERK1/2. To determine the effect of PED and Rac1 interaction on ERK 1/2 activation, we transfected A459 cells with control vector, PED-MYC or RacQL cDNAs and then evaluated the downstream effects on ERK 1/2 phosphorylation. PED and RacQL alone were able to activate ERK 1/2. Interestingly, when PED and RacQL were co-transfected the levels of ERK 1/2 phosphorylation were even stronger (fig. 29D). As previously described, we found that PED transfection resulted in an inhibitory effect on ERK 1/2 nuclear translocation, as attested by the reduction of the phosphorylation of their nuclear substrate ELK1 (fig. 29D). On the contrary when PED was overexpressed together with RacQL, ELK1 phosphorylation was stronger compared to control. This effect was probably due to the Rac1-induced phosphorylation on serine 104. To this aim, we generated a mutant PED protein which could not be phosphorylated in Ser^{104} (S104G PED). Transfection of S104G PED mutant, alone or co-transfected with RacQL, abolished the phosphorylation of ELK1 (fig. 29D). These results suggest that PED, upon Rac-induced Ser^{104} phosphorylation, lost its capability to retain ERK 1/2 into cytosol, while its unphosphorylable mutant S104G blocked ERK 1/2 into cytosol, even in presence of constitutively active Rac mutant.
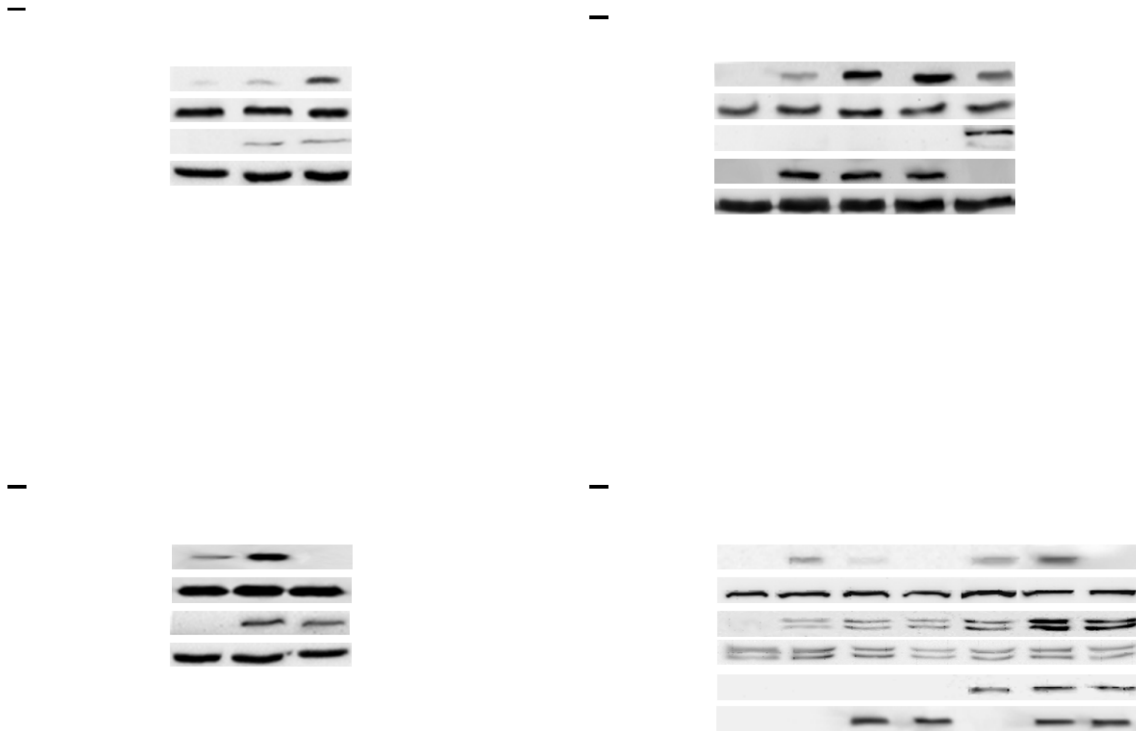
Figure 29. Rac1 activation induces PED-Ser[104] phosphorylation. (A) A459 cells were transfected with control vector, Rac and RacQL. Overexpression of constitutively active Rac resulted in a strong increase of Ser[104]–PED phosphorylation, as attested by immunoblotting with specific Ser[104]–PED antibody. (B) Confirmation of Rac-induced PED phosphorylation using another active mutant of Rac (12V) and with Vav1 overexpression. A459 cells were transfected with control vector, Rac, RacQL, Rac12V and Vav1 respectively and then Ser[104]–PED phosphorylation was evaluated. (C) A459 cells were transfected with 2 μg of RacQL and then treated with 108 nM PKC inhibitor Ro-32-0432 for 16 h. PKC inhibition resulted in abolishment of Rac-induced Ser[104]–PED phosphorylation. (D) A459 cells were transfected with control vector, PED, PED S104G or RacQL. Then cells were starved for 16 h and treated with 20% FBS. Expression of PED and Rac-QL resulted in an increase of ERK 1/2 phosphorylation and Elk1 activation upon serum stimulation, while Elk1 phosphorylation, but not ERK 1/2 phosphorylation, was abrogated by transfection of unphosphorylable PED mutant S104G, even with RacQL, indicating that ERK 1/2 were restrained into cytosol.

Role of PED on cell migration. One of the most important effects of the activation of ERK1/2

pathway is regulation of cellular migration and invasion. For this reason we asked wheter

PED/Rac1 interaction was involved in these phenomena. Interestingly, overexpression of

PED-MYC resulted in increased migration and invasion of A459 cells. The effect was similar

to that obtained with constitutive active Rac (fig. 30A and 30B). When PED-MYC and RacQL

were cotransfected, the effects on cell migration and invasion were even stronger than

controls. Similar results were obtained by transfecting the same constructs into HeLa cells

(data not shown). Moreover, unphosphorylable S104G PED mutant was able to inhibit both

cell migration and invasion (fig. 30A), demonstrating the importance of Rac1-induced PED

phosphorylation in serine 104. Indeed S104G PED mutant was able to bind ERK 1/2, sequestrate them into cytosol, not allowing them to migrate into nucleus and promote cell migration and invasion. On the other hand, A459 PED knock-down clones had reduced migratory and invasive capabilities (fig. 30B). Furthermore, PED knock-down clones showed also a reduced wound healing capability, compared to control cells (fig. 30C). To determine the pathway involved in the regulation of PED-mediated migration and invasion, PED overexpressing A459 cells were treated with 100 µM Rac1 inhibitor NSC23766 or 108 nM PKC inhibitor Ro-32-0432 for 16 h. PED-MYC transfected cells lost their capability to migrate and invade upon treatment with inhibitors (fig. 31A), demonstrating that PED requires Rac1 and PKC activity to promote migration and invasion. To finally prove Rac1 involvement in PED-mediated cell migration and invasion, we down-regulated Rac1 with the transfection of specific siRNAs. Upon Rac1 downregulation, PED could not promote cell migration and invasion anymore (fig. 31B). These results show for the first time that PED expression promote cell migration and invasion through a mechanism involving the activation of Rac1, PKC and ERK1/2.
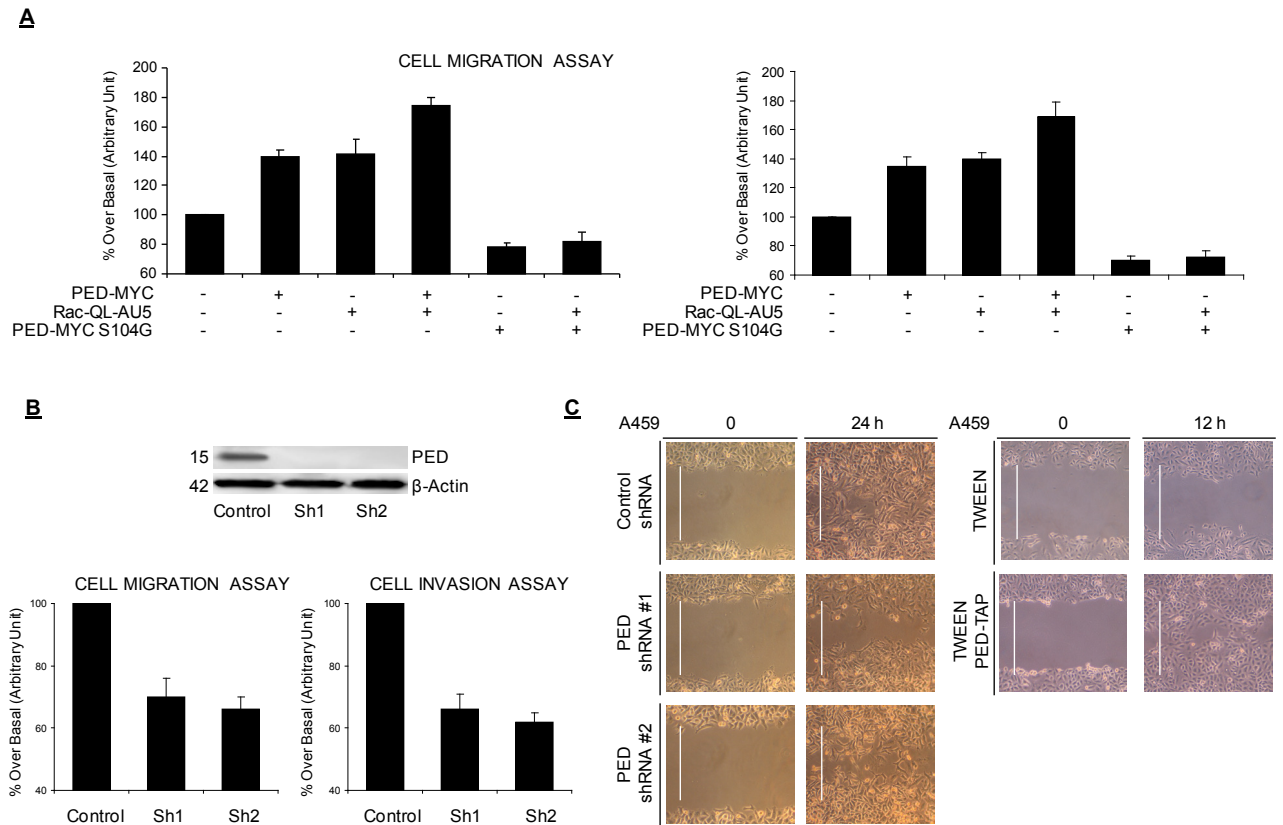
Figure 30. Effects of PED and Rac1 interaction on cell migration and invasion. (A) A459 cells were transfected with control vector, PED, PED S104G or mutant RacQL, and transwell migration and invasion assay was performed as described above. (B) A459-PED KO clones, obtained with transfection of specific PEDshRNA vector and then selected with 2.5 µg/ml of Puromycin. A459-PED KO clones showed a reduction of migration and invasion upon serum stimulation, compared to control cells expressing Scrambled shRNA (control). (C) Wound healing assay of A459 shScrambled cells and PED shRNA clones (Sh1 and Sh2). Cells were grown to confluence and then wound was performed using a pipette tip. Then cells were incubated and grown for 24 h.
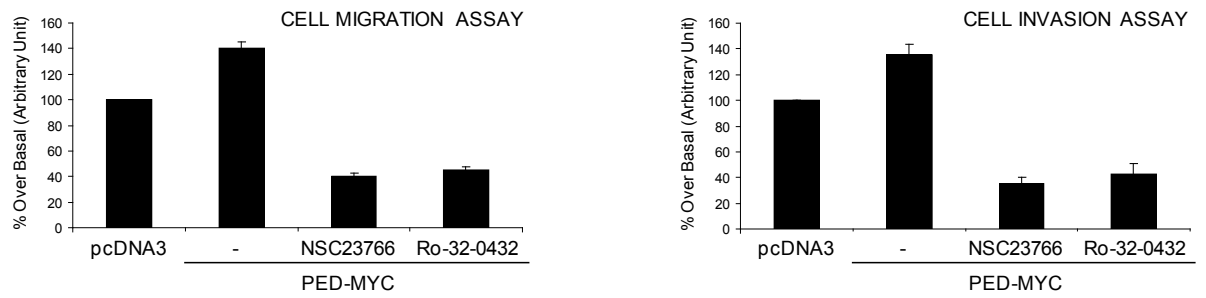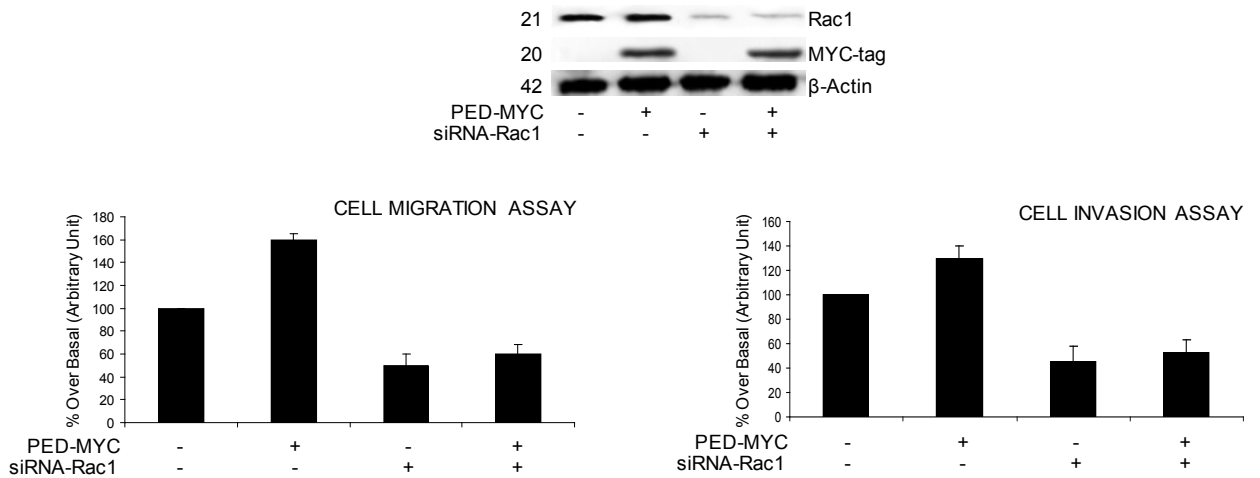
Figure 5. Pathways of PED-mediated migration and invasion. (A) A459 cells were transfected with control vector or PED cDNA. Then cells were plated on transwell chambers to perform migration and invasion assays and treated with Rac1 and PKC inhibitors (NSC23766 and Ro-32-0432 respectively). Migrated cells were evaluated 24 h later. Cells were stained in 25% methanol and 0.1% crystal violet. Then it was eluited with 1% SDS and the migration rate was established by reading absorbance at λ 570 nm. (B) A459 cells were transfected with control vector, PED-MYC and Rac1-siRNAs. Rac1 downregulation was evaluated by immunoblotting with Rac1 antibody. Transwell chambers were used to perform migration and invasion assays. 10^5 cells were plated onto the upper chamber of tranwell and cells were incubated for 24 h. Rac1 downregulation blocked PED-mediated migration and invasion.

DISCUSSION

There is much evidence implicating an important role for PED in human cancer. PED, being a member of DED protein family (24), induces resistance to TRAIL, FasL, TNFα-mediated death in cancer cells (22-30), making therapy often ineffective. Increased expression of DED family members with anti-apoptotic functions, such as PED, represents a possible mechanism by which tumor cells escape apoptosis. PED acts primarily by preventing the interaction between the adaptor molecule, FADD, and procaspase-8. We have reported that PED inhibits the anti-apoptotic signal of death receptors in many different cell types, including breast carcinoma and glioma, in which it is overexpressed.

Lung tumors are among the most aggressive types of cancer and are frequently resistant to drug-induced cell death. 80% of lung cancers are of the NSCLC type. Advances in standard treatment for this tumor, such as surgery, radiotherapy, and chemotherapy, have not significantly increased patient survival. Thus, novel treatment strategies are urgently needed to improve the clinical management of this serious disease. Recent studies have demonstrated that targeting TNF superfamily death receptors is a promising strategy for the treatment of cancer. Apoptosis-based anti-cancer therapies are designed to achieve tumor eradication through the use of death-inducing molecules capable of activating the apoptotic program selectively in neoplastic cells. Due to its specific toxicity for transformed cells, recombinant forms of TRAIL are among the most promising apoptosis-based anti-tumor agents. In fact, a number of biotech and pharmaceutical companies developed recombinant TRAIL/Apo2L as well as humanized agonistic mAb targeting TRAIL-R1 or TRAIL-R2 that are currently being evaluated in Phase I and Phase II clinical trails. Mice that are genetically deficient in the TRAIL gene, exhibit increased susceptibility to experimental and spontaneous tumors, suggesting an important role of endogenous TRAIL in tumor surveillance. However, in a number of patients, tumor cells evade death signals generated by drugs through the activation of effective anti-apoptotic mechanisms. We demonstrated that PED is overexpressed in lung cancer tissue obtained from 27 NSCLC-affected patients.

Interestingly, TNM staging revealed that PED expression is greater during the first phase of the disease (T1) than in T2 lesions. The analysis of PED expression in pre-malignant lesions, such as metaplastic bronchial lesions, could shed light on the role of PED in tumor initiation, progression and invasiveness. This study shows that PED regulates the susceptibility to TRAIL-induced death in lung cancer cells. In fact, while the levels of PED differs significantly in CALU-1 (TRAIL-insensitive) and H460 (TRAIL-sensitive) cells, the levels of the other signaling components (such as TRAIL receptors caspases, and FADD) were comparable. Modulation of the sensitivity to TRAIL by PED was confirmed by down regulating PED expression with PED siRNA: when transfected, the otherwise TRAIL-insensitive CALU-1 cells became susceptible to this cytotoxic cytokine. Moreover, PED overexpression in H460 cells was able to change their phenotype from TRAIL-sensitive to TRAIL- insensitive.

Because resistance of different tumors may be mediated by diverse survival mechanisms, we investigated the role of c-FLIP in TRAIL resistance by down-regulation of c-FLIP expression with a specific siRNA. As already observed in other tumor types such as glioma and B-cell chronic leukemia, the effects of PED are prevalent over those mediated by c-FLIP for sensitivity to TRAIL. Thus, it is possible that c-FLIP and PED contribute differently, depending to the cell type or tumor type to induce resistance to TRAIL. Our data thus demonstrate that PED plays a major role in TRAIL resistance in NSCLC. Although PED expression was completely and specifically inhibited by the transfection with PED siRNA duplex, TRAIL sensitivity was not fully recovered. These results suggest that it is likely that there might be alternative mechanisms for TRAIL resistance.

Thus, the overexpression of a gene involved in resistance to TRAIL could be important for responsiveness to chemotherapy. Since expression levels of PED are a focal point for the regulation of apoptosis, PED represents a key target for treatment of cancer.

We furthermore analyzed the molecular mechanisms by which PED expression is regulated. In collaboration with the group of Theo Rein, Max Planck Institute of Psychiatry, Munich, Germany, we searched for vitamin D3-regulated targets in the proteome of human brain-

derived cells. Up-regulation of PED was the most prominent feature on the used antibody array. We investigated this up-regulation further and conclude from our experiments with different cell lines (human Non Small cell Lung Cancer A549 cell line, with low endogenous PED levels) that vitamin D3 leads to an increase in promoter activity of PED already after 3-6 h and with a little delay to an increase in protein phosphorylation after 6h, most likely via activation of AKT1, which is known to phosphorylate PED. The increase in mRNA and the protein stabilization through phosphorylation in combination lead to an increase in total PED protein level after 12h. Our finding of increased AKT1 activity after vitamin D3 exposure not only provides a potential mechanism for activation of PED, but also adds another pathway through which vitamin D3 exerts anti-apoptotic effects. Our discovery that PED is strongly responsive to vitamin D3 potentially links vitamin D3 to any of the actions of PED. Although extensive work needs to be done to test the degree of overlapping activities, we already showed in this work that vitamin D3 significantly affected apoptosis and cell survival in A549 cells in a PED-dependent manner.

Recently, Peacock et al. demonstrated that PTEN can regulate PED phosphorylation and activity in an AKT-dependent manner, and thus modulate the ability of Bcl-2 to suppress Fas-induced apoptosis (36). A new role for PED in cancer was then proposed by Bartholomeusz et el. by suggesting a mechanism involving activation of ERK 1/2 pathway and induction of autophagy (37). The ability of PED to bind ERK 1/2 was the focus of many studies that indicated that PED can restrain ERK 1/2 within the cytosol, avoid their nuclear translocation and this way block the nuclear effects mediated by these signaling molecules, among them transcription, migration, invasion. Moreover, PED, through the control of activated-ERK1/2 localization, can act as a tumor suppressor gene in inducing senescence and reducing the transforming effects of oncogenic Ras (38). Further evidence that PED is connected to ERK activation derives from its capability to bind RSK2 in a phosphorylation-regulated manner and act as a scaffold protein to strengthen its role in ERK activation (39). The emerging scenario is complex, with a single protein involved in many cellular pathways, varying from apoptosis to cell migration, invasion, autophagy, senescence, cell signaling. In order to give

new insights in PED's role in cancer, we aimed to discover new interactors of PED. We performed a generic purification method for protein complexes characterization, the tandem affinity purification method. This method has two purification steps, obtained with IgG-Agarose and Calmodulin chromatographic supports, which allow high binding specificity of interaction partners. Upon mass spectrometry analysis of final eluition, we identified several new candidate partners of PED, one of which was Rac1. We first confirmed the interaction between PED and Rac1 through independent immunoprecipitation experiments, using both exogenous and endogenous proteins. It was interesting to note that phosphorylation status of PED did not interfere with its interaction with Rac1. Indeed, unphosphorylable Ser[104] and Ser[116] PED mutants still interacted with Rac1 (not shown). In order to investigate the effect of PED on Rac1 GDP/GTP bound state, we performed a GST-pull down assay using the p21-binding domain (CRIB) of p21-activated kinase 1 (PAK1) to isolate the active GTP-bound Rac1 from the total extract. We demonstrated that PED augmented GTP-bound state upon stimulation with both unspecific stimulus of 20% FBS or specific Rac1 activator as EGF (not shown) in a mechanism involving GEFs action. Downregulation of PED, obtained with specific PED-siRNAs, did not significantly alter GDP/GTP exchange compared to control samples (data not shown). PED did not act as a scaffold protein in promoting GEFs-Rac1 binding, since in co-immunoprecipitation experiments, PED could not bind neither Tiam1 nor TrioN, two of the most abundant Rac1 GEFs. Moreover, we did not identify any GEFs from tandem affinity purification analysis and mass spectrometry experiments that bind to the PED complex. Our data show that PED was able to inhibit AKT-mediated Rac1 Ser[71] phosphorylation. It was previously shown that this phosphorylation inhibits GEFs binding to Rac1, thus preventing Rac1 activation (35). To better elucidate this point, we generated two stable PED knock out (KO) clones with PED-specific shRNA plasmid vectors and then we evaluated Rac1 phosphorylation by blotting with phospho-serine 71 Rac1 antibody. PED downregulation resulted in 30% increase in Rac1 phosphorylation, compared to control cells (not shown). The mechanism of PED effects on Rac1 phosphorylation is not clear yet. Since

it was reported that AKT/PI3K pathway is involved in motility of tumor cells and AKT has negative regulatory role on Rac1 (35), we hypothesized that PED promotes GTP loading to Rac1, by reducing AKT inhibitory effects on Rac1.

Interestingly, PED and Rac1 interefered with each other's function once bound together. In facts, when Rac1 is active, promotes PED Ser^{104} phosphorylation, as shown with two different Rac constitutively active mutants (RacQL, Rac12V) or with the overexpression of Vav1. This mechanism involves PKC activation. In facts, treatment with specific PKC inhibitors completely abolished PED Ser^{104} phosphorylation. The mechanism by which Rac1 promotes PKC-dependent PED phosphorylation is under investigation in our lab.

PED and Rac1 are involved in many cellular process. To understand the biological meaning of their interaction we focused on the regulation of ERK 1/2 activation status as well as their cellular localization. We observed that co-expression of PED and constitutively active Rac induced a strong ERKs phosphorylation as well as Elk-1 activation, indicating that ERKs were able to translocate from the cytosol into the nucleus. We propose that PED alone coadiuvates Rac1-mediated ERKs activation and the expression of active Rac facilitates PED phosphorylation on Ser^{104} and the consequent release of ERKs. Furthermore, in this study we demonstrate that PED is involved in promoting cell migration and invasion. Previous findings described that PED mediated inhibition of cell migration/invasion. Our data suggest that Rac1's effects on PED phosphorylation determine a reduction of PED's inhibitory role of ERK 1/2 nuclear translocation, which is required to promote migration/invasion. We propose a model in which when Rac1 is activated, PED phosphorylation on Ser^{104} is increased and its binding with ERK 1/2 is reduced. This results in abrogation of its regulatory role on ERK 1/2 (involving nuclear migration, cell invasion and proliferation).

Besides Rac1-induced effects on PED phosphorylation, we did not observe any interference in PED-mediated TRAIL resistance (our unpublished observations). Ramos et al. previously reported that PED activates ERK MAP Kinase through a Ras-dependent pathway (38). PED-

Rac1 interaction gives a new explanation of how PED can mediate its effects on MAPK signaling. Here we demonstrate that regulation of PED phosphorylation can modify its ability to promote or repress cell migration and invasion.

Our findings about PED interactome demonstrate that PED overexpression is linked to cancer not only because of an anti-apoptotic role but also because this promotes migration and invasion of malignant cells. This protein might result, therefore, to be a good target for anti-neoplastic therapy.

BIBLIOGRAPHY

1. Herbst RS, Heymach JV and Lippman SM. *Lung cancer* N Engl J Med. 2008 Sep 25;359(13):1367-80.

2. Cotran, Kumar and Collins. Robbins. *Le basi patologiche delle malattie.* Sesta Edizione.

3. Sun S, Schiller JH, Gazdar AF. *Lung cancer in never smokers--a different disease.* Nat Rev Cancer. 2007 Oct;7(10):778-90.

4. Lababede O., Meziane MA and Rice TW. *TNM staging of lung cancer.* Chest 1999;115;233-235.

5. Okamoto I. *Epidermal growth factor receptor in relation to tumor development: EGFR-targeted anticancer therapy.* FEBS J. 2009 Nov 18. [Epub ahead of print]

6. Johnstone RW, Frew AJ and Smyth MJ. *The TRAIL apoptotic pathway in cancer onset, progression and therapy.* Nat Rev Cancer. 2008 Oct;8(10):782-98. Review.

7. Sakamoto H, Shimizu J, Horio Y, Ueda R, Takahashi T, Mitsudomi T, Yatabe Y. *Disproportionate representation of KRAS gene mutation in atypical adenomatous hyperplasia, but even distribution of EGFR gene mutation from preinvasive to invasive adenocarcinomas.* J Pathol. 2007 Jul;212(3):287-94.

8. Wistuba II, Berry J, Behrens C, Maitra A, Shivapurkar N, Milchgrub S, Mackay B, Minna JD, Gazdar AF. *Molecular changes in the bronchial epithelium of patients with small cell lung cancer.* Clin Cancer Res. 2000 Jul;6(7):2604-10.

9. Sengupta S, Harris CC. *p53: traffic cop at the crossroads of DNA repair and recombination.* Nat Rev Mol Cell Biol. 2005 Jan;6(1):44-55.

10. Sharma SV, Bell DW, Settleman J, Haber DA. *Epidermal growth factor receptor mutations in lung cancer.* Nat Rev Cancer. 2007 Mar;7(3):169-81.

11. Keith RL, Miller YE, Gemmill RM, Drabkin HA, Dempsey EC, Kennedy TC, Prindiville S, Franklin WA. *Angiogenic squamous dysplasia in bronchi of individuals at high risk for lung cancer.* Clin Cancer Res. 2000 May;6(5):1616-25.

12. Dash P. *Apoptosis.* Basic Medical Sciences, St.George's, University of London.

13. Taylor RC, Cullen SP, Martin SJ. *Apoptosis: controlled demolition at the cellular level.* Nat Rev Mol Cell Biol. 2008 Mar;9(3):231-41.

14. Cotter TG. *Apoptosis and cancer: the genesis of a research field.* Nat Rev Cancer. 2009 Jul;9(7):501-7.

15. Youle RJ, Strasser A. *The BCL-2 protein family: opposing activities that mediate cell death.* Nat Rev Mol Cell Biol. 2008 Jan;9(1):47-59.

16. Lowe SW, Lin AW. *Apoptosis in cancer.* Carcinogenesis. 2000 Mar;21(3):485-95.

17. Sander EE, Collard JG. *Rho-like GTPases: their role in epithelial cell-cell adhesion and invasion.* Eur J Cancer. 1999 Dec;35(14):1905-11.

18. Vega FM, Ridley AJ. *Rho GTPases in cancer cell biology.* FEBS Lett. 2008 Jun 18;582(14):2093-101.

19. Price LS, Collard JG. *Regulation of the cytoskeleton by Rho-family GTPases: implications for tumour cell invasion.* Semin Cancer Biol. 2001 Apr;11(2):167-73.

20. Raftopoulou M, Hall A. *Cell migration: Rho GTPases lead the way.* Dev Biol. 2004 Jan 1;265(1):23-32.

21. Pullikuth AK, Catling AD. *Scaffold mediated regulation of MAPK signaling and cytoskeletal dynamics: a perspective.* Cell Signal. 2007 Aug;19(8):1621-32.

22. Sharif A, Canton B, Junier MP, Chneiweiss H. *PEA-15 modulates TNFalpha intracellular signaling in astrocytes.* Ann N Y Acad Sci. 2003 Dec;1010:43-50.

23. Renault F, Formstecher E, Callebaut I, Junier MP, Chneiweiss H. *The multifunctional protein PEA-15 is involved in the control of apoptosis and cell cycle in astrocytes.* Cell Mol Life Sci. 2009 Mar;66(5):814-30.

24. Valmiki MG, Ramos JW. *Death effector domain-containing proteins.* Cell Mol Life Sci. 2009 Mar;66(5):814-30.

25. Ungaro P, Teperino R, Mirra P, Cassese A, Fiory F, Perruolo G, Miele C, Laakso M, Formisano P, Beguinot F. *Molecular cloning and characterization of the human PED/PEA-15 gene promoter reveal antagonistic regulation by hepatocyte nuclear factor 4alpha and chicken ovalbumin upstream promoter transcription factor II.* J Biol Chem. 2008 Nov 7;283(45):30970-9. Epub 2008 Sep 2.

26. Obradovic D, Zanca C, Vogl A, Trümbach D, Deussing J, Condorelli G, Rein T. *Vitamin D(3) signalling in the brain enhances the function of Phosphoprotein Enriched in Astrocytes - 15 KDa (PEA-15).* J Cell Mol Med. 2009 Mar 27. [Epub ahead of print]

27. Todaro M, Lombardo Y, Francipane MG, Alea MP, Cammareri P, Iovino F, Di Stefano AB, Di Bernardo C, Agrusa A, Condorelli G, Walczak H, Stassi G. *Apoptosis resistance in epithelial tumors is mediated by tumor-cell-derived interleukin-4.* Cell Death Differ. 2008 Apr;15(4):762-72. Jan 18 Epub 2008

28. Hao C, Beguinot F, Condorelli G, Trencia A, Van Meir EG, Yong VW, Parney IF, Roa WH, Petruk KC. *Induction and intracellular regulation of tumor necrosis factor-related apoptosis-inducing ligand (TRAIL) mediated apotosis in human malignant glioma cells.* Cancer Res. 2001 Feb 1;61(3):1162-70.

29. Garofalo M, Romano G, Quintavalle C, Romano MF, Chiurazzi F, Zanca C, Condorelli G. *Selective inhibition of PED protein expression sensitizes B-cell chronic lymphocytic leukaemia cells to TRAIL-induced apoptosis.* Int J Cancer. 2007 Mar 15;120(6):1215-22

30. Zanca C, Garofalo M, Quintavalle C, Romano G, Acunzo M, Ragno P, Montuori N, Incoronato M, Tornillo L, Baumhoer D, Briguori C, Terracciano L, Condorelli G. *PED is overexpressed and mediates TRAIL resistance in human non-small cell lung cancer.* J Cell Mol Med. 2008 Dec;12(6A):2416-26. Epub 2008 Feb 15.

31. Stassi G, Garofalo M, Zerilli M, Ricci-Vitiani L, Zanca C, Todaro M, Aragona F, Limite G, Petrella G, Condorelli G. *PED mediates AKT-dependent chemoresistance in human breast cancer cells.* Cancer Res. 2005 Aug 1;65(15):6668-75.

32. Heasman SJ, Ridley AJ. *A generic protein purification method for protein complex characterization and proteome exploration.* Nat Rev Mol Cell Biol. 2008 Sep;9(9):690-701

33. Condorelli G, Vigliotta G, Cafieri A, Trencia A, Andalò P, Oriente F, Miele C, Caruso M, Formisano P, Beguinot F. *PED/PEA-15: an anti-apoptotic molecule that regulates FAS/TNFR1-induced apoptosis.* Oncogene. 1999 Aug 5;18(31):4409-15.

34. Benard V, Bohl BP, Bokoch GM. *Characterization of rac and cdc42 activation in chemoattractant-stimulated human neutrophils using a novel assay for active GTPases.* J Biol Chem. 1999 May 7;274(19):13198-204

35. Kwon T, Kwon DY, Chun J, Kim JH, Kang SS. *Akt protein kinase inhibits Rac1-GTP binding through phosphorylation at serine 71 of Rac1.* J Biol Chem. 2000 Jan 7;275(1):423-8.

36. Peacock JW, Palmer J, Fink D, Ip S, Pietras EM, Mui AL, Chung SW, Gleave ME, Cox ME, Parsons R, Peter ME, Ong CJ. *PTEN loss promotes mitochondrially dependent type II Fas-induced apoptosis via PEA-15.* Mol Cell Biol. 2009 Mar;29(5):1222-34. Epub 2008 Dec 22.

37. Bartholomeusz C, Rosen D, Wei C, Kazansky A, Yamasaki F, Takahashi T, Itamochi H, Kondo S, Liu J, Ueno NT. *PEA-15 induces autophagy in human ovarian cancer cells and is associated with prolonged overall survival.* Cancer Res. 2008 Nov 15;68(22):9302-10

38. Ramos JW, Hughes PE, Renshaw MW, Schwartz MA, Formstecher E, Chneiweiss H, Ginsberg MH. *Death effector domain protein PEA-15 potentiates Ras activation of extracellular signal receptor-activated kinase by an adhesion-independent mechanism.* Mol Biol Cell. 2000 Sep;11(9):2863-72.

39. Vaidyanathan H, Opoku-Ansah J, Pastorino S, Renganathan H, Matter ML, Ramos JW. *ERK MAP kinase is targeted to RSK2 by the phosphoprotein PEA-15*. 1. Proc Natl Acad Sci U S A. 2007 Dec 11;104(50):19837-42. Epub 2007 Dec 6.

40. Huber LA. *Is proteomics heading in the wrong direction?* Nat Rev Mol Cell Biol. 2003 Jan;4(1):74-80.